A Study on Exchange Processes of Carbon Monoxide and Hydrogen Molecule between the Atmosphere and the Biosphere

by Seiichiro YONEMURA

A dissertation for the degree of Doctor of Science in the Graduate School of the University of Tokyo

Acknowledgments

I would like to pay special thanks to Professor N. Iwagami who gave me the opportunity to submit this thesis to the University of Tokyo and suggested valuable comments through this thesis. I am much indebted to Professor T. Ogawa in NASDA for the instruction during my Master thesis. I am deeply obliged to Dr. S. Kawashima, the chief of Laboratory of Air Quality Conservation and Agroclimatology in NIAES for his comments with deep insight on the processes of analysis of data and of writing papers to journals and summarizing this study. I would like to pay sincere thanks to Dr. H. Tsuruta, the chief of Laboratory of Impact Assessment in NIAES, for suggesting this themes on gas exchange studies between the atmosphere and the biosphere and for offering me the opportunity to participate in various projects.

I owed to Dr. M. Yokozawa in NIAES who is a mathematical ecologist for his techniques in mathematics, physics, numerical simulation, and daily-conversation about present research topics on environmental studies. I am indebted to Dr. S. Sudo in NIAES who is an analytical atmospheric chemist and an ideal co-researcher for his techniques of experiments and analytical atmospheric chemistry, for the cooperation in the combustion experiments, and for daily discussion on atmospheric chemistry. I owed to Dr. A. Miyata who is a micrometeorologist for the cooperation in field measurements and the comments on this thesis.

I owed to Dr. K. Kita of the university of Tokyo who is an atmospheric chemist for the improvement of RGA3 measurements systems. I owed to Dr. H. Matsueda in Meteorological Research Institute who is an atmospheric chemist for the discussion on atmospheric behavior of CO and H_2 and for comparing my standards with the NOAA/CMDL scale. I owed to Dr. H. Sakai in NIAES who is a agronomist specializing in CO_2 exchange of plants for offering plants samples in the experiments of CO emission from plant leaves. I owed to Dr. M. Morokuma in Kagawa university who is an agronomist specializing in plant physiology for the experimental set-up and analysis in plant experiments. I owed to many researchers in NIAES for interdisciplinary discussion. I am indebted to Professor Makide in the university of Tokyo and Dr. T. Machida in National Institute for Environmental Studies for the

improvement of oral presentation of this thesis. I owed to Mrs. I. Utagawa for official works through this study. I thank to the members of Division of Experimental Farm of NIAES for help in the field experiments and to many other members in NIAES for various helps.

Further, I could obtain up-to-date information from Dr. R. Conrad in Max-Planck Institute in Germany who is a pioneer microbiologist in terrestrial microbial uptake of trace gases including CO and H_2 by soil and Dr. G.M. King in Main University in U.S.A. who is a pioneer microbiologist in soil uptake of CH_4 , Dr. I. MacTaggart and Dr. B.C. Ball in Scottish Agricultural College who corrected English and contents of my second paper (Yonemura et al., 1999b) and who have novel works in soil science, and Dr. P.C. Novelli in NOAA/CMDL in U.S.A. who is a prominent atmospheric scientist specializing in atmospheric behavior of CO and H_2, and offered me his up-to-date manuscript (Novelli et al., 1999), during their short visits in Japan or in international conferences. The recent CO and H_2 concentration data at various world sites of Chapter 1 were owed to NOAA/CMDL (http://www.cmdl.noaa.gov/ccg). I can have information on H_2 cycles thankfully from Professors Ehhalt and Schmidt in Germany by letters and e:mails. I thank Environmental Institute of Metropolitan Tokyo for providing the surface data in Chapter 3. The quality of this study was highly improved by valuable and constructive suggestions from instructive anonymous referees in reviewing several papers submitted to journals.

This study is mainly supported mainly by the budgets of NIAES and partly by projects of Environmental Agency of Japan.

Lastly, I would like to pay thanks to my wife, Mayumi for her daily help and to my intimate friends for giving me advice when I was against obstacles during this study.

Contents

Chapter 1 Introduction 1
1.1 Preface 1
1.2 Global CO and H_2 sources 2
1.2.1 Formation from hydrocarbons in the atmosphere 2
1.2.2 Technological 3
1.2.3 Biomass burning 4
1.2.4 Ocean and water 5
1.2.5 Vegetation 5
1.2.6 Soils 6
1.3 Global CO and H_2 sinks 6
1.3.1 Reaction with OH radical in the atmosphere 7
1.3.2 Uptake by soils 8
1.4 Life time of CO and H_2 in the atmosphere 10
1.5 CO and H_2 distribution in the atmosphere 10
1.5.1 Long-term or secular trends of CO and H_2 concentrations 10
1.5.2 Distribution of CO and H_2 in the atmosphere 11
1.6 The objectives 13

Chapter 2 CO and H_2 concentrations at two heights above a grass field 22
2.1 Introduction 22
2.2 Methods 22
2.2.1 Instrumental 22
2.2.2 Micometeorological estimation of deposition velocity 23
2.3 CO and H_2 concentrations and micrometeorology near ground 25
2.4 Deposition of CO, H_2, and CH_4 to the grass field 27
2.5 Summary 29

Chapter 3 CO and H_2 measurements and methods to measure CO and H_2 uptake by soil 39
3.1 Introduction 39
3.2 Measurement of CO and H_2 39
3.3 Analysis of CO and H_2 by RGA3 40
3.4 Analysis of CO, CH_4, and CO_2 by GC-FID with a methanizer and GC-TCD or NDIR 41
3.5 Analysis of related gases--THC and light hydrocarbons 42
3.6 Methods to measure atmosphere-biosphere interaction of gases 43
3.7 Closed-chamber technique 44
3.8 Open-flow technique 46

Chapter 4 Field measurements of CO and H_2 uptake by soil 61
4.1 Introduction 61
4.2 Field description and experiments 62
4.2.1 Arable field 62
4.2.2 Forest 63
4.3 Measurements 64
4.3.1 Characteristics of the gas profiles in the soil 64
4.3.2 Continuous measurements by the OFT 65
4.3.3 Long-term measurements by the CCT 65
4.3.4 Measurements of $[CO]_{equiv}$ in the arable field 67

4.3.5 Measurements of factors on deposition velocities- soil temperature and moisture 67
4.3.5.1 During OFT measurements
4.3.5.2 During measurements by CCT
4.4 Results 69
4.4.1 Characteristics of the gas profiles in the soil 69
4.4.2 Deposition velocities continuously obtained by the OFT 70
4.4.3 Deposition velocities and production rates in the arable field obtained by CCT experiments 71
4.4.3.1 CO production from the arable soil
4.4.3.2 Variation in deposition velocities in the arable field
4.4.4 Deposition velocities and production rates in the forest obtained by CCT experiments 74
4.4.3.1 CO production from the forest soil
4.4.3.2 Variation in deposition velocities in the forest
4.5 Discussion 76
4.5.1 Differences in exchange between emitted and absorbed gases by soil 76
4.5.2 CO, H_2, and CH_4 deposition velocities 77
4.5.2.1 General
4.5.2.2 Soil moisture and deposition velocities
4.5.2.3 Soil temperature and deposition velocities
4.5.3 Differences in deposition velocities resulting from management practices in the arable field 82
4.5.4 Relationship between deposition velocities 84
4.5.5 CO production in soil 85
4.6 Summary 87

Chapter 5 Model analysis of CO and H_2 uptake by soil 119
5.1 Introduction 119
5.2 Model to soil uptake of CO and H_2 119
5.2.1 Diffusion model 119
5.2.2 Analytical solutions for a mono-layered model 123
5.3 Experiment to obtain model parameters, $u_{in\text{-}situ}$ and $P_{in\text{-}situ}$ in regard to soil temperature 124
5.4 Results 125
5.4.1 $u_{in\text{-}situ}$ and $P_{in\text{-}situ}$ 125
5.4.2 Calculations using experimental in-situ uptake and production rates 126
5.4.3 Calculations incorporating changes in in-situ uptake rates 127
5.4.4 Analysis of the contribution of the various factors affecting CO and H_2 uptake by soil 128
5.5 Discussion 128
5.5.1 Diffusion control of CO and H_2 uptake by soil 128
5.5.2 Factors affecting CO and H_2 uptake by soil 129
5.5.3 Relationship between deposition velocities of different gas species 131
5.6 Summary 132

Chapter 6 A process-based model to estimate global CO-, H_2-, and CH_4-uptake strengths by soils 145
6.1 Introduction 145
6.2 Data and model 145
6.2.1 In-situ uptake and production rates of CO, H_2, and CH_4 146
6.2.2 Dependence of in-situ uptake and production rates of CO, H_2, and CH_4

on soil temperature and moisture content 146
6.2.3 Surface environmental data 149
6.2.4 Atmospheric concentrations of CO, H_2, and CH_4 150
6.2.5 Global gross uptake and net uptake 150
6.2.6 Comparison of process-based models to estimate global uptake strengths of CO and H_2 151
6.3 Results and discussion 151
6.3.1 Global CO and H_2 uptake 151
6.3.2 Influence of global CO- and H_2- uptake by soil on global CO and H_2 concentrations 155
6.3.3 Global CH_4 uptake 156
6.3.4 Comparison of global CO-, H_2-, and CH_4- uptake and their changes under changes under global changes 157
6.5 Summary 158

Chapter 7 CO emission processes from vegetation 178
7.1 Introduction 178
7.2 Materials and methods 178
7.3 Results and discussion 180
7.4 Summary 182

Chapter 8 Production of CO and other carbon gases during combustion processes 190
8.1 Introduction 190
8.2 Material and methods 191
8.2.1 Closed-chamber experiments 191
8.2.2 Time-series experiments 192
8.2.3 Method for expressing gas emissions 192
8.3 Results 193
8.3.1 Estimation of gas emission in closed-chamber experiments 193
8.3.2 Time-series of gas concentrations in combustion plume 194
8.3.2.1 Case 1: efficient combustion
8.3.2.2 Case 2: inefficient combustion
8.3.3 Relationship between temperature, $ER_{CO2}(X)$ and THC, and time-series of $ER_{CO2}(X)$ 197
8.4 Discussion 197
8.4.1 $ER_{CO}(X)$ values from the closed-chamber experiments and comparisons with previous studies 197
8.4.2 Time-series of gas concentrations in the combustion plume and $ER_{CO2}(X)$ 199
8.4.3 Relationship between the results of the closed-chamber experiments and the time-series of gas concentrations 202
8.5 Summary 204

Chapter 9 Summary and further studies 226
9.1 Summary 226
9.2 Further studies 227
9.2.1 Soil uptake 227
9.2.2 CO photoproduction from vegetation 228
9.2.3 Biomass burning 229

References 230
Appendix 243

Chapter 1

Introduction

1.1 Preface

Recent changes in the concentrations of atmospheric constituents are conspicuous and social attention is concerned for their impacts on the global environment. Concentrations of some gases including greenhouse gases such as carbon dioxide (CO_2), methane (CH_4), and nitrous oxide (N_2O) are increasing rapidly as man increases its activity. Each nation is required to grasp her source and sink strengths of trace gases to control atmospheric concentrations of the gases.

Presence of carbon monoxide (CO) in the atmosphere was discovered by infrared measurement of solar radiation (Migeotte, 1949). CO is an insignificant greenhouse gas itself, but is related to greenhouse effect as well as nitrogen oxides and hydrocarbons. CO plays important roles in the tropospheric chemistry by regulating the concentration of OH which controls oxidation of reduced gases in the atmosphere. About 75% of the removal of OH is attributed to the reaction with CO (Thompson, 1992). Therefore, it is expected that if the CO concentration increases, more OH will be lost through the reaction with CO and less OH will be available for the reaction with reduced greenhouse gases such as CH_4. Actually, recent trends in CO and CH_4 concentrations are linked each other (Dlugokencky et al., 1994; Novelli et al., 1998). The atmospheric CO level increased consistently until 1980s (Zander et al., 1989; Novelli et al., 1998). In 1990s, the concentration increase ceased and a decrease was observed. Recent level of atmospheric CO is about 80-200 ppbv in the northern hemisphere and 40-60 ppbv in the southern hemisphere.

Among chemically-active trace gases in the atmosphere, molecular hydrogen (H_2) is the secondly most abundant. H_2O produced from H_2 is an important source of H_2O in the stratosphere. Recent atmospheric H_2 level is about 450-550 ppbv (Schmidt, 1974; Novelli et al., 1999). Concentrations in the northern hemisphere are lower than those in the southern hemisphere because of the H_2 uptake by soil in the northern hemisphere (Chapter 6).

To understand these trends of atmospheric CO and H_2 concentrations, atmospheric balances of these gases must be made clear. In particular, the influence of the biosphere on the concentration of CO and H_2 must be investigated because there are much uncertainties in the estimations of the biosphere source/sink strengths of the gases and their exchange mechanisms involved in the biosphere.

1.2 Global CO and H_2 sources

The sources of CO and H_2 have been considered to be similar (Tables 1.1 and 1.2). This is partly because both gases are reduced gases in the atmosphere. All the sources of CO and H_2, both anthropogenic and natural ones, can be related to oxidation processes of organic compounds. The uncertainty in the biospheric sources such as biomass burning, ocean, and vegetation is larger than that in the technological sources and the formation in the atmosphere.

1.2.1 Formation from hydrocarbons in the atmosphere

In the atmosphere, CO and H_2 are produced in a chain reaction from hydrocarbons. If the relevant hydrocarbon is expressed by RCH_3, the reactions leading CO and H_2 formation are:

$$RCH_3 + OH \rightarrow RCH_2 + H_2O \quad (1.1)$$

$$RCH_2 + O_2 + M \rightarrow RCH_2O_2 + M \quad (M=N_2, O_2) \quad (1.2)$$

$$RCH_2O_2 + NO \rightarrow RCH_2O + NO_2 \quad (1.3)$$

If R=H (methane),

$$CH_4 + OH \rightarrow CH_3 + H_2O \quad (1.4)$$

$$CH_3 + O_2 + M \rightarrow CH_3O_2 + M \quad (M=N_2, O_2) \quad (1.5)$$

$$CH_3O_2 + NO \rightarrow CH_3O + NO_2 \quad (1.6)$$

Formaldehyde is destroyed by either the reaction with OH or photolysis.

$$HCHO + OH \rightarrow HCO + H_2O \quad (1.7)$$

$$HCHO + h\nu \rightarrow H_2 + CO \quad (1.8a)$$

$$HCO + OH \quad (1.8b)$$

The formyl radical, HCO, rapidly reacts with O_2:

$$HCO + O_2 \rightarrow HO_2 + CO \quad (1.9)$$

Globally, the average yield of CO from CH_4 is about 0.82 molecules of CO per molecules of methane destroyed (Tie et al., 1992). From non-methane hydrocarbons (NMHC), CO is produced by 0.6 molecules per carbon number of non-methane hydrocarbons destroyed in the presence of NO_x and 0.23 molecules in the absence of NO_x , and the yield in the real atmosphere was evaluated as 0.3 molecules (Miyoshi et al., 1994). The pathways in reaction (1.8) forming H_2 depend on cross section, photon flux as a function of wavelength, and HCHO and OH concentrations. From CH_4, H_2 is formed by 0.3-0.4 molecules per CH_4 destroyed and from NMHC, H_2 is formed by 0.1-0.2 molecules per NMHC destroyed (Novelli et al., 1999).

1.2.2 Technological

CO and H_2 are emitted from various technological (anthropogenic) processes including fossil fuel combustion (Badr and Probert, 1995a). In most developed countries, motor vehicles represent a major source of CO and H_2. The CO emission rates from these combustion sources have been identified with relatively high certainty by employing data on fuel consumption and emission factors for various combustion processes. This source increases with the economical development accompanied by the vehicle-population growth.

1.2.3 Biomass burning

Biomass burning, namely combustion processes in the biosphere, is very important when considering CO and H_2 exchanges between the atmosphere and the biosphere as well as biogeochemical cycles (e.g., Crutzen and Andreae, 1990). Furthermore, in the combustion processes, CO is regarded as a key parameter to determine emissions of other trace gases such as greenhouse gases and ozone precursor gases.

Gas emission from biomass burning is characterized by combustion phases, flaming and smoldering. The transition time between the two phases is defined as the time when d[CO]/dt reaches a maximum (Crutzen and Andreae, 1990; Lobert et al, 1991). During the flaming phase, which appears first, combustion is efficient and CO_2 and nitrogen oxides are emitted. During the following smoldering phase, combustion is inefficient and CO and various hydrocarbons are emitted.

Generally, wet and high-density materials have a tendency for inefficient combustion. Savanna and agricultural residue fires burn with high combustion efficiency due to their low water content and/or low density. Forest fires, on the other hand, burn with low combustion efficiency due to the high water content of the material and/or little permeability of O_2, as well as by the high density of the fuel.

The emission of hydrocarbons is roughly related to the emission of CO (inefficient combustion). CH_4 production relative to combustion efficiency from biomass burning is higher in forests with little duff, while it is lower in savannas, agricultural residues, pine needles, pine forest litter, chaparral, and wetlands (Delmas et al., 1991; Hao and Ward, 1993). Nguye et al. (1994) measured CO, CO_2, and OCS in the air mass from the combustion of rice straw in the wet and dry seasons, and concluded that rice straw combustion produces much more CO and OCS than other known biomass sources. Emissions of individual non-methane hydrocarbon species are, in general, positively correlated with the ratio of carbon monoxide concentration to CO_2 concentration in excess of background atmospheric concentration, $[CO]/\Delta[CO_2]$ (Cofer et al., 1989; Lobert et al., 1991; Laursen et al., 1992). However, Bonsang et al. (1995) suggested that major hydrocarbons are not produced simultaneously with CO. CO and H_2 are produced in the numerous reactions in the combustion processes. In biomass burning, CO is a secondary last product of oxidation reactions. CO

and H_2 are well emitted under incombustion conditions which are expected in the burning of wood.

CO and H_2 emissions from biomass burning occupy about 30-40% of CO and H_2 budgets (Tables 1.1 and 1.2). It should be noted that climate or social conditions influence the activity of biomass burning; the annual global emissions from the biomass burning vary greatly ; some studies (e.g., Novelli et al., 1998, 1999) mentioned that recent decrease in CO and H_2 concentrations be due to the decrement in the activity of biomass burning.

1.2.4 Ocean and water

CO and H_2 are emitted from photo-oxidation of organic matters in ocean and water. In ocean (Swinnerton and Lamontagne, 1974; Conrad et al., 1982; Johnson and Bates, 1996; Matsueda et al., 1997) or in wetlands (Moxley and Smith, 1998b), both CO and H_2 are supersaturated under daylight at the equilibrium concentration of ~10 ppmv. In a similar way in soil (see 1.3.2), the equilibrium concentration in water is determined on the net balance between photochemical or algal production (Troxler and Dokos, 1973; Conrad et al., 1982), and microbial (single bacterial cells) consumption (Conrad et al., 1982). Due to their gradients CO and H_2 are emitted to the atmosphere. However, the H_2 concentration in ocean is relatively low at 1-10 ppm levels, because H_2 is rapidly oxidized by microbial processes.

Although large area of the earth surface is covered by ocean, the CO and H_2 emissions from this source seem to be small. Bates et al. (1995) estimated CO emission from ocean to be 13 Tg yr^{-1}; Moxley and Smith (1998b) estimated CO emission from wetlands in the northern hemisphere to be 0.2 Tg yr^{-1} .

1.2.5 Vegetation

Until recently, vegetation has been considered to have a minor roll in the atmospheric budget of CO. Also note that plants do not directly exchange H_2. Under dark conditions, CO is reported to be metabolized by plants. Bidwell and Fraser (1972) showed that CO uptake rates by plants were roughly proportional to the CO concentration in the surrounding air. High concentration of ambient CO is useful to keep vegetable fresh (Peiser et al., 1982).

Previous studies agree on a level of CO emission from plant leaves under light at the ambient atmospheric CO concentration. Two mechanisms have been proposed for CO

photoproduction in plant leaves: one is as a by-product of photorespiration (Fischer and Lüttge, 1978; Lüttge and Fischer, 1980), and another is as a product of the photodegradation of plant cellular material, including porphyrin (Troxler and Dokos, 1973; Bauer et al., 1980; Tarr et al., 1995).

Lüttge and Fischer (1980) reported that light-dependent CO production rate by green leaves of C_3 and C_4 plants depends on the CO_2/O_2 ratio in the ambient atmosphere by laboratory experiments. They concluded that photoproduced CO is a by-product of photorespiration.

Tarr et al. (1995) showed that CO is emitted through stomata. Further, they showed that senescent leaf matter photoproduced CO at rates 1.3–5.4 times higher than green leaves per unit area. They concluded that formation of CO was the result of direct photochemical transformation on or in the plant matter.

Previous studies (Seiler and Conrad, 1987; Khalil and Rasmussen, 1990a) estimated that direct CO emission from living plants to be 50-200 Tg yr^{-1}. Tarr et al. (1995) additionally estimated global CO emission from dead plant matters to be 60-90 Tg yr^{-1}.

1.2.6 Soils

H_2 is released as a by-product from biological N_2 fixation in the roots of *Legumes* as clover (Conrad and Seiler, 1980a). However, this source is considered to be little (2-5 Tg yr^{-1}) in the global budgets. This is far smaller than H_2 uptake by normal soils.

CO is thermally produced in soil from organic matters (Conrad and Seiler, 1985b; Moxley and Smith, 1998b). The production of CO in soil has been mentioned in previous global estimates independent from soil uptake. However, this is not reasonable because production and consumption occur simultaneously in soil and are interactive each other. Hence, this production is described later, together with the uptake by soil section (1.3.2).

1.3 Global CO and H_2 sinks

The reaction with OH radicals in the atmosphere and soil uptake are sinks of atmospheric CO and H_2. Transition of global CO uptake strengths estimated by previous studies is summarized in Table 1.3. Although previous studies listed CO uptake strengths by soil, most

of estimations are almost copies from preceding studies. Large uncertainty exists in the CO uptake by soil and much more strenuous efforts are needed to reveal fundamental mechanisms in it. The uncertainty in H_2 soil uptake strengths by soil is larger than sink strengths by the reaction with OH, which can be determined photochemically.

1.3.1 Reaction with OH radicals in the atmosphere

The sink reactions of CO and H_2 with OH radicals (Fishman and Crutzen, 1978; Logan et al., 1981; Thompson, 1992) are:

$$CO + OH \rightarrow CO_2 + H, \quad (1.10)$$

$$H_2 + OH \rightarrow H_2O + H. \quad (1.11)$$

Furthermore, in the troposphere, eqs. 1.10 and 1.11 lead to the formation of tropospheric O_3 through the following reaction under the condition of NO_x>30pptv. This level of NO_x is expected in the continental air masses.

$$H + O_2 + M \rightarrow HO_2 + M \quad (1.12)$$

$$NO + HO_2 \rightarrow NO_2 + OH \quad (1.13)$$

$$NO_2 + h\nu \rightarrow NO + O(^3P) \quad (1.14)$$

$$O(^3P) + O_2 + M \rightarrow O_3 + M \quad (1.15)$$

Under the lower level of NO_x expected in the marine air masses, O_3 is destroyed by reactions after eq. (1.12).

$$HO_2 + O_3 \rightarrow 2O_2 + OH \quad (1.16)$$

Tropospheric O_3 is a greenhouse gas. CO is thus related to greenhouse effect through the chemical reactions in the atmosphere.

The CO and H_2 accumulated in the troposphere are transported to the stratosphere,

and also destroyed by the reaction with OH (eqs. 1.10 and 1.11). Equation (1.11) is a stratospheric source of water vapor which is a strong greenhouse gas in the stratosphere and play an important role in the stratospheric atmosphere.

1.3.2 Uptake by soil

Uptake of CO and H_2 by soil is caused by the oxidation of the gases by soil bacteria or enzymes, as shown by carbon radioactivity experiments (Bartholomew and Alexander, 1982; Duggin and Cataldo, 1985). Various bacteria oxidize CO (Bédard and Knowles, 1989; Bender and Conrad, 1994a; Conrad, 1996). Among them, nitrifiers are reported to be the most powerful oxidizers of atmospheric CO (Jones and Morita, 1983; Conrad, 1988; Moxley and Smith, 1998a). Conrad (1988) concluded that *Nitrosomonas* species are the actual oxidizers of CO at atmospheric levels, and Bender and Conrad (1994a) showed that CO was oxidized by various types of bacteria such as carboxydotrophs, methanotrophs, and nitrifiers. CO is used as a source of energy and not as a subtrate of cell constituents. H_2 is utilized by Knallgas bacteria under the concentration greater than 1 ppmv (Schuler and Conrad, 1991). H_2 consumption by soil under atmospheric concentration level (0.5 ppmv) is thought to be due to extracellular enzymes in the soil (Conrad et al., 1983).

Generally, it depends on the balance between production and uptake by the soil whether gases are absorbed by or emitted from soil. The production obeys a zero-order kinetics whereas uptake obeys a first-order kinetics with respect to gas concentration. If there is no transport of the gas in the soil, the compensation (equilibrium) concentration of the gas in the soil, C_{eq}, is determined by the balance between the in-situ uptake rate on the spatial base, $u_{in\text{-}situ}$ (s^{-1}), and the in-situ production rate on the spatial base, $P_{in\text{-}situ}$ (s^{-1}) as follows:

$$C_{eq} = \frac{P_{in\text{-}situ}}{V_a u_{in\text{-}situ}} \tag{1.17}$$

where V_a is air-filled porosity (volumetric content of gas phase, dimensionless) (see Chapter

5 for the detailed formulations). The gas is emitted from the soil when $C_{eq} > C_{atm}$ (atmospheric concentration), while the gas is absorbed by the soil when $C_{eq} < C_{atm}$. H_2 production rates in aerated soils are low, and C_{eq} is much smaller than C_{atm}..

For CO, processes of production and uptake occur simultaneously in soil. CO is thought to be produced abiologically from organic-matter (Conrad and Seiler, 1985b; Moxley and Smith, 1998b). The absolute value of the activation energy of CO production is higher than that of the uptake rate. So when the temperature is higher, the compensation concentration of CO is higher. In temperate regions, CO is generally absorbed by soil (Liebl and Seiler, 1976; Conrad and Seiler, 1980b; Moxley and Smith, 1998a; Sanhueza et al., 1998). During the daytime in arid, tropical (Conrad and Seiler, 1985a; Scharffe et al., 1990; Sanhueza et al., 1994a, b; Zepp et al., 1996) or forested regions (Zepp et al., 1997), where surface-soil temperature and/or carbon content is higher and/or uptake activity is less, the CO compensation concentration in surface-soil is greater than the atmospheric concentration, and CO is released to the atmosphere

Model calculations of Volz et al. (1981) using isotope fractionation of ^{12}CO and ^{14}CO, resulted in a global uptake strength of CO by soils of 320 Tg yr^{-1}. Seiler and Conrad (1987) suggests that the CO consumption by soils within humid tropical area (i.e., tropical forests and grasslands) is 105±35 Tg yr^{-1}, with a total global uptake strength of 390±140 Tg yr^{-1}, by extending a deposition-velocity value of 0.02 to 0.04 cm s^{-1} over all ecosystems. However, Potter et al. (1996a) estimated the global uptake strength to be 16-50 Tg yr^{-1} which is much smaller value than that by Seiler and Conrad (1987). The model by Potter et al. (1996a, b) used a modified version of Fick's first law based on computation for diffusivity in aggregated media, together with a bucket model to obtain soil moisture. In contrary to this, Sanhueza et al. (1998) estimated global gross CO uptake by soils to be 115-230 Tg yr^{-1}, extrapolating similar deposition velocity value over all ecosystems. The differences among previous studies are partly due to different estimation of the atmospheric boundary concentration of CO (see 1.4). The estimation of global uptake strength of CO by soils is under progress (Table 1.3, Chapter 6).

The global sink strength of H_2 by soils has been estimated only by extrapolation from European and African soil data (Liebl and Seiler, 1976; Conrad and Seiler, 1980a; Seiler and Conrad, 1987). The estimation of the global H_2 sink strength, 80-110 Tg y^{-1} (Seiler and

Conrad, 1987) is not consistent with those estimated from isotopic evidence (10-70 Tg yr^{-1}; Ehhalt et al., 1989; Ehhalt, 1999) (Table 1.2). There is a large gap between these two estimations for H_2.

According to recently published reports on carbon monoxide uptake in the forest (Zepp et al., 1997; Kuhlbusch et al., 1998; Sanhueza et al., 1998), the net uptake of CO in the forest is repressed by the high organic-matter content of the soil. Moreover, the leaf layer on the soil surface plays important role by resisting CO gas diffusion from the atmosphere into the soil much more than it does for CH_4 (Dong et al., 1998; Sanhueza et al., 1998). However, other reports (Hendrickson and Kubiseski, 1991; Moxley and Smith, 1998a) show that CO uptake rates of soil samples correlate positively with organic-matter content of the soil, and that forest soil therefore has a high potential to absorb CO.

1.4 Lifetime of CO and H_2 in the atmosphere

Tropospheric CO and H_2 burdens are approximately 360 and 150 Tg integrating the atmospheric concentrations, respectively (Ehhalt, 1999). We can calculate their tropospheric mean lifetime to be 1.5 months and 2.3 years, respectively. Their local lifetimes vary with season, latitude, and local source and sink strengths. During the winter, at high and middle latitudes, CO has a lifetime of more than a year, but during the summer at mid-latitudes, the lifetime may be closer to the average global value.

1.5 CO and H_2 distribution in the atmosphere

1.5.1 Long-term or secular trends of CO and H_2 concentrations

From the long term record of the CO column abundance above the Jungfraujoch derived from solar infrared spectra, Zander et al. (1989) deduced that a mean relative increase between 1950 and 1985 is (0.85±0.20)% yr^{-1} and that the increase coincided with the increase of anthropogenic contributions. Khalil and Rasmussen (1988) measured the CO concentration at 6 sites located in both hemispheres by the flask-sampling method, and derived rates of increase from 1978 to 1988 equal to 1.4% yr^{-1} in the northern hemisphere and 0.8% yr^{-1} in the southern hemisphere. After the proceeding years, they reported a decreasing trend in recent

years (Khalil and Rasmussen, 1994; Novelli et al., 1994). It should be noted that these trends in CO concentration are related to those in CH_4 through the chemical reactions in the atmosphere: the global CH_4 increase rate decreased from +14ppbv yr^{-1} in 1983 to +10 ppbv yr^{-1} in 1990, and it was a temporary as low as 0 ppbv yr^{-1} in 1992 (Dlugokencky et al., 1994). In other words, the concentration level of CO is important to estimate the oxidizing capacity of atmosphere. Global decrease in CO seems to be continuing, but the decreasing rate may be decelerated, and recently maintains an almost constant level.

Khalil and Rasmussen (1990b) deduced a global increase rate in the H_2 concentration of 0.6±0.1% yr^{-1}. In the late 1980s the increasing trend in H_2 reversed to a decrease, just like that observed for CO (Ehhalt, 1999). There are other data in 1960s and 1970s (Schmidt, 1974; Schmidt, 1978) and 0.5 ppmv in old times in 1923 (Warneck, 1988). However, because of the problems of standard gas scale and its stability, systematic trends cannot be obtained from these data. Recent trend in H_2 concentration (Novelli et al., 1999) is a decrease, in the marine boundary layer at a global rate of 2.3±0.1 ppbv yr^{-1} (0.4% yr^{-1}), or maintained a certain level.

Because of its reactivity and permeability, CO and H_2 at prehistoric times cannot be measured by glacial evidence, different from CH_4. However, from the balance of sources and sinks, pre-industrial level of atmospheric CO is estimated to be 30-50 ppbv, half as present level (Khalil and Rasmussen, 1994); pre-industrial level of atmospheric H_2 is estimated to be as low as 200 ppbv (Khalil and Rasmussen, 1990b).

1.5.2 Distribution of CO and H_2 in the atmosphere

In the continental air masses, vertical gradients exist for CO and H_2, which are influences by local sources or sinks (Fig. 1.1). H_2 concentrations in the boundary layer were lower in the clean continental air masses than the free tropospheric concentrations, probably because of uptake by soil.

The strong latitudinal gradient in CO concentration (Fig. 1.2) indicates that CO is transported from the northern mid-latitudes to the tropics and the southern hemisphere. High CO concentrations in the northern hemisphere (e.g., Seiler and Fishman, 1981; Yonemura and Iwagami, 1996) is due to large anthropogenic sources on land surfaces. In contrary to CO, the atmospheric concentration of H_2 is lower in the northern high-latitudes (Novelli et

al., 1999). The inter-hemispheric difference in H_2 concentration is about 3%.

The seasonal variation of CO at high-latitudes in both hemispheres (Fig. 1.3) is , to a large extent , caused by the seasonal variation of the CO removal rate by the reaction with OH. As a consequence, the CO concentration shows a minimum in late summer, i.e., August-September in the northern hemisphere and February in the southern hemisphere, despite the fact that some of the sources of CO also show a summertime maximum, viz., the atmospheric oxidation of CH_4 and NMHC. Although the absolute amplitude differs greatly, the relative amplitudes are nearly the same at northern and southern hemisphere about 25-30%. Seasonal variation of CO in the southern hemisphere seems sinusoidal, with additional modulation in the northern hemisphere.

The spatial and temporary distributions of H_2 in the troposphere are more uniform than those of CO, reflecting longer life time of H_2 in the atmosphere. The seasonal trends of H_2 could be explained by the seasonal variation of OH. The seasonal variation of H_2 concentration in the norther hemisphere showed an expected variation, high in late winter and low in late summer, which was similar to the seasonal variations of CO and CH_4. The seasonal variation of H_2 in the southern hemisphere, however, is nearly in phase with that in the northern hemisphere, in contrast to observed seasonal variations of CO and CH_4. This might be attributable to the seasonal variation in soil uptake strength of northern hemisphere (see Chapter 6).

The trends in CO and H_2 concentrations on land are much more complex and inhomogeneous than those in background regions because they are influenced by local sources and sinks. Recent trends in CO at several sites are shown in Fig. 1.4. Seasonal variations can be seen at these sites. Although continental air masses are inhomogeneous, CO concentrations in the Eurasian Continent seems be larger than those in the North American Continent. In Europe and Ease Asia (Korea), CO concentrations were high probably due to the anthropogenic sources. Generally, in northern mid-latitudes, concentrations in the west side of continents tend to be low while those in the east side of continents tend to be high because of prevailing westerly wind which conveys polluted air masses.

Recent trends in H_2 concentration (Fig. 1.5) on land show low values at central continental sites whose seasonal variations were larger than those at marine background sites; at Utah and Ulaan Uul, minimum values were as low as 400 ppbv. This should be attributed

to the uptake by soil (Chapter 6). At some sites (e.g., Malta Mediterranean), seasonal variations were different from those at normal background sites. This may exhibit geographical distribution of sources and sinks and may be influenced by local circulation (memory of air masses).

Please note that the data at these sites are not representative of mean values in the continents because these sites were selected because the influence of pollution resulting from human activities is relatively small.

1.6 The objectives

To understand the atmospheric balance of CO and H_2 on the global scale, more knowledge on the mechanisms involving the exchange between the atmosphere and the biosphere is needed.

Here, the objectives of this study are as follows:

1, To make clear the processes and key factors regulating CO and H_2 exchange between the atmosphere and biosphere such as biomass burning, vegetation, and soil uptake. More precise understanding of CO and H_2 uptake processes by soils are needed because such measurements of CO and H_2 uptake by soil are few except those in Europe and Africa, and because it is only a sink of the two gases except the reaction with OH. These two sinks are competitive but uncertainty in their strengths are large. Especially, this study aims at the understanding of CO and H_2 uptake by soil from the atmosphere into soil, because this process has been ignored so far.

2, To model these processes and to simulate global uptake strengths of CO and H_2 by soil in order to fill the gaps among previous estimations. By the simulation, the global sink strengths by soils can be estimated and the global budget of CO and H_2 can be revised. These up-to-date estimations will be reflected in the understanding of the present trends in CO and H_2 concentrations in the atmosphere.

Table 1.1 Global budget of CO in the troposphere from previous studies

	Volz et al. (1981)	Seiler and Conrad (1987)	WMO (1995)	Ehhalt (1999)
		SOURCES		
Technological	640	640±200	440	440
Biomass burning	300-2200	1000±600	660	770
Methan oxidation	600-1300	600±300	210	600
NMHC oxidation	200-1800	900±500	790	800
Vegetation	50	75±25	80	75
Ocean	100	100±90	150	50
Total	2800±300	3300±1700	2330	2800±1000
		SINKS		
Oxidation by OH	1650-3550	2000±600	2000	2400
Uptake by soils	320	390±140	400	400
Total sinks	2800±800	2500±750	2400	2800

Table 1.2 Global budget of H_2 in the troposphere from previous studies

	Seiler and Conrad (1987)	Warneck (1988)	Ehhalt (1999)	Novelli et al. (1999)
		SOURCES		
Technological	20±10	17	20±10	16±10
Biomass burning	20±10	15	10±5	16±5
Methan oxidation	15±5	29	15±5	26±9
NMHC oxidation	25±10	21	20±10	14±7
Biogenic N_2 fixation	3±2	3	3±2	3±1
Ocean	4±2	4	3±2	3±2
Total	87±38	89	71±20	78±16
		SINKS		
Oxidation by OH	8±3	11	25±5	19±5
Uptake by soils	90±20	78	40±30	55±40
Total sinks	98±23	89	65±30	74±40

Table 1.3 Estimation of CO sinks from previous studies.
This table is obtained by adding recent estimation to a Table (Badr and Probert, 1995b)

Reference	Reaction with OH	Uptake by soil	Stratospheric inputs
Seiler (1974) Seiler and Schmidt (1974)	1940-5000	450	110
Seiler (1976)	-600	450	110
Zimmerman et al. (1978)	1390-4870	450	110
Freyer (1979)	2700-5000	500	110
Volz et al. (1981)	1650-3550	320	
Logan et al. (1981)	1600-4000	250	
Seiler and Warneck (1972)	2054	318-636	
Gammon et al. (1986) McElroy and Wofsy (1986)	1213-2613	257	
Seiler and Condrad (1987) Conrad and Seiler (1985a)	1400-2600	250-530	80-140
Khalil and Rasmussen (1990a)	2200	250	100
Fung et al. (1990)	3170	250	
Bouwman (1990)	1600-4000	190-580	170
Crutzen and Zimmermann (1991)	2050	280	
Potter et al. (1996a)		15-50	
Sanhueza et al. (1998)		115-230	
Ehhalt (1999)	2400	400	

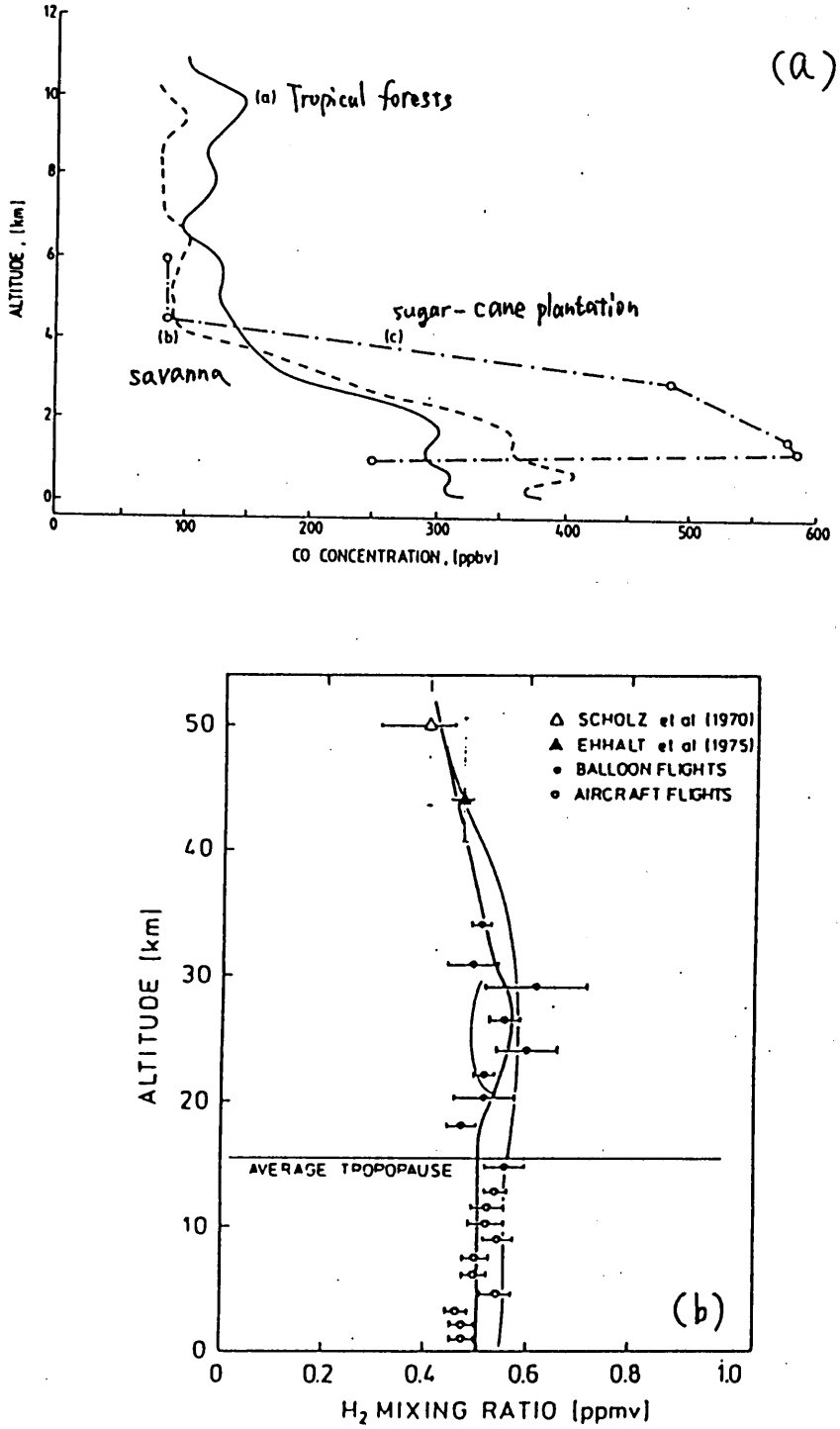

Figure 1.1 Vertical distribution of (a) CO in Brazil from Crutzen et al. (1985) and Kirchhoff et al. (1991) and (b) H_2 from Ehhalt and Schmidt (1977).

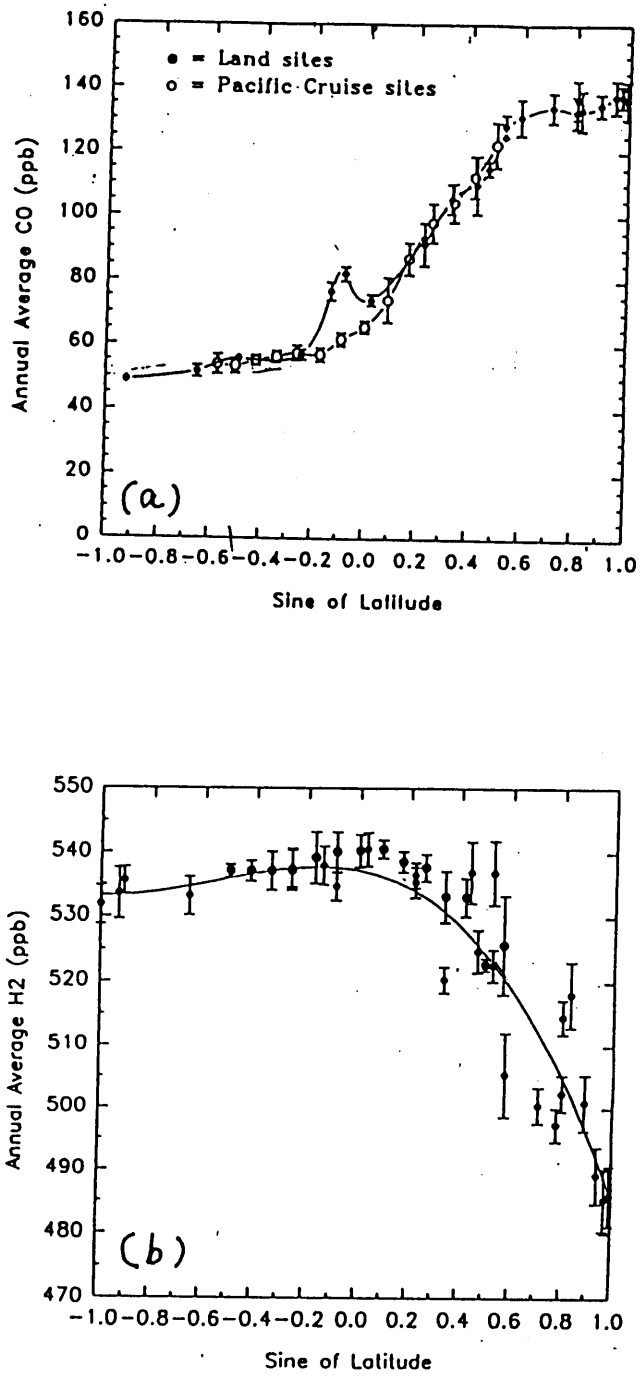

Figure 1.2 Latitudinal distribution of (a) CO and (b) H_2 (Novelli et al., 1998, 1999)

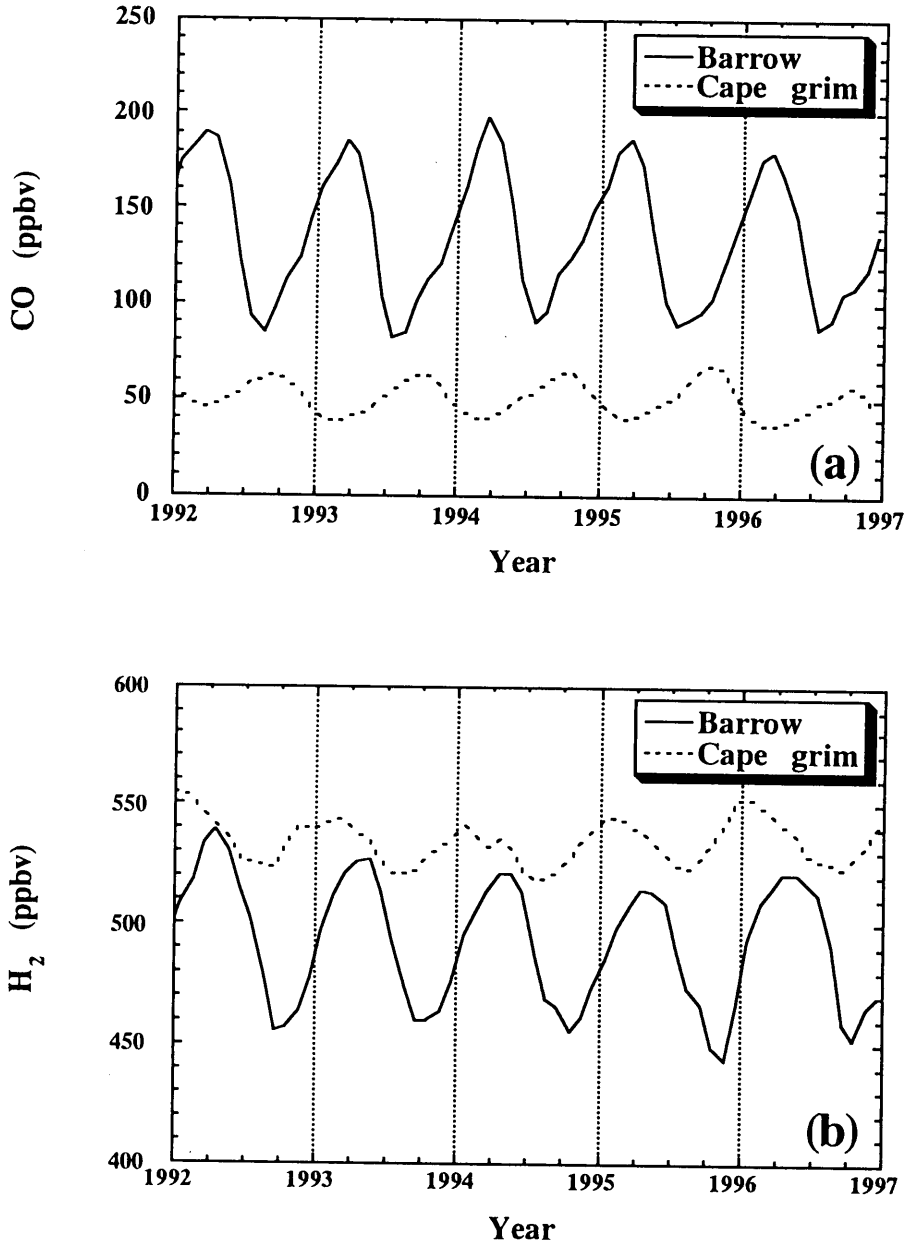

Figure 1.3 Seasonal trends in (a) CO and (b) H_2 in recent years at Barrow (71°19'N, 156°36'W) and at Cape Grim, Tasmania Australia (40°41'S, 144°41'E). Data are monthly values derived from weekly data (Novelli et al., 1998, 1999).

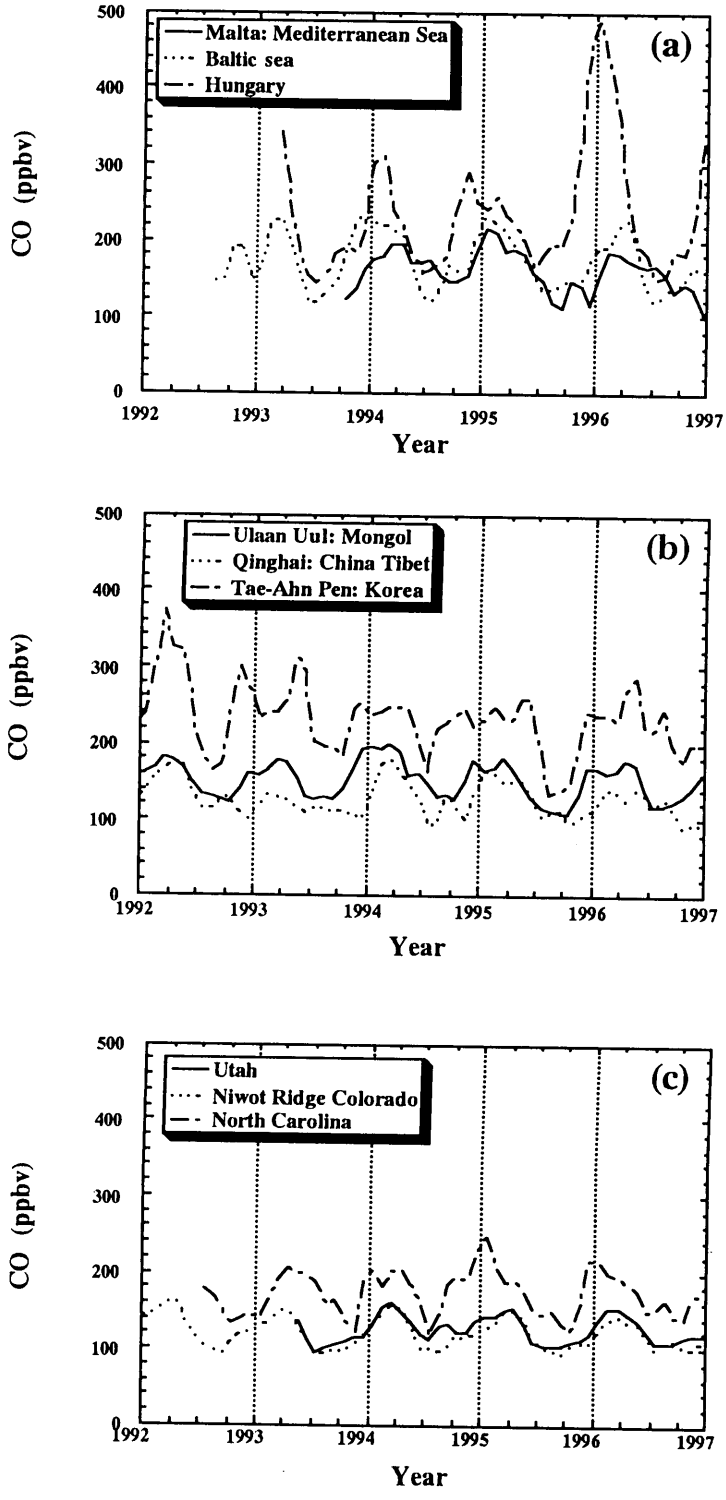

Figure 1.4 CO concentration trends at land sites (Malta: 36°03'N 14°11'E, Baltic sea: 55°30'N 16°40'E, Hungary: 46°58'N 16°23'E , Ulaan Uul: 44°27'N 116°06'E, Qinghai China: 36°16'N 100°55'E, Tae-Ahn Pen Korea: 36°44'N 126°08'E, Utah: 39°54'N 113°43'W, Niwot Ridge Colorado: 40°03'N 105°35'W, North Carolina:35°21'N 77°23'W). Data were from web sites (Novelli et al., 1998).

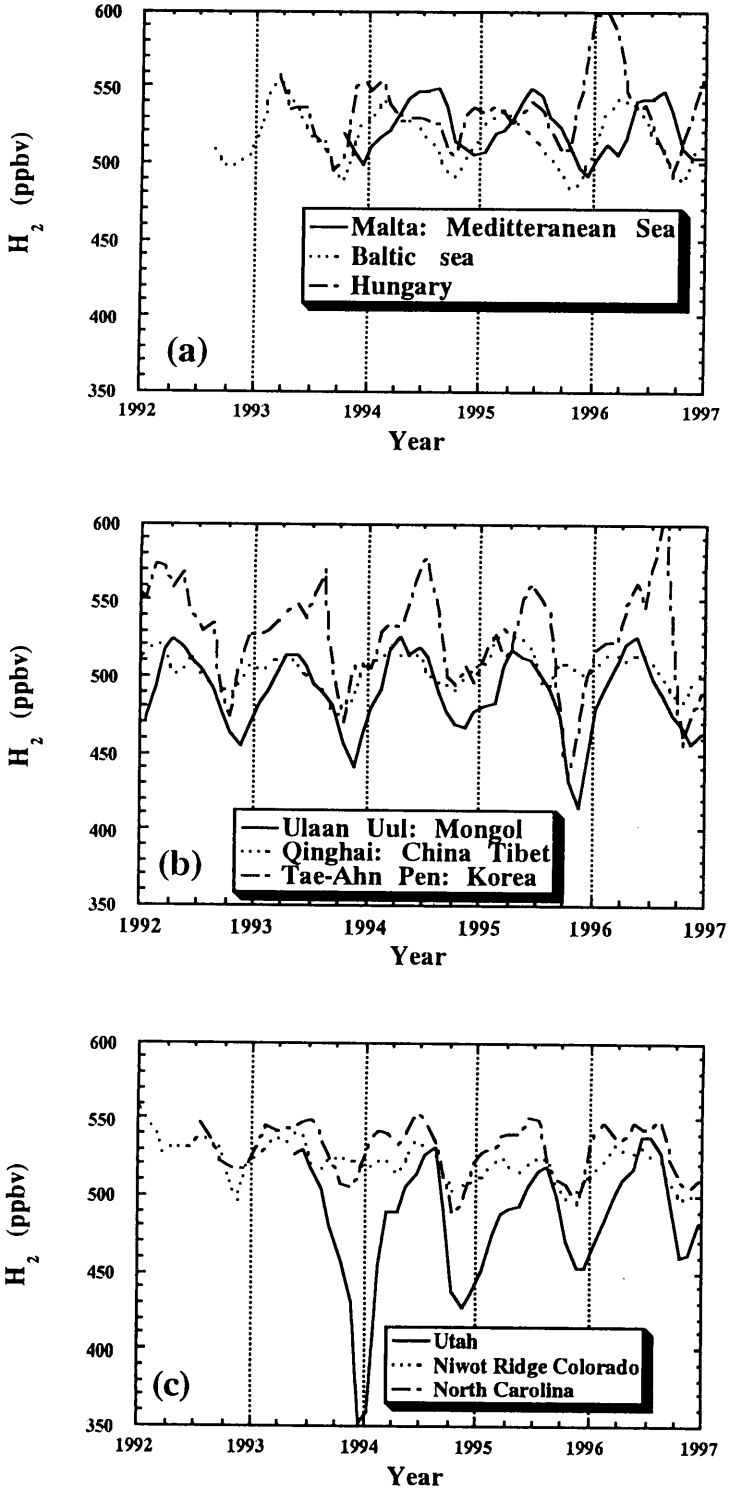

Figure 1.5 H_2 concentration trends at land sites. Data were from web sites (Novelli et al., 1999). A minimum in H_2 concentration at Utah reflects two very small concentration data.

Chapter 2

CO and H_2 concentration at two heights above a grass field

2.1 Introduction

Concentration difference above fields could be one information on the soil uptake of gases. When a gas is absorbed by soil, the concentration at a lower height should be lower than that at a higher heights. This Chapter reports the concentrations of CO, H_2, (and CH_4) at two heights above a grass field in NIAES (Yonemura et al., 2000b). Furthermore, deposition velocities of the gases were calculated by micrometeorological technique.

2.2 Methods

2.2.1 Instrumental

Observations of CO and H_2 concentrations were carried out from 21 November to 26 December 1994 in a grass field in the campus of National Institute of Agro-Environmental Sciences (NIAES) (150 m east-west and 100 m north-south) to investigate the variation pattern in the CO concentration on lands (Photo 2.1). No mineral fertilizers have been applied since the application (N, P, K = 11.5, 11.5, 11.5 kg ha^{-1}) on 14 October 1992. The vegetation coverage was almost 100%, and the dominant species was clover. Plants were cut short about every month during their growing season, but the cut biomass was not removed from the site. The grass height of the field was about 5 cm during the measurements. Sunny days continues during the measurement periods.

Air inlets and micrometeorological sensors were mounted on a mast at the center of the grass field. Two gas inlets with Teflon® filters were mounted on the mast at heights of 0.33 and 1.30 m. Sampled air was drawn through a 50-m length of 10-mm ϕ Teflon® tube and a 15-liter Teflon-coated buffer, then pumped to an air-conditioned laboratory building at

a flow rate of 15 liter min^{-1}. The air sampled from each of the 2 heights was selected in turn at 3-minute intervals by switching solenoid valves. Selected air was analyzed for CO, H_2, CH_4, and CO_2 concentrations (see Chater 3). At the laboratory building RGA3 system was installed. The analysis of CO and H_2 was conducted at the interval of 3 min by turns for the two gas sample lines. Absolute concentrations of CH_4 at the 2 heights were measured with an non-dispersive infrared (NDIR) analyzer (GA-360E; Horiba Ltd., Kyoto, Japan), while another NDIR analyzer was used to measure differences in CH_4 concentrations between the 2 heights (Miyata 1998). Uncertainties in the absolute concentration of CH_4 and differences between CH_4 concentrations were estimated to be 5 and 2 ppbv, respectively, on the basis of 30-minute averages. The CH_4 analyzer was calibrated several times during the measurements using cylinders of high-grade air and 4.0 ppmv CH_4 in air (Takachiho Chemical Industry Co. Ltd., Japan). CO_2 concentrations were measured using an NDIR CO_2 analyzer (VIA-510, Horiba Ltd., Kyoto, Japan) calibrated once a day using cylinders of pure N_2 and 480 ppmv CO_2 in N_2 (Takachiho Chemical Industry Co. Ltd., Japan).

Three components of wind speed were measured with a sonic anemometer (DA-600; Kaijo, Tokyo, Japan) installed on the mast at a height of 0.74 m. Variations in CO_2 and H_2O concentrations were measured using an open-path fast response infrared gas analyzer (E009; Advanet Inc., Okayama, Japan) installed at the same height as the sonic anemometer. The data from the sonic anemometer and the infrared gas analyzer were sampled at 10 Hz and recorded. Friction velocity, sensible and latent heat fluxes, and CO_2 flux were calculated by the eddy correlation method from the covariance between the vertical wind speed and corresponding scalar quantities. Several corrections required were applied such as coordinate rotation (Tanner and Thurtell, 1969), corrections for path length averaging of the sonic anemometer and the gas analyzer, and for the separation of the 2 sensors (Moore, 1986; Leuning and Moncrieff, 1990). The present study also applied corrections for density fluctuations that arise from fluctuations of temperature and water vapor (Webb et al., 1980); these are necessary for the use of the open-path gas analyzer.

2.2.2 Micometeorological estimation of deposition velocity

Deposition velocities of gases can be estimated from concentrations at two heights above fields with micrometeorological measurements. There are several sub-techniques in

micrometeorological technique.

First sub-technique employed in this study is gradient technique. Deposition velocity that is important in studying soil uptake of CO and H_2, was estimated by using basic equations in micrometeorology. From the Monin-Obukhov similarity theory, an integrated relationship between the gas flux and the concentration gradient of the gas is expressed as follows (Miyata et al. 2000):

$$\frac{\kappa u_*(CN_2 - CN_1)}{-F_n} = \int_{\zeta_1}^{\zeta_2} \frac{\phi_C}{\zeta} d\zeta \qquad (2.1)$$

where F_n is the gas flux (molecules m^{-2} s^{-1}), CN is the number density of the gas (molecules m^{-3}), u_* is the friction velocity (m s^{-1}), ζ is the Monin-Obukhov stability parameter (= z/L, where z is the height above the ground and L is the Monin-Obukhov length), ϕ_c is the universal function for mass transfer, κ is von Karman's constant (0.4), and subscripts 1 and 2 represent the values at the lower (= 0.33 m) and upper height (= 1.30 m), respectively. The values for u^* and ζ were obtained by the eddy correlation method. Based on the results of previous field studies over short vegetation, ϕ_c is assumed to be equal to the universal function for heat transfer ϕ_h (Denmead, 1994). The value of ϕ_h was cited from previous studies (Dyre and Hicks, 1970; Webb, 1970).

F_n, CN_1, and CN_2 are expressed by (net) deposition velocity, v_{nd}, and the volume mixing ratios (ppbv) of the gas, C_1 and C_2:

$$F_n = -\rho C_0 v_{nd} \qquad (2.2)$$

$$CN_1 = \rho Conv\ C_1; \qquad CN_2 = \rho Conv\ C_2 \qquad (2.3)$$

where ρ is the number density of air (molecules m^{-3}), $Conv$ is a mass conversion factor from air to the gas and C_0 is CO volume mixing ratio (ppbv) at the soil surface. Equation (2.2)

implicitly incorporates the first-order kinetics of CO, H_2, and CH_4 uptake by soil bacteria (e.g., Bender and Conrad, 1994a, b; Conrad and Seiler, 1980a, b). From eqs. (2.1) to (2.3), v_{nd} is obtained by:

$$v_{nd} = \frac{ku_* \dfrac{C_2 - C_1}{C_0}}{\displaystyle\int_{\zeta_1}^{\zeta_2} \frac{\phi_c}{\zeta} d\zeta} \cong \frac{ku_* \dfrac{C_2 - C_1}{C_1}}{\displaystyle\int_{\zeta_1}^{\zeta_2} \frac{\phi_h}{\zeta} d\zeta} \qquad (2.4)$$

The value of C_0 is replaced by that of C_1 (in the second part of this equation) because the concentration at the soil surface is cannot be measured. Following previous publications, the rate of CH_4 deposition is expressed by the flux density (ng CH_4 m^{-2} s^{-1}) rather than by deposition velocity itself. The CH_4 influx was calculated from the deposition velocity, assuming the CH_4 concentration to be 1800 ppbv.

Second sub-technique employed in this study is a method that uses CO_2 as a tracer (Miyata et al., 2000):

$$F = Conv \frac{C_2 - C_1}{[CO_2]_2 - [CO_2]_1} F_{CO2} \qquad (2.5)$$

where *Conv* is a mass conversion factor from CO_2 to the gas in question and F_{CO2} is the CO_2 flux. This method assumes that ϕ_c functions for CO, H_2, CH_4, and CO_2 in eq. (2.1) are all equal each other, and hence no stability corrections to the flux estimates are required.

2.3 CO and H_2 concentrations and micrometeorology near ground

During the measurement period, slight precipitations of 2.5, 1.0, 2.0, and 1.0 mm were recorded on 11, 12, 13, and 14 December, respectively. This range of slight precipitation is considered to have little effect on the changes in soil moisture, which controls gas diffusion

in soil (see Chapter 4). After 12 December, nocturnal temperatures of soil and air at 0.33 m show a decreasing trend (Fig. 2.1a). During the measurements, northwesterly winds prevailed due to the influence of a continental anti-cyclone, as is often the case in Japan in winter. Wind speed often exceeded 5 m s^{-1} (Fig. 2.1b). The measurement site was not subject to direct pollution from Tokyo (population 10 million) under the prevailing northwesterly winds. Combustion of agricultural wastes was sometimes visible in the agricultural fields located to the south of the measurement site.

CO and CH_4 concentrations were > 200 and >1800 ppbv (Fig. 2.1c), respectively, reflecting the concentrations in the northern mid-latitudes in winter (Dlugokencky et al., 1994; Novelli et al., 1998; Pochanart et al., 1999). CO and H_2 concentrations were highly variable compared to CH_4 concentrations. The CO and H_2 concentrations tended to be large in the mornings (7:00-9:00 JST) and in the evenings (18:00-20:00 JST), probably influenced by vehicle emissions since it coincided with periods of greatest vehicle use. Furthermore, when air masses of high CO and CO concentrations came, a few minutes' delay in concentration was observed at the lower height, showing that horizontal uniformity was not realized.

In the daytime (Fig. 2.2), under conditions of high wind speed, CO, H_2, and CH_4 concentrations were low and showed small temporal variations. The differences in concentration between the 2 heights were small. At night (Fig. 2.3), the CO, H_2, and CH_4 concentrations increased under the stable layer that developed, and temporal variations were larger than in the daytime. The differences in concentrations between the 2 heights also increased gradually. The correlation between wind speed and CO, H_2, and CH_4 concentrations under conditions of low wind speed was not clear at night, partly because there was not enough mixing of air masses emitted to the atmosphere from ground sources.

The inverse relationships between wind speed and concentrations of CO, H_2, and CH_4 (Fig. 2.4) show that these gases are emitted from ground sources at a regional scale. The ratios of CH_4 concentrations to CO concentrations in excess of the background level decreased as the CO concentrations increased (Fig. 2.5). Air masses that contained higher CO concentrations may be heavily influenced by combustion processes because the ratio approached 0.1 (e.g., Lobert et al., 1991; Chapter 8). The large increases in the concentrations of CO and CH_4 are probably attributable to high CO emissions from ground sources near the measurement site.

It is expected that the CH_4:CO ratio increases as the air masses are subject to photochemical oxidation. Because air masses containing lower concentrations of CO may be aged after local emission, the ratio would increase as CO decreases (Fig. 2.5). However, some large CH_4 sources other than combustion also appears to be present on the ground because some of the air masses show ratios larger than 0.5. The ratios were in the same order as those in urban-impacted air (0.36-0.84; Harriss et al., 1994; Bakwin et al., 1995; Barlett et al., 1996), probably reflecting local CH_4 sources.

2.4 Deposition of CO, H_2, and CH_4 to the grass field

The inverse relationships between wind speed and gradients of CO, H_2, and CH_4 (Fig. 2.6) indicate that these gases were deposited onto the grass. Direct application of eq. (2.4) resulted in deposition velocities that fluctuated greatly. This was partly due to the relatively low confidence of determination of CO, H_2, and CH_4 concentrations under conditions of higher wind speeds, and partly due to the absence of horizontal uniformity because of the highly variable CO, H_2, (and CH_4) concentrations at the measurement site (Fig. 2.1c). Therefore, several periods were selected when the changes in CO and CH_4 concentrations were small (<10% of the mean concentration) and when the wind speed was lower than 1.5 m s^{-1}. Such periods suitable for applying the micrometeorological techniques were restricted to the nighttime (Table 2.1).

The first 2 estimations of CO deposition velocities (shown in Table 2.1) were 2.9 and 3.9 $\times$ 10^{-2} cm s^{-1}, while the last 2 were about 1.7 $\times$ 10^{-2} cm s^{-1}. The difference in CO deposition velocities between the first 2 and the last 2 periods cannot be attributed to the changes in soil moisture because there was little precipitation during the measurement periods. Rather, the smaller deposition velocities in the last 2 days can probably be attributed to lower soil temperatures. The air temperature at 0.33 m stayed as high as 8°C on the mornings of 12 and 13 December, whereas in the early mornings of 18 and 21 December, it decreased to below -5°C (Fig. 2.1a). In the latter 2 days, it was expected that the temperature of the topsoil at a few centimeters depth decreased to below zero, although the soil temperature at 5 cm stayed above 2°C (Fig. 2.1a). Temperatures below 0°C considerably reduce bacterial

uptake activity (Kuhlbusch et al., 1998). In the early morning of 18 and 21 December, bacterial CO oxidation in the topsoil was reduced at subzero temperatures, and CO could be oxidized only in the deeper soil where the temperature was several degrees Celsius. Under these conditions, the topsoil acted to resist CO diffusion from the air to the oxidizing soil layer, and consequently the total CO uptake by the soil was reduced.

The CH_4 flux obtained ranged between 12 and 17 ng m^{-2} s^{-1}, in the same range as CH_4 flux observed in other grass fields measured by the closed-chamber technique (Steudler et al., 1989; Tate and Striegl, 1993; Minami et al., 1993; Mosier et al., 1996). It was also in the same range as values obtained by micrometeorological techniques in the same field in other seasons (Miyata, 1998). The effect of low temperature in the topsoil is less critical for the CH_4 oxidation because this reaction occurs in deeper soil (>a few centimeters) than does the CO oxidation.

Deposition velocities were also obtained using CO_2 as a tracer. Good correlations (R^2 ≈ 0.7) were found between the gradients of CO_2 and CO concentrations and between the gradients of CO_2 and CH_4 concentrations (Fig. 2.7). Large deviations from the regression line were found when the CO concentration gradient was large (Fig. 2.7a). These deviations were probably due to the highly variable CO concentration in the high concentration range, together with horizontal uniformity not being satisfied. By applying eq. (2.5), a CO deposition velocity of 3.4 × 10^{-2} cm s^{-1}, a H_2 deposition velocity of 6.6 × 10^{-2} cm s^{-1}, and a CH_4 influx of 13 ng m^{-2} s^{-1}, were obtained. The CO deposition velocity is in the middle of the range of values in Table 2.1 and it can be considered to reflect the mean value of CO deposition velocity during the measurement period. Results of the closed-chamber technique (Chapter 4), showed CO deposition velocities in a nearby arable field to be 2 to 4 × 10^{-2} cm s^{-1} in winter (excluding a period of several days following precipitation of greater than 10 mm). The agreement between the deposition velocity estimated by the micrometeorological technique and that estimated by the chamber technique indicates that CO deposition to the soil is not markedly accelerated by wind when the wind speed is less than 1.5 m s^{-1}. The CH_4 influx as calculated by eq. (2.5) is also in the middle of the range of values in Table 2.1, and is similar to those measured in the same grass field by applying the same micrometeorological method (Miyata, 1998).

2.5 Summary

This Chapter reported that the vertical gradients of CO, H_2, and CH_4 concentrations were observed, indicating the uptake of these gases by the grassland. Deposition velocities of the gases estimated by micrometeorological techniques were generally comparable to those of previous studies. Therefore, soil uptake is an significant sink of CO and H_2.

In Chapter 4, factors controlling the deposition velocities of CO and H_2 to soils are investigated more intensively by chamber techniques.

Table 2.1

Selected deposition velocities on periods when conditions applying micrometeorological technique to estimate fluxes were satisfied. In the first two periods, CH_4 difference between the two depths was not obtained because of measurement trouble.

Period (JST)	CO v_d (10^{-2} cm s^{-1})	CH_4 v_d (10^{-4} cm s^{-1})	(CH_4 influx) (ng m^{-2} s^{-1})	Averaged wind speed by sonic anemometer (m s^{-1})	Averaged air temperature at 0.33m (°C)
12.Dec 1:00 - 7:00	3.9 ± 1.8			1.51	5.5
13.Dec 1:00 - 5:30	2.9 ± 1.7			0.79	9.3
18.Dec 2:30 - 5:00	1.8 ± 0.9	13 ± 8 (17 ± 11)		0.75	-3.2
21.Dec 3:00 - 6:00	1.6 ± 0.8	9 ± 6 (12 ± 7)		0.45	-4.1

Photo 2.1 Meteorological measurement grass field in NIAES.

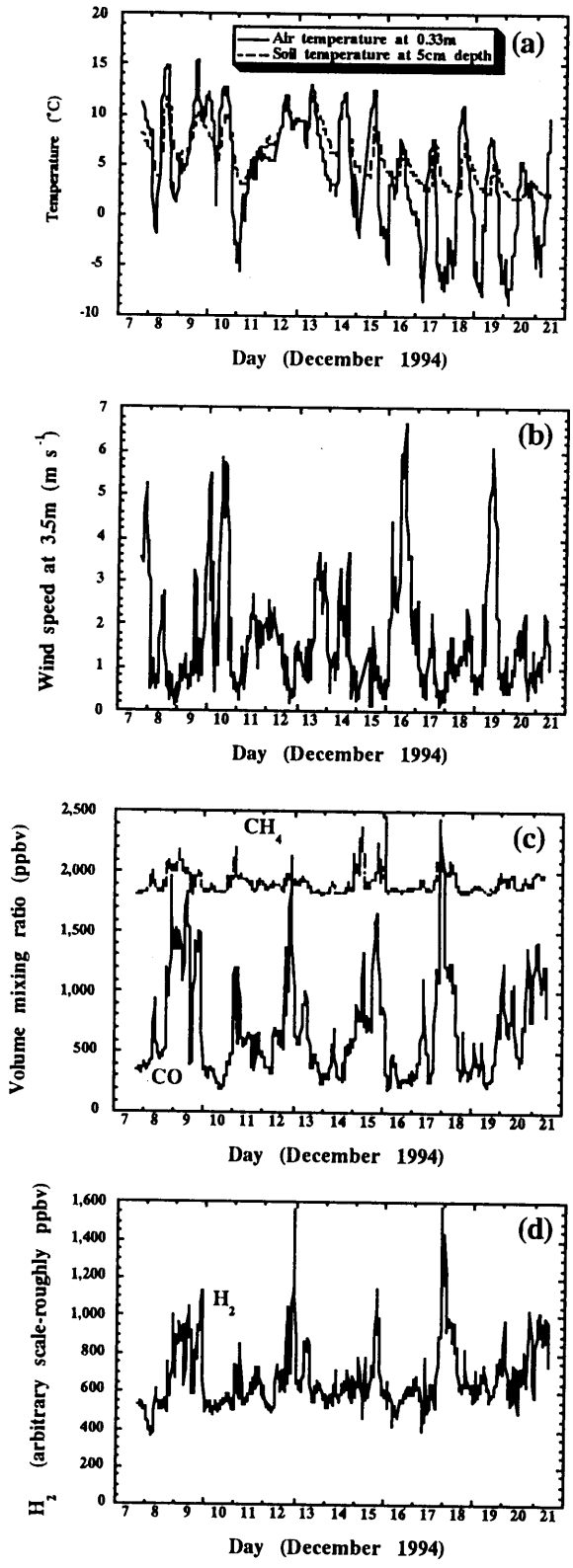

Figure 2.1 (a) Air temperature at 0.33 m height, soil temperate at 5 cm depth; (b) wind speed at 3.5 m; and (c) CO and CH_4 and (d) H_2 concentrations 1.30 m above a grass field in NIAES from 7 to 21 December 1994. Data were 30-min averages.

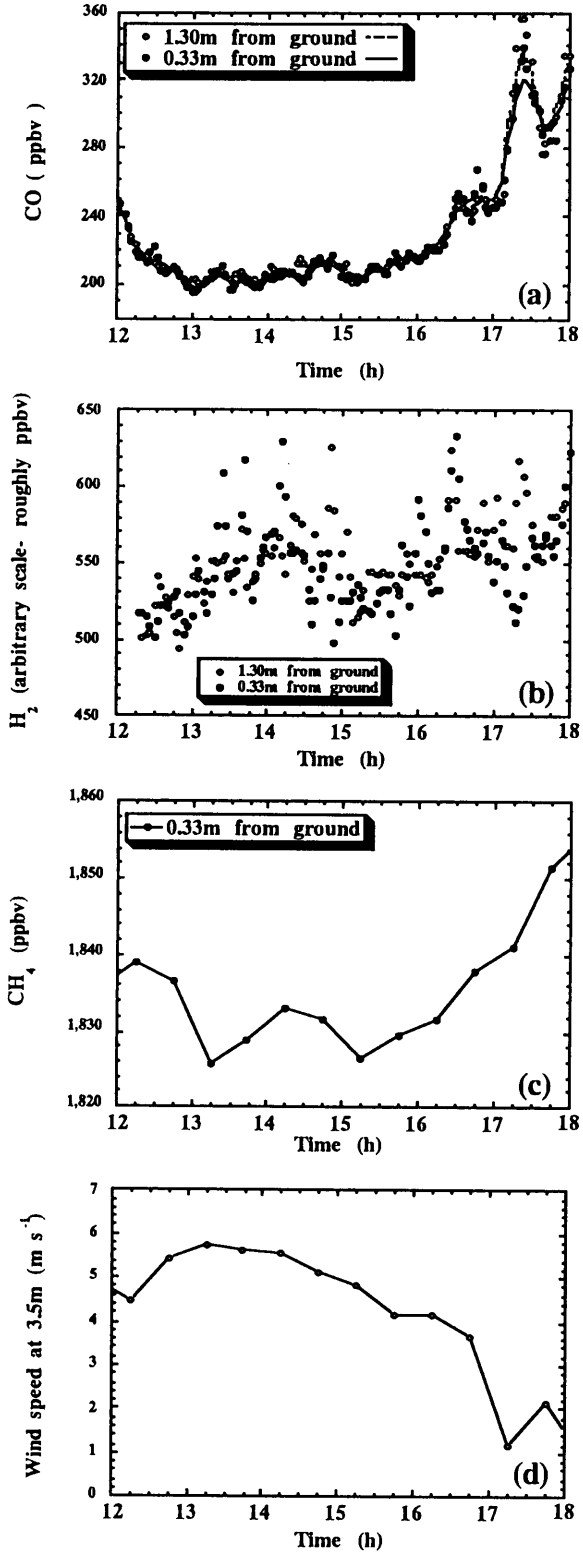

Figure 2.2 (a) CO concentration, (b) H_2 concentration, (c) CH_4 concentration, and (d) wind speed during the day on 10 December 1994. CH_4 concentrations at 1.30 m are not shown due to a measurement trouble Data of CO and H_2 were obtained every 3 min. The curves for CO were drawn by spline method.

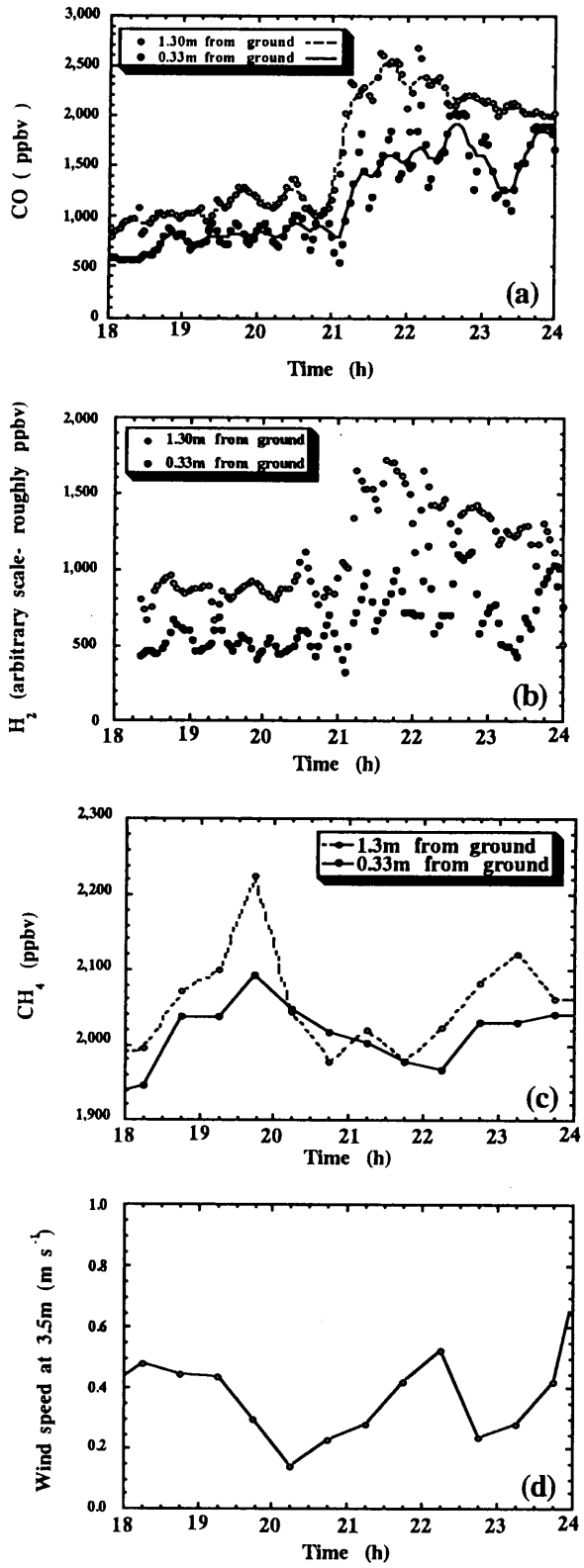

Figure 2.3 (a) CO concentration, (b) H_2 concentration, (c) CH_4 concentration, and (d) wind speed at night day on 17 December 1994.

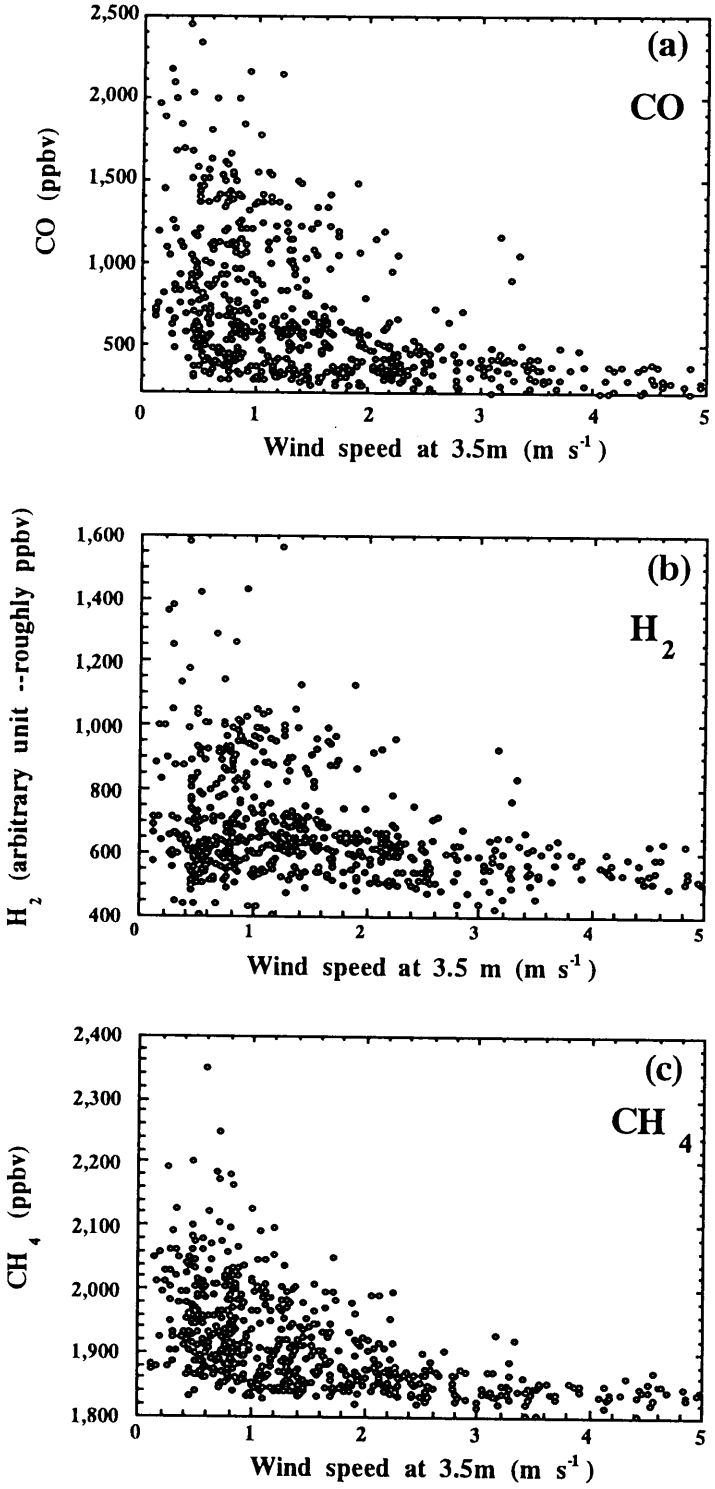

Figure 2.4 Relation between wind speed and (a) CO, (c) H_2, and (b) CH_4 concentrations. Data were 30-min averages.

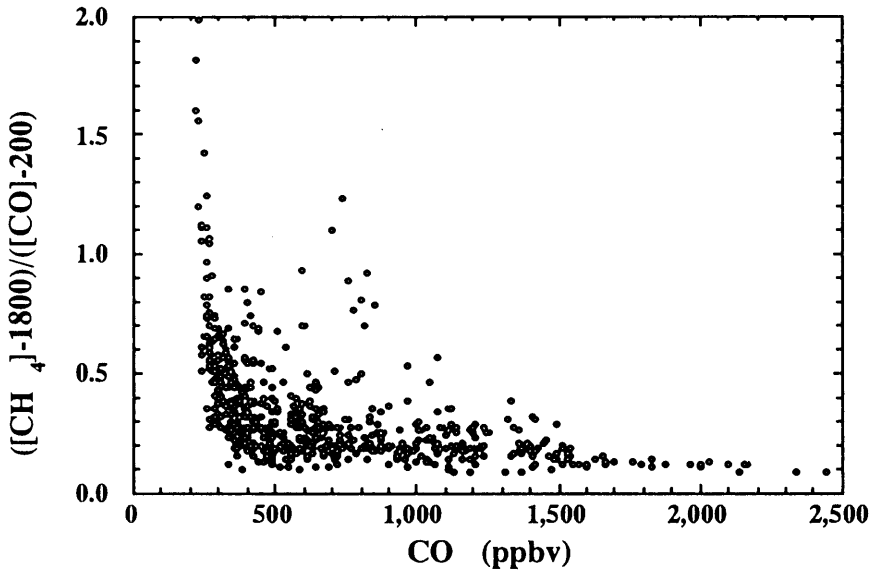

Figure 2.5 Relation between CO concentration and the ratio of excess CH_4 to excess CO above background levels (200 ppbv for CO and 1800 ppbv for CH_4). Data were 30-min averages.

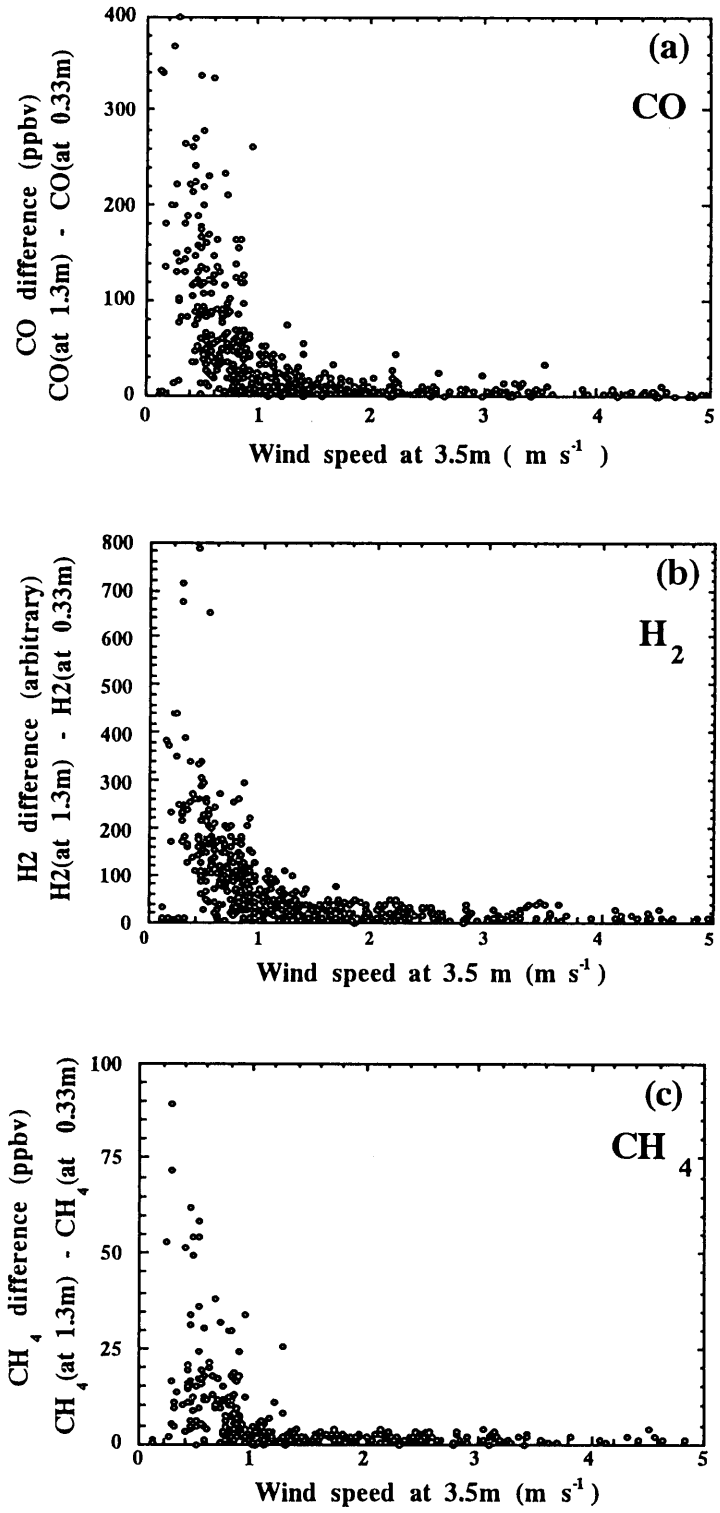

Figure 2.6 Relation between wind speed and differences between concentrations of (a) CO, (b) H_2, and (c) CH_4 at 0.33 and 1.30 m. Data were 30-min averages.

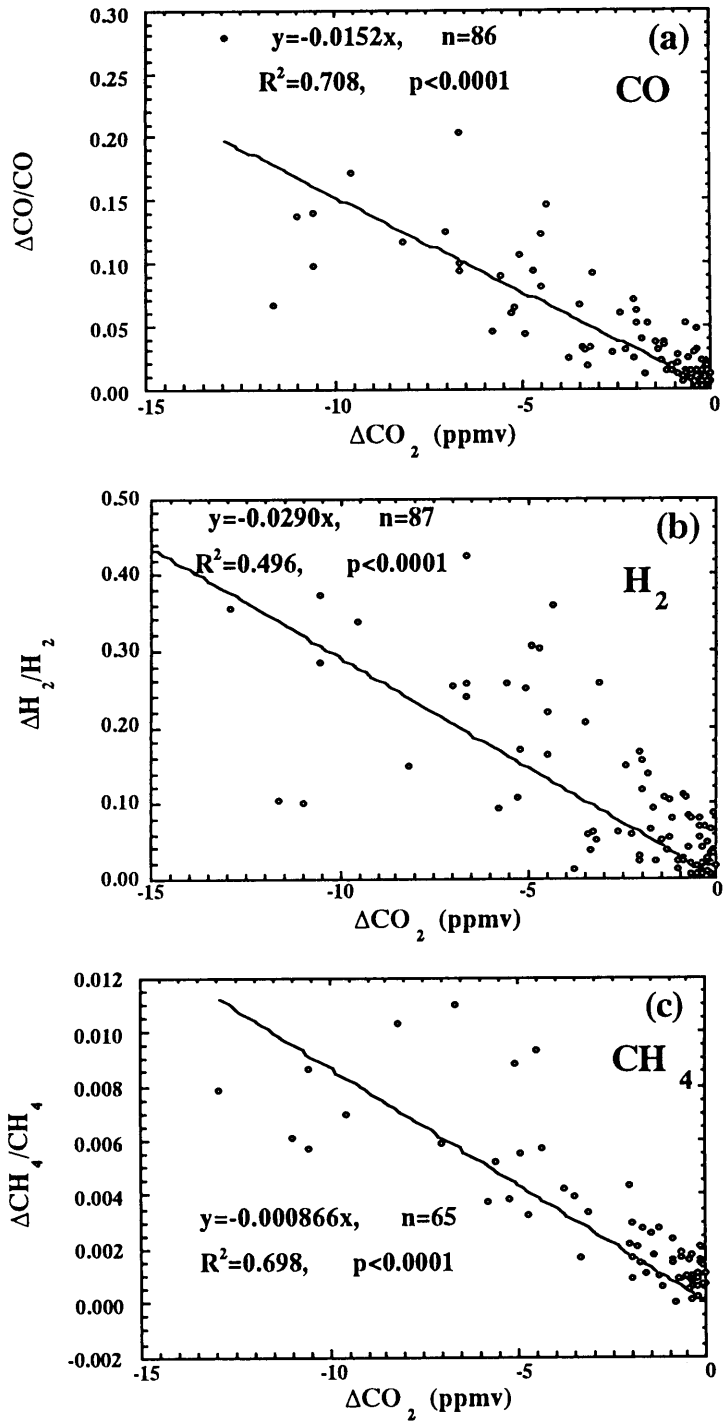

Figure 2.7 Relationship between ΔCO_2 (the difference in CO_2 concentrations at the 2 heights of 1.30 and 0.33 m) and $\Delta X/[X]$ (the ratios of: the differences in (a) CO, (b) H_2, and (c) CH_4 concentrations at the 2 heights to the relevant concentration at 0.33 m). ΔCH_4 data from 17 Dec used was because of measurement trouble.

Chapter 3

CO and H_2 measurements and techniques to measure CO and H_2 uptake by soil

3.1 Introduction

This Chapter presents methodology in gas analyses, field measurements, and laboratory experiments, which are common in Chapters of the present study. In the first half of this Chapter, analytical methods of CO, H_2, and related gases such as CH_4, CO_2, and hydrocarbons, are described. In the latter half of this Chapter, several techniques to measure CO and H_2 uptake by soil and their properties are described.

3.2 Measurements of CO and H_2

There are several methods to measure atmospheric CO (Crill et al., 1995; Fehsenfeld, 1995). CO exhibits moderately strong IR absorption of rotation-vibration lines of the molecule. Then, the applications of IR absorption are non-dispersive infrared analyzer (NDIR) used for measuring high-concentration of in-situ CO, solar spectroscopy or fourier transform infrared spectrometry (FTIR), satellite measurements such as MAPS (Reichle et al., 1990), and tunable diode laser (TDL) spectroscopy (Kolb et al., 1995). NDIR is used for the monitoring of the urban atmosphere at ppm levels. Solar spectroscopy is powerful to deduce secular trends of atmospheric CO (Zander et al., 1989). FTIR and TDL are suited for determining the fine vertical or horizontal structure of trace gases in the atmosphere. MAPS from Space shuttle was designed to detect CO in the free troposphere.

CO can be measured by GC, using various detectors such as reduction gas detector (RGD), electron capture detector (ECD), and FID with methanizer, depending on the concentration level and usage. For the accurate measurements of CO at atmospheric level, RGD is most reliable and has been used at background sites. FID with methanizer is linear over several orders of magnitude and is extremely useful when a wide range of concentrations

will be encountered as in ecological studies.

At present, atmospheric H_2 is reliably measurable only by in-situ measurements by GC equipped with RGD. H_2 cannot be detected optically because H_2 has not transition lines in UV or IR regions due to its symmetrical structure of the molecule.

3.3 Analysis of CO and H_2 by RGA3

Analysis of CO and H_2 in this study was carried out mainly using a RGA3 Reduction Gas Analyzer (Trace Analytical, California U.S.A.) (Fig. 3.1). The RGA3 consists of a microprocessor-controlled gas chromatograph with a back-flush system, fitted with a RGD. In this instrument, the mercuric oxide technique is applied to detect CO and H_2 as low as the atmospheric concentration level (Seiler et al., 1980). The analyzer was improved to allow CO to be analyzed automatically and was improved to analyze various kinds of samples such as stored in syringes and Tedler® bags. The chromatographic data from the RGA3 system were downloaded to a CR5A integrator (Shimadzu Corporation, Japan) and gas concentrations were calculated. Then, analyzed data were transmitted to a PC through RS232C port. At the same time, the CR5A controlled the RGA3 and solenoid valves controlling the automatic sampling system. Sample gases were injected about 30 sec after the sample gases were introduced into the sample loop in RGA3, not to be pressurized. Samples were usually dried before analysis, using $Mg(ClO_4)_2$.

The chromatograph of RGA3 showed that H_2 and CO can be completely independent from other gases (Fig. 3.2). Column and detector temperatures of RGA3 were maintained at 105 and 265 or 280°C, respectively. The detection limits of CO and H_2 were about 1 ppbv and 50 ppbv, respectively, and the averages of 10 standard deviations of CO and H_2 were 1.2 and 5 ppbv at about 500 ppbv, respectively (standard deviation (s.d.) for number of samples (n)=20). The trends of a few percentages found in the precision analysis in laboratory should be attributed to the temperature variation because the response is related to diurnal temperature cycle and because retention times changed simultaneously.

For the calibration of CO and H_2 concentrations, standard gases enclosed in aluminum and iron cylinders at 95.6, 488, 494, 998 ppbv, 1 ppmv CO, and 537 ppbv and 1.1 ppmv H_2 with N_2 balance, respectively, commercially supplied (Takachiho Chemical Industry Co.

LTD.; Nihon Sanso Corporation, Japan) were used. The difference between the CO 494 ppbv standard and the NOAA/CMDL scale used by the Meteorological Research Institute of Japan (Matsueda et al., 1998) was less than 3%. Reasonable relations between standards were obtained for CO. Several calibration standards were used for the normal use.

The linearities of CO and H_2 concentration measurements by RGA3 in the range ≤1 ppmv, using a dilutor and cylinders containing 95.6 ppbv, 1 ppmv and 9.9 ppmv CO and 1.1 ppmv H_2, fell within a 5 % precision level and within the precision of analysis, respectively (Fig. 3.3). Over ppmv levels of CO concentration, the linearity is no longer maintained because the response of photodiode optically saturated. For the analysis of high concentration samples by RGA3, dilution or changing sample loops from 1 ml to less volume was necessary. It should be noted that the resolution was better from the calculation from height values although the linearity was better from the calculation from area values. Then, under normal used, height values were used for the calculation of concentrations.

CO and H_2 permeability of the 0.5 L Tedler® bags which was used for field and laboratory experiments was checked and found to be less than 1 and 4 ppbv h^{-1} for CO and H_2, respectively, which was acceptable for measurements in this study if the measurements were conducted within several hours.

3.4 Analysis of CO, CH_4 and CO_2 by GC-FID with a methanizer and GC-TCD or NDIR

To analyze samples containing high concentration of CO, CO should be measured by GC-FID with a methanizer. This means that simultaneous measurements of CO and CH_4 are possible by GC-FID. At the same time, the GC system was improved to measure CO, CH_4, and CO_2, simultaneously by installing double flow lines in the GC system (Fig. 3.4).

CO and CH_4 were measured by flame ionization detector (FID) with a methanizer (MTN-1; Shimadzu Corporation, Kyoto), which converts CO to CH_4. The GC-FID used a backflush system with Unibeads1S (60/80mesh 0.5 m) as the pre-cut column and molecular sieve 5A (60/80mesh 1.8 m) as the main column, using N_2 as carrier gas. CO_2 was measured by a thermal conductivity detector (TCD) using a dehumidifier ($Mg(ClO_4)_2$) and separation by Porapack Q column (60/80 mesh 7.2 m) mounted on a gas chromatograph (GC-9A;

Shimadzu Corporation, Kyoto), using He as carrier gas. Samples of CO, CH_4, and CO_2 were automatically injected from the sample loop (3.3 ml for FID, 5 ml for TCD). The column temperature of the GC-9A was maintained at 60°C. For calibration of CO, 9 standard gas cylinders containing 0.998 to 9970 ppmv (0.997%) CO with N_2 balance were used. For calibration of CH_4, 10 standard gas cylinders containing 1.67 to 999 ppmv CH_4 with N_2 balance were used (Takachiho Chemical Industry Co. LTD., Japan). For calibration of CO_2, 9 standard gas cylinders containing 289 to 100,000 ppmv (10%) CO_2 with N_2 balance were used (Takachiho Chemical Industry Co. LTD., Japan). Several calibration standards were used for the normal use.

Area values on the chromatogram (Fig. 3.5) were used for the calculation in the TCD and FID. The linearity of the TCD and FID response to gas concentration was good and validated the analysis within the wide range of concentrations expected in the ecological studies (Fig. 3.6). The R^2 values of linear regressions for the CO_2, CH_4 and CO calibrations in the concentration range were 0.99992, 0.99990,0.99985, respectively.

The CO_2 concentration was obtained also by infrared gas analyzer as well as the GC-TCD (Chapter 4, 5, and 8). The infrared analyzer used was Model LI6250 (LI-COR Inc., Nebraska U.S.A.) or Model ZRC non-dispersive infrared gas analyzer (Fuji Electric, Tokyo, Japan) with 289, 396, 1000, and 2000 ppmv CO_2 cylinder, commercially supplied (Takachiho Chemical Industry Co. LTD., Japan).

For small amounts of samples stored in vials, 1 ml of sample gas was injected into a carrier gas line and conveyed to GC-TCD or the infrared gas analyzer (Bekku et al., 1995). CO_2 concentration measurement precision was within 3.0% (s.d. for n=5). CH_4 concentration was measured with a precision within about 2% for vial samples (s.d. for n=5).

3.5 Analysis of related gases--THC and light hydrocarbons

In combustion experiments (Chapter 8), total hydrocarbon (THC) and light hydrocarbons were measured to study the emission of CO in view of the oxidation from organic matter. THC was measured by FID on a GC8A (Shimadzu Corporation, Kyoto). A mixture of 20 ml min^{-1} N_2 gas and 20 to 50 ml min^{-1} sample gas pumped from the stack was continuously introduced into the FID. Linearity was checked using 199 and 999 ppmv CH_4 standard gases

with N_2 balance. However, in Chapter 8, only the relative response of FID is reported due to the difficulty of maintaining flow rates and the interpretation of the CH_4 measurements. The response of the FID was transmitted every second to the 21XL data logger (Campbell Scientific, California USA), as was the temperature.

Light hydrocarbons were measured by double GC-FID with a cryofocusing system (Fig. 3.7). C_2 gas species were analyzed by FID1 after the separation by Porapack Q (1 m) and Unibeads 1S (3 m). The C_3 to C_5 gas species were analyzed by FID2 after the separation by Porapack Q (1 m), cryofocusing by cryofocus B, and separation by capillary columns of CP-PoraBOND Q + CP-Sil 13B. These FIDs for light NMHCs also had good linearity and validated the analysis over the wide range of concentrations expected in the combustion experiment. An example of a chromatograph is shown in Fig. 3.8. The chromatograph was changed from FID1 to FID2 between the C_2 and C_3 species.

The standard hydrocarbon gas used was synthetic air mixed with 1.512 ppmv C_2H_6, 1.391 ppmv C_2H_4, 1.391 ppmv C_2H_2, 1.482 ppmv C_3H_8, 1.524 ppmv C_3H_6, 1.578 ppmv n-C_4H_{10}, 1.568 ppmv i-C4H_{10}, 1.473 ppmv n-C_5H_{12}, and 1.469 ppmv i-C_5H_{12} with N_2 balance (Sumitomo Seika Chemicals Co., Ltd., Osaka).

3.6 Techniques to measure CO and H_2 uptake by soil

A variety of techniques (Fig. 3.9) have been developed to measure surface-atmosphere gas exchange, including micrometeorological, enclosure and diffusion theory approaches. Each has advantages and disadvantages, and no single approach is applicable to all studies.

The diffusion theory technique (Fig. 3.9a) has been used for the uptake measurement of CH_4 by soil (Born et al., 1990). Gas fluxes are calculated from gas profiles and diffusivities in soil. However, this approach is not suitable for CO and H_2 uptake by soil because the gradients of CO and H_2 in soil are far more steep than that of CH_4. The gradient of CO and H_2 change with mm-scale (see Fig. 5.4) and cannot be easily obtained due to the problems of limited sample amount or the measurement of soil depth.

The disadvantages of micrometeorological technique are that various complex measurement system is needed and costly; experimental approaches are not easy because large area is object; high resolution and rapid response of gas analysis are necessary. Hence,

until now, the gas species available in the micrometeorological technique are limited for CO_2 and CH_4 (Miyata, 1998). However, micrometeorological technique (Kaimal and Finnigan, 1992; Lenschow, 1995) has advantages that average fluxes over large area are available. The present study has already shown the applicability of the micrometeorological technique in Chapter 3.

Here, chamber techniques adopted in the subsequent Chapters are introduced.

3.7 Closed-chamber technique (CCT)

Closed-chamber technique (Livingston and Hutchinson, 1995) is relatively low cost and simple to operate, and especially useful for addressing research objectives served by discrete observations in space and time. In combination with appropriate sample allocations, it is adaptable to a wide variety of studies on local to global spatial scales and particularly well suited to in situ and laboratory-based studies addressing physical, chemical and biological controls on surface-atmosphere trace gas exchange. Then, previous studies has used CCT for the soil uptake of CO and H_2.

The concentrations of CO and H_2 in the closed-chamber over soil decrease exponentially with time (Fig. 3.10). From the mass balance in the chamber (see Chapter 5), deposition velocities were calculated by curve fitting assuming first-order kinetics. If the concentrations in the chamber, C, is fitted by

$$C=C_0\exp(-kt), \tag{3.1}$$

where t is time (s), and C_0 and k (s^{-1}) are the fitting parameters. To understand uptake processes of CO and H_2 by soil, the unit used to express the uptake must not be direct influx values because deposition onto soils obeys first-order kinetics for gas concentration at atmospheric level (e.g., Bender and Conrad, 1993; Conrad and Seiler, 1985a) and because atmospheric CO and H_2 concentrations are highly variable. The net deposition velocity, v_{nd} ($cm\ s^{-1}$), can be given by

$$v_{nd}=kh. \tag{3.2}$$

where h is the chamber height (cm). For CO (Fig. 3.10b), due to the simultaneous presence of production as well as uptake in soil, the concentrations should be fitted by

$$C=C_0\exp(-k_g t)+[CO]_{eq}, \tag{3.3}$$

where C_0, k_g (s^{-1}), and $[CO]_{eq}$ are fitting parameters. $[CO]_{eq}$ is the compensation (equilibrium) concentration between uptake and production as given in eq. (1.17). The gross deposition velocity, v_{gd} (cm s^{-1}) and production rate, P_{CO} (molecules cm^{-2} s^{-1}), are calculated as follows:

$$v_{gd}=k_g h, \tag{3.4}$$

$$P_{CO}=\rho\,[CO]_{eq} v_{gd}=\rho[CO]_{eq} k_g h, \tag{3.5}$$

where ρ is the number density of air (molecules cm^{-3}).

The net influx, F (molecules $cm^{-2}s^{-1}$), is obtained by

$$F=\rho C_{atm} v_{nd}=\rho(C_{atm}-C_{eq})v_{gd}. \tag{3.6}$$

To estimate the deposition flux onto soil, the flux value (Scharffe et al., 1990; Sanhueza et al., 1994a, b), net deposition velocity (Liebl and Seiler, 1976; Moxley and Smith, 1998a) , and gross deposition velocity and gross production rate (Conrad and Seiler, 1985a) were employed. In the present study, net or gross deposition velocities, and (gross) production rates were used to study property of soil uptake of the gases.

The repeatability of the closed-chamber experiments is better than 15%, similar to previous studies (e.g., Conrad and Seiler, 1985a). In experiments with changes in chamber heights as 9, 20, and 50 cm (Fig. 3.11), showed that deposition velocities were not affected by chamber height when the range of deposition velocities were $0\sim10\times10^{-2}$ cm s^{-1}.

3.8 Open-flow technique (OFT)

The systems by open-flow technique are inherently vented because of their open-path circulation (Fig. 3.12). The OFT measures the concentration difference through a chamber from which the net flux (F) between soil and the atmosphere was calculated. Direct flux values were not employed because of the first order kinetics of CO and H_2 deposition and the rapid changes in CO and H_2 concentrations at Tsukuba probably due to human activities. Several advantages of the OFT are that continuous measurements are possible and the precision and detection limit of flux can be low by repeated analysis and that concentration gradients in soil is less perturbed than the CCT. The OFT was applied to monitor CO and H_2 uptake continuously and deduce diurnal trends and a-few-days trends in deposition velocities. However, it should be noted that soil condition gradually changed by the enclosure; soil becomes gradually wet by enclosure.

The chambers used for the OFT in this study were made of poly vinyl chloride cylinders, 20 cm diameter cut to 15 cm length, of which 5 cm was inserted into the soil. During the measurements, a lid was loosely attached to the top of the chamber and a sun shade consisting of a white cone funnel was placed above the lid to avoid excessive temperature increase.

Air taken from the atmosphere was pumped through a large container acting as a buffer (>200 liter) with fans and introduced to the chamber to smooth the concentrations which display rapid changes. Two air inlets and outlets were connected to the middle of the cylinder wall to mix the airflow effectively. During the measurements, the air flow rate was controlled by mass flow meters with needle valves (Kojima Co. LTD., Japan), and was set at values ranging between 3.0 and 3.3 liters min^{-1} to match the high deposition rates of CO and H_2 onto the soil. The air samples were pumped from the inlet and outlet of the chamber to the RGA3 system and the CO_2 analyzer. To calculate deposition velocities by the OFT, the mass balance of the target gas in the chamber can be written as:

$$\rho\frac{d(VC_{ch})}{dt} = f\rho(C_{in} - C_{out}) - \rho A v_{nd} C_{surface} + P_{vinyl} \qquad (3.7)$$

t: time (s)

C_{ch}: mean concentration in the chamber (ppbv)

C_{in}: concentration at the inlet (ppbv)

C_{out} : concentration at the outlet (ppbv)

$C_{surface}$: concentration on the soil surface (ppbv)

f: flow rate (liter min^{-1})

A : soil surface area in the chamber (cm^2)

V: volume of the chamber (cm^3)

P_{vinyl}: production from the vinyl chloride chamber (molecules s^{-1})

Only net deposition velocity v_{nd} can be obtained by the OFT. In measurements of this study, time series of C_{in} and C_{out} were analyzed in turn every six minutes. Interpolating these data, the values at three minute intervals were calculated. From the advective term on the left hand side of eq. (3.7), the correction of the CO_2 efflux was < 1 %, and the correction for CO and H_2 deposition velocities amounted to a maximum of several percentage points in measurements of this study due to the rapid changes of CO and H_2 concentrations in the air , although the concentrations were smoothed by the buffer. CO deposition velocities were corrected for temperature-dependent CO flux from the vinyl chloride chambers.

Here, it was assumed as follows:

$$C_{ch} = C_{surface} = \frac{C_{in} + C_{out}}{2} \tag{3.8}.$$

The assumption that C_{ch} is the mean of C_{in} and C_{out} does not result in any large error because the chamber was ventilated at the high flow rate. On the other hand, the interpretation of $C_{surface}$ can lead to a bias of calculated deposition velocities. Finally, v_{nd} was calculated as follows:

$$v_{nd} = \frac{2f(C_{in} - C_{out}) - \frac{d}{dt}\{V(C_{in} + C_{out})\} + \frac{2}{\rho}P_{vinyl}}{A(C_{in} + C_{out})} \tag{3.9}.$$

Measured deposition velocities showed relatively high repeatability (resolution) much more than those by the CCT.

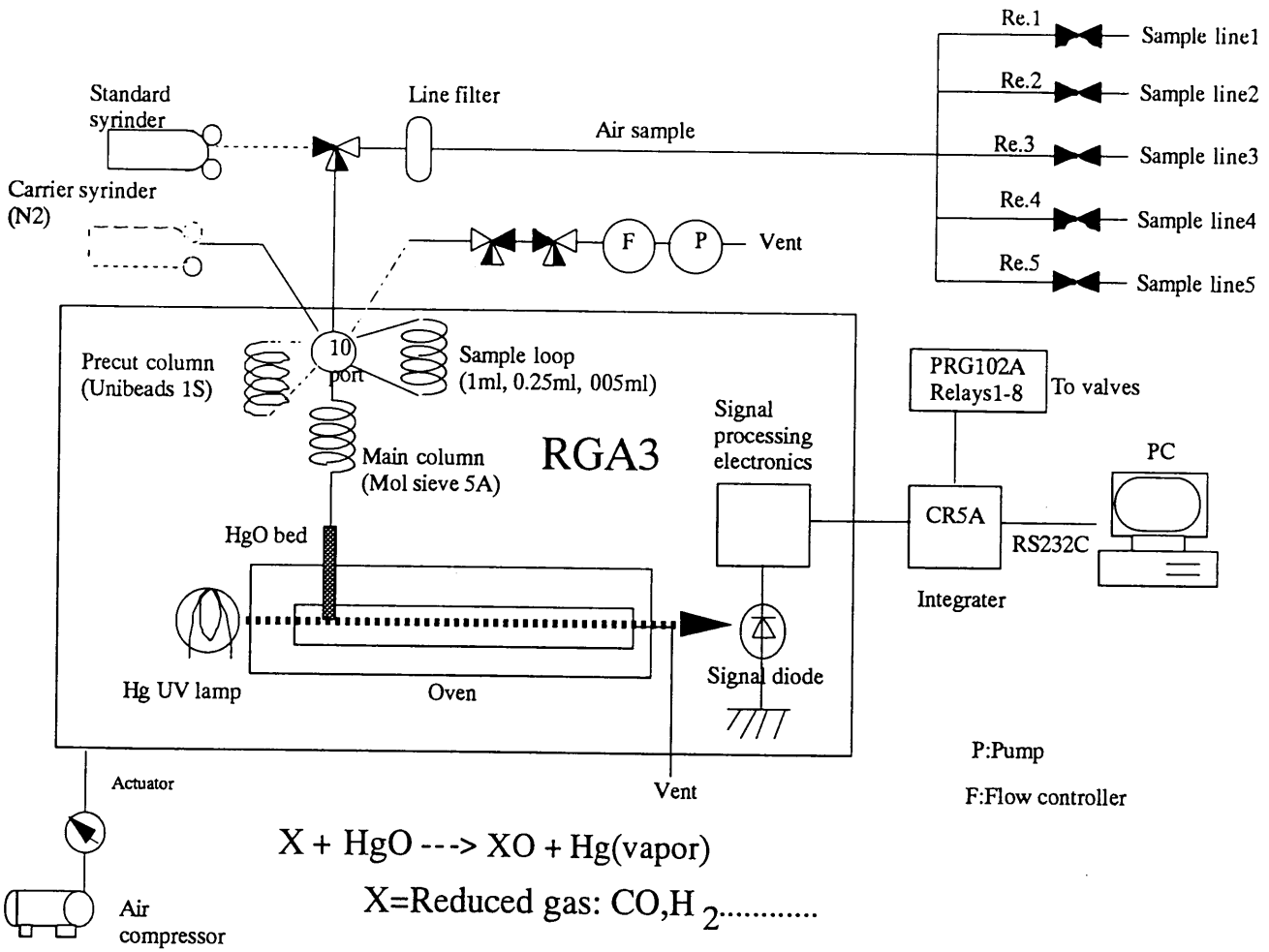

Fig. 3.1 RGA3 system

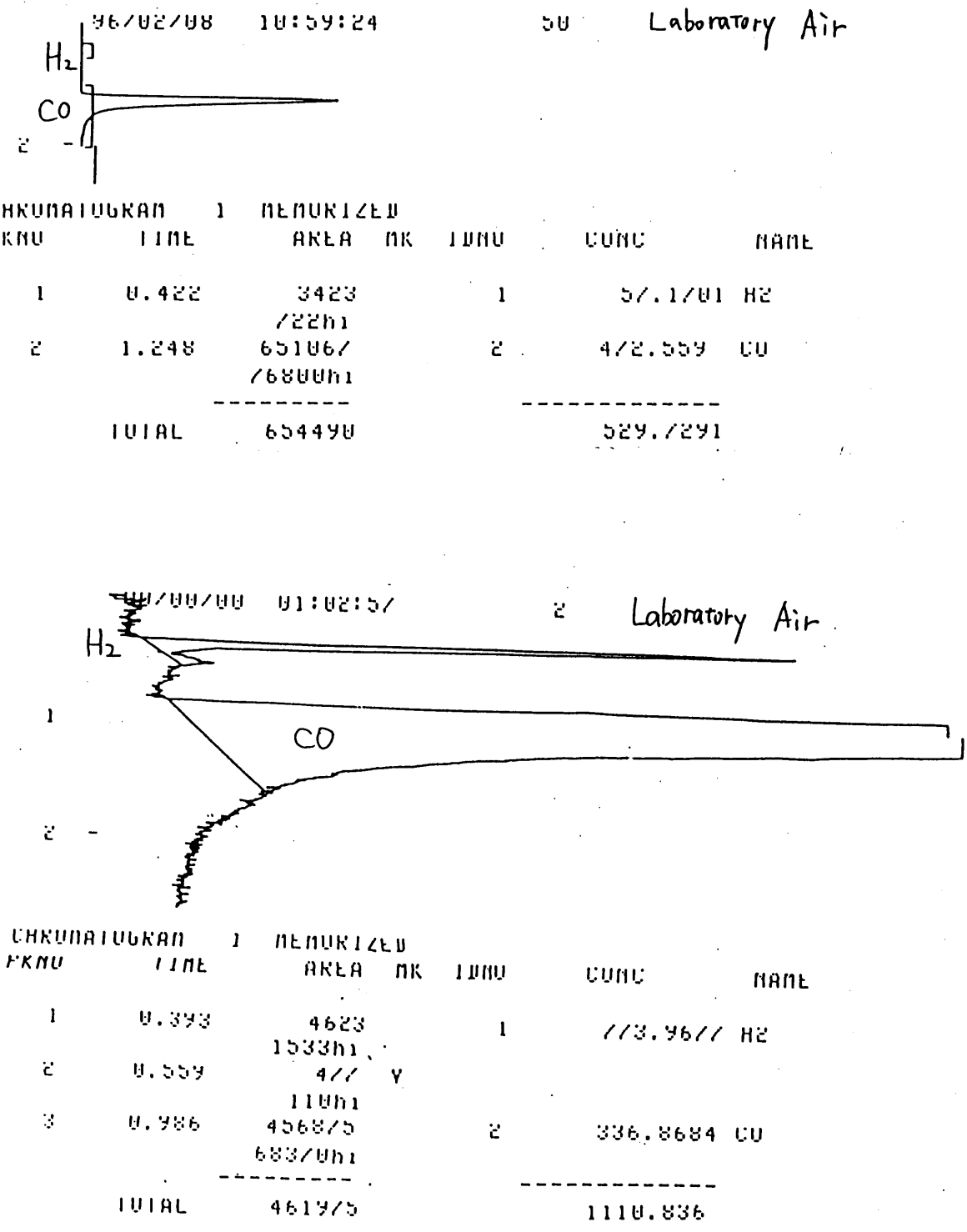

Figure 3.2 An example of chromatograph of RGA3

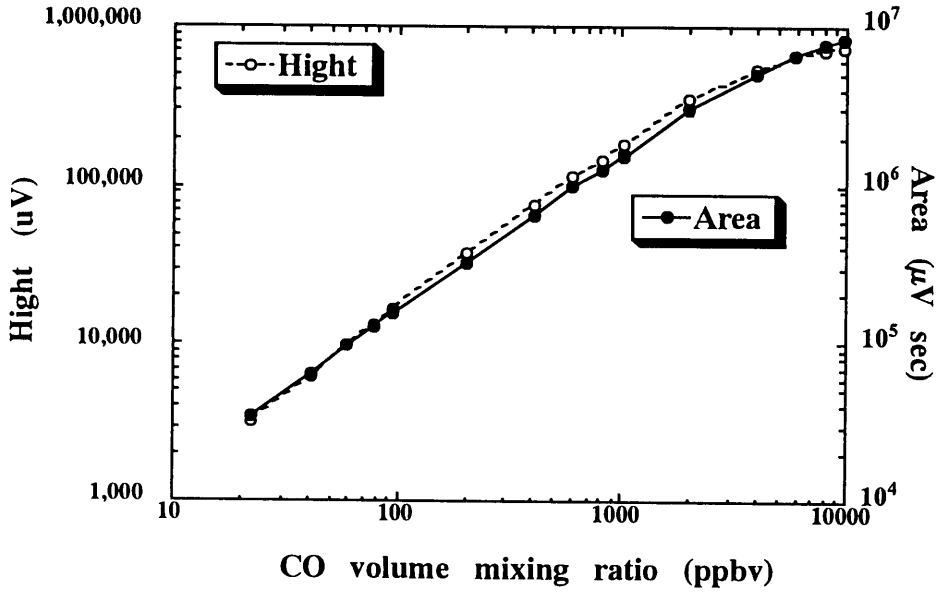

Figure 3.3 Calibration curves for CO by RGA3

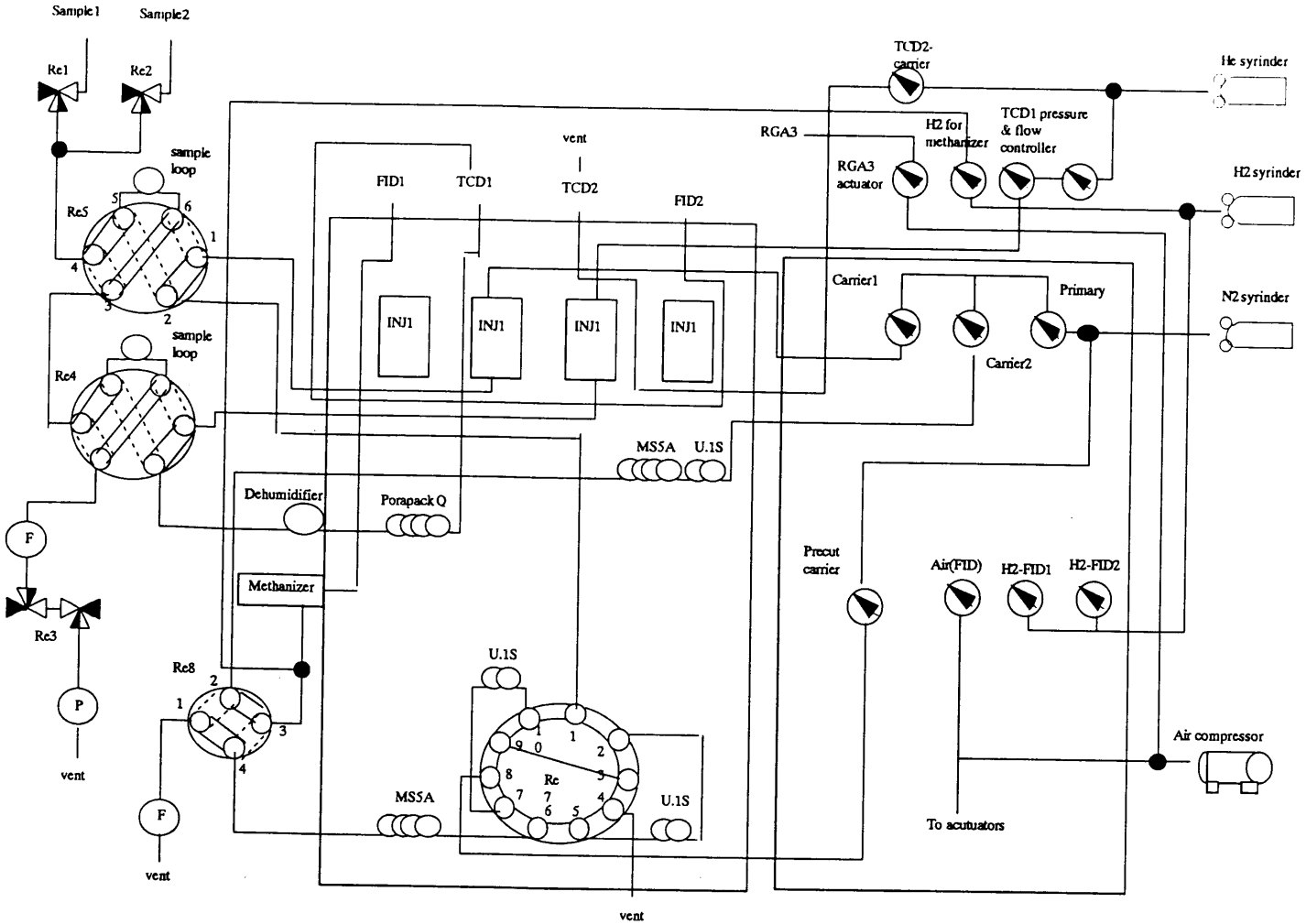

Figure 3.4 GC-TCD and FID system with methanizer

CHROMATOPAC C-R7A CH=1 REPORT No.=11 ｸﾛﾏﾄ=1:@CHRM1.C00 99/08/15 15:17:48

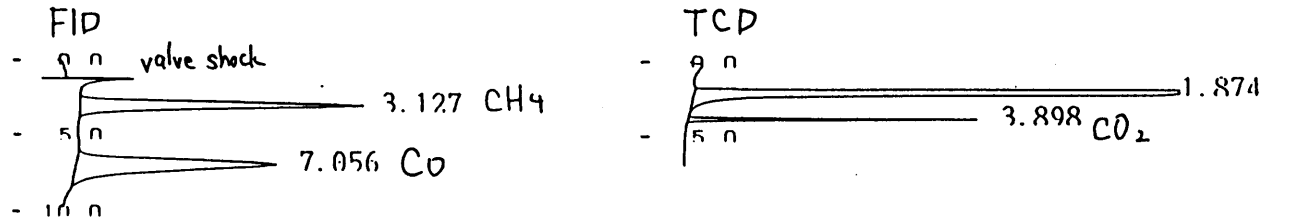

** 定量計算結果 **

CH	PKNO	TIME	AREA	HEIGHT	MK	IDNO	CONC	NAME
1	2	3.127	77785	2350		1	77785.3984	CH4
	17	7.056	88027	1669				
		TOTAL	165813	4018			77785.3984	

CHROMATOPAC C-R7A CH=2 REPORT No.=11 ｸﾛﾏﾄ=1:@CHRM2.C00 99/08/15 15:17:48

** 定量計算結果 **

CH	PKNO	TIME	AREA	HEIGHT	MK	IDNO	CONC	NAME
2	1	1.874	7946225	1059544	E		99.9268	
	2	3.898	5824	585			0.0732	
		TOTAL	7952049	1060129			100	

Figure 3.5 An example of chromatogram of GC-FID with methanizer and GC-TCD

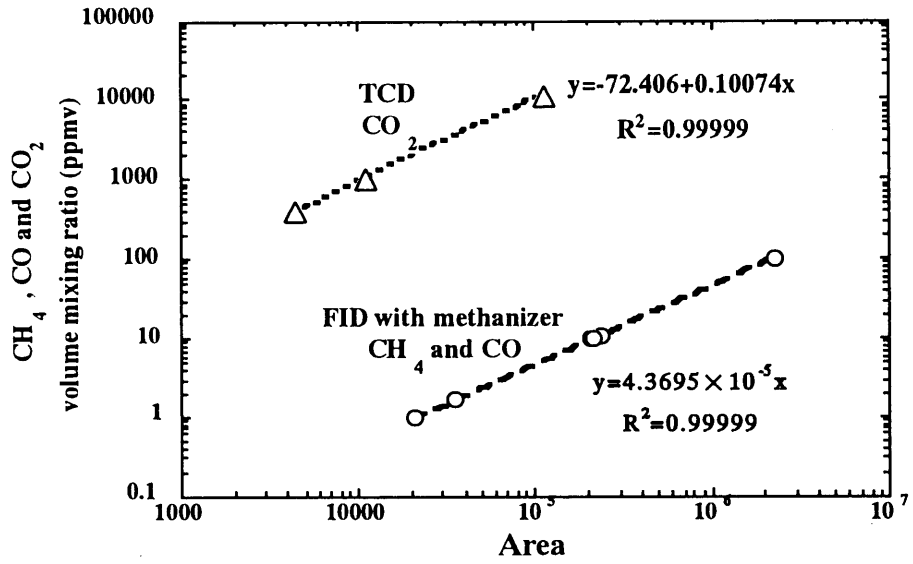

Figure 3.6 Sensivitity of CO and CH_4 peaks by GC-FID with a methanizer and CO_2 peak by GC-TCD.

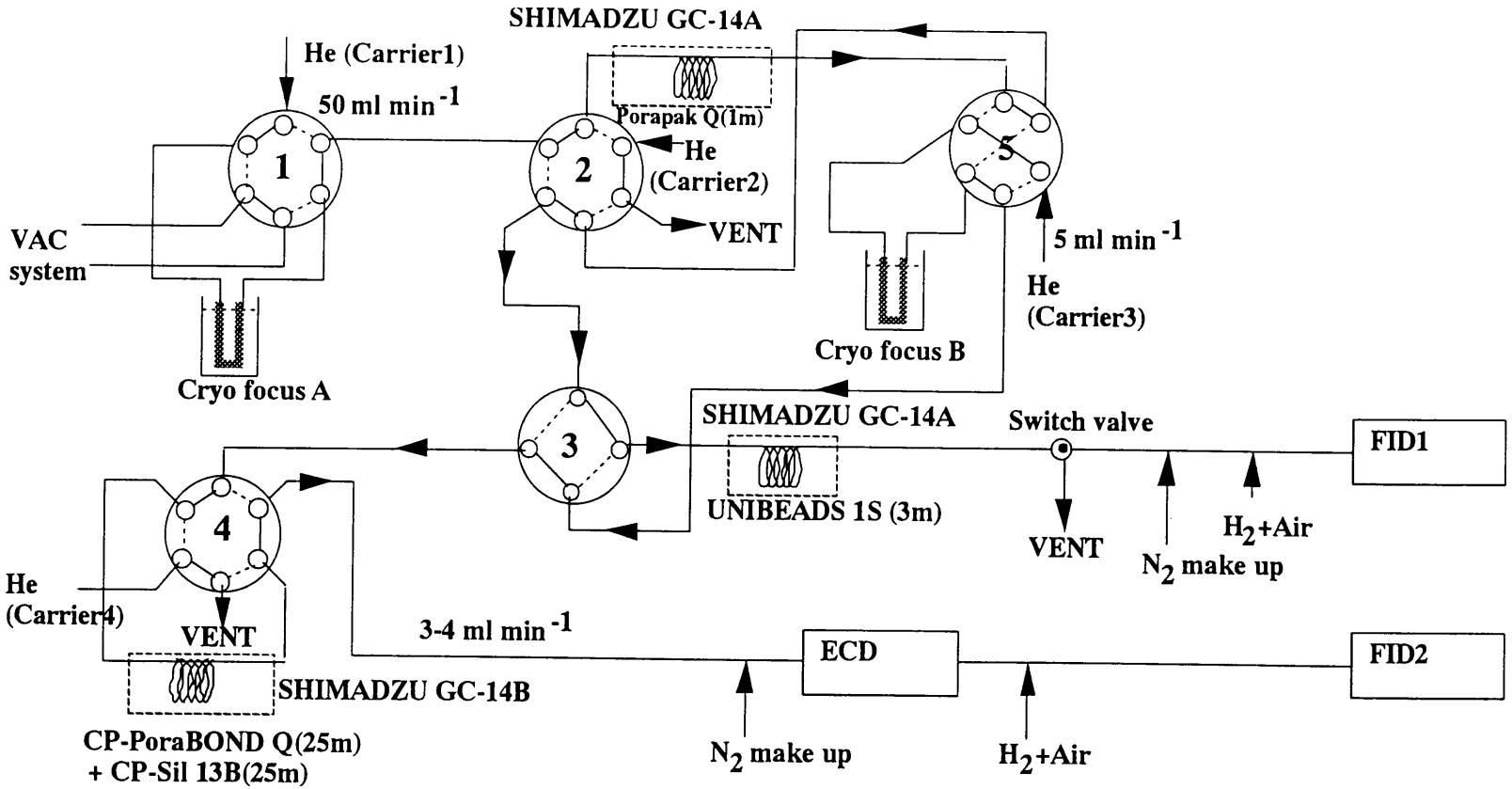

Figure 3.7 Schematic diagram of the system for analyzing hydrocarbons.

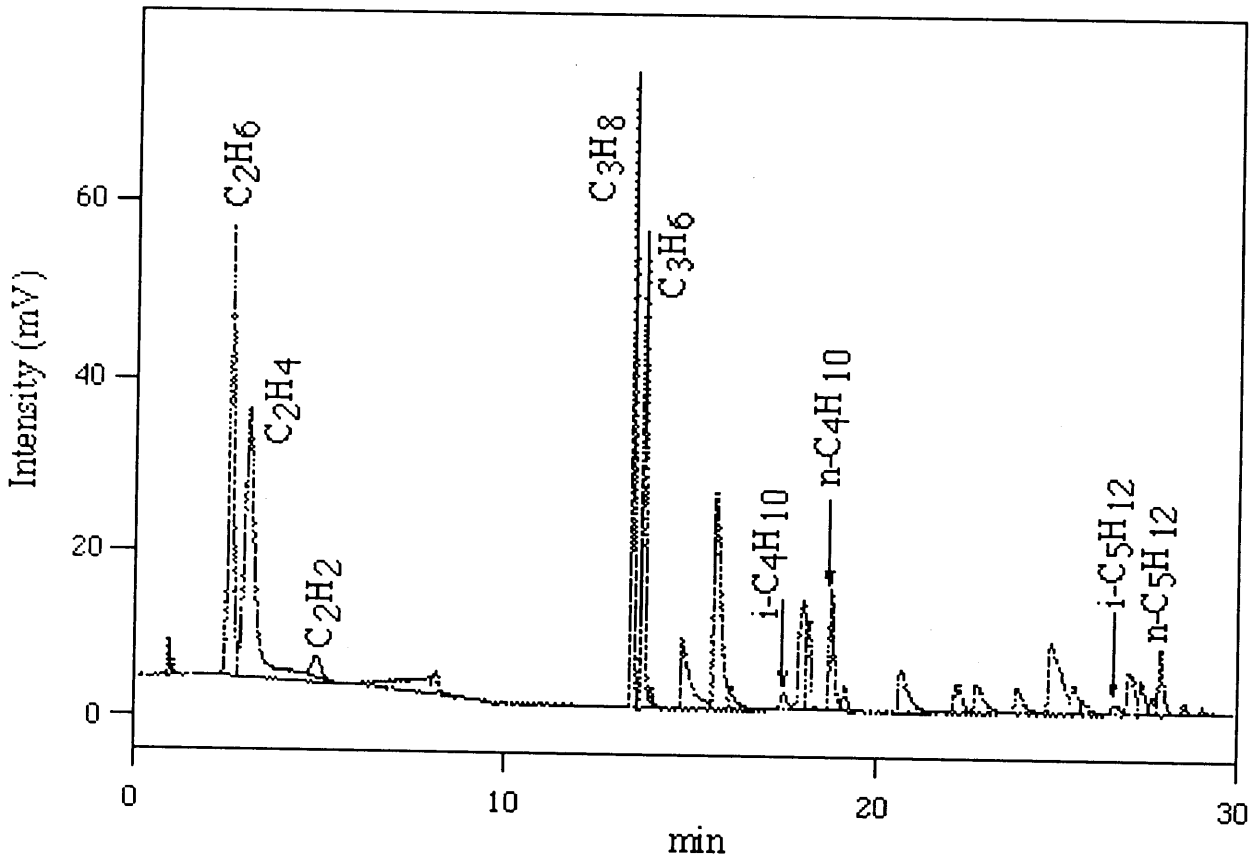

Figure 3.8 An example of a chromatogram for C_2-C_5 hydrocarbons by GC/FID with cryofocusing system.

(a) Duffusion theory technique

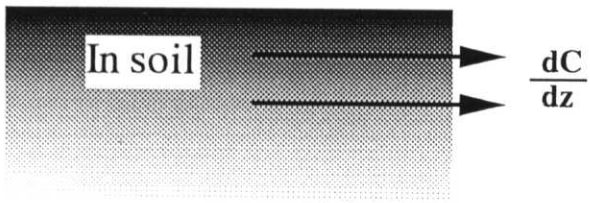

(b) Closed-chamber technique

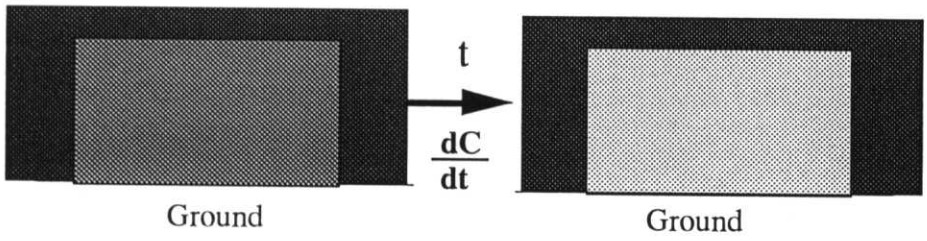

(c) Open-flow chamber technique

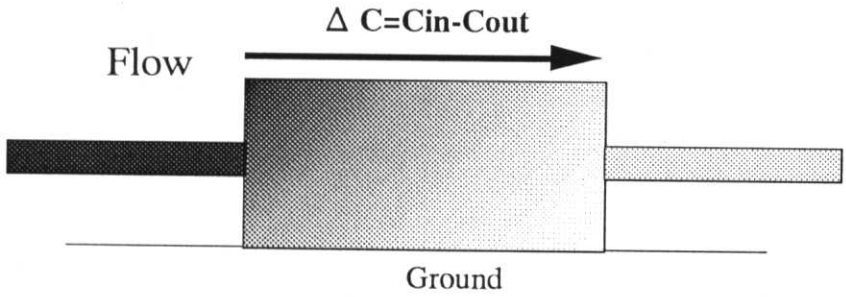

(d) Micrometeorological technique

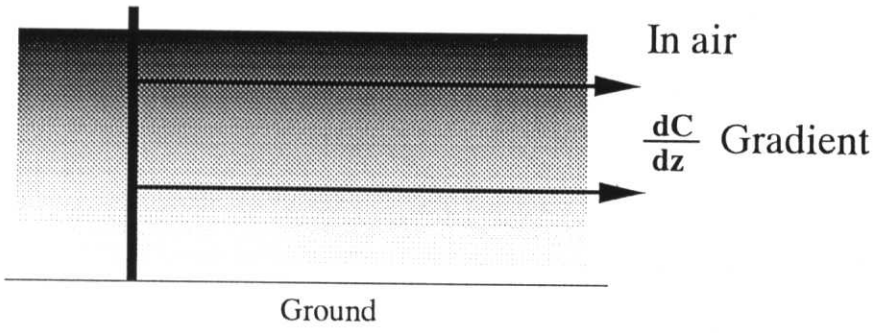

Figure 3.9 Techniques to measure surface uptake fluxes of gases.

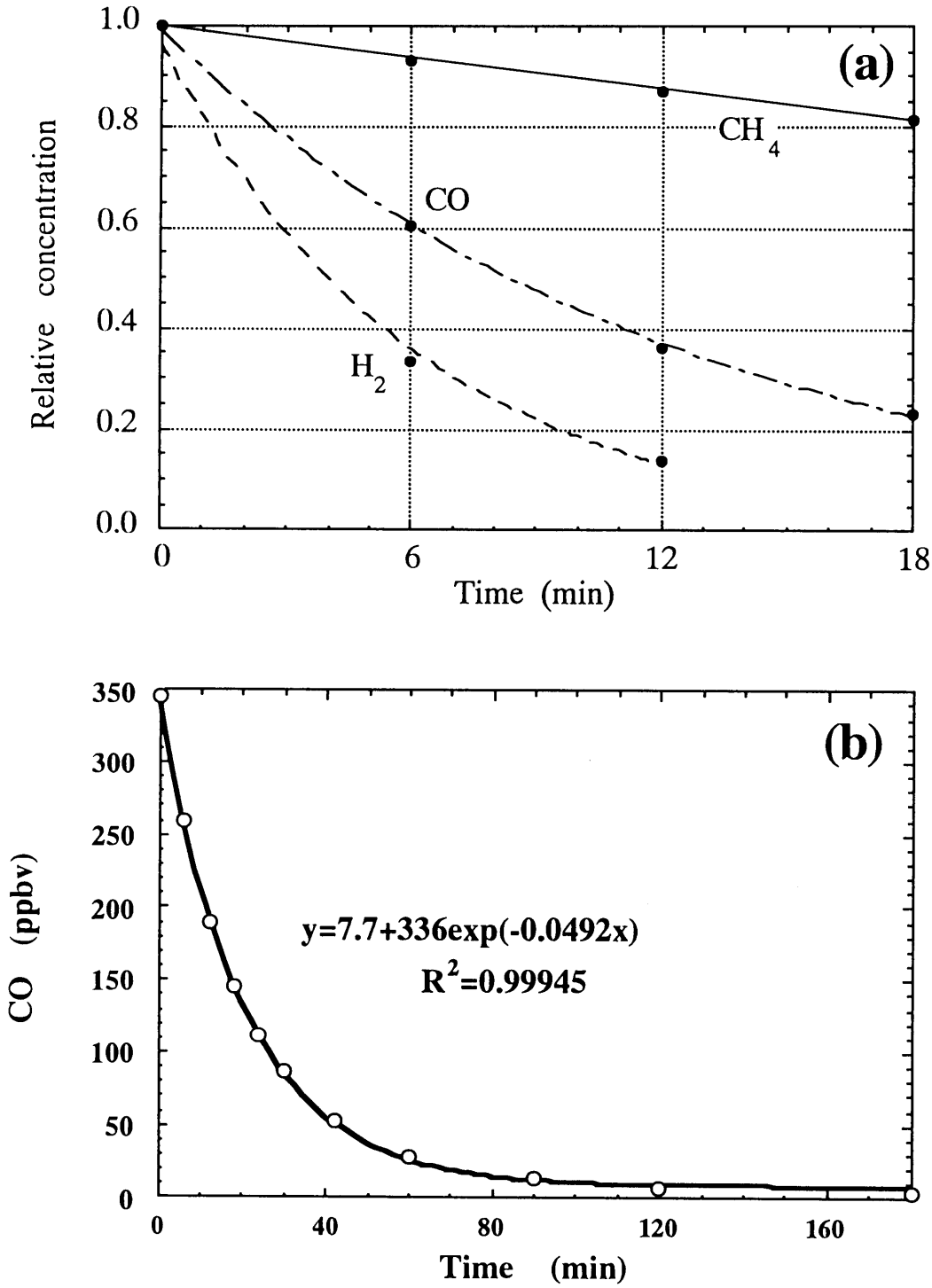

Figure 3.10 Changes in concentrations in closed-chamber. Data taken at (a) forest and (b) agricultural field in the campus of NIAES. Chamber height was 20 cm.

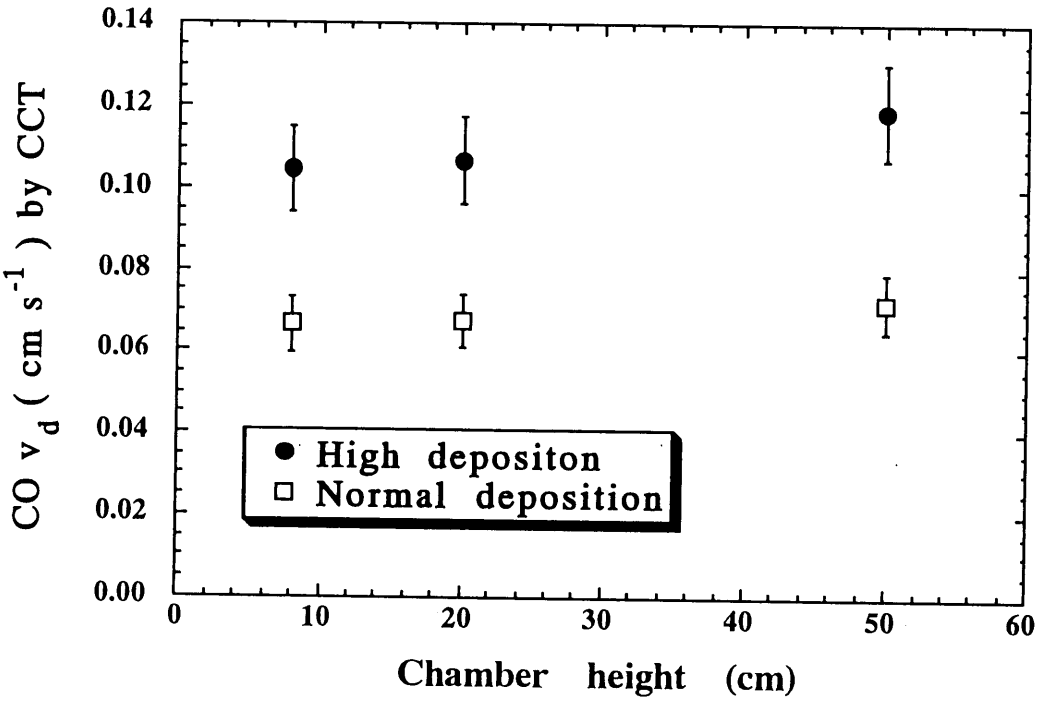

Figure 3.11 CO deposition velocities with changes in chamber height. Used chamber was 20cm by 20cm.

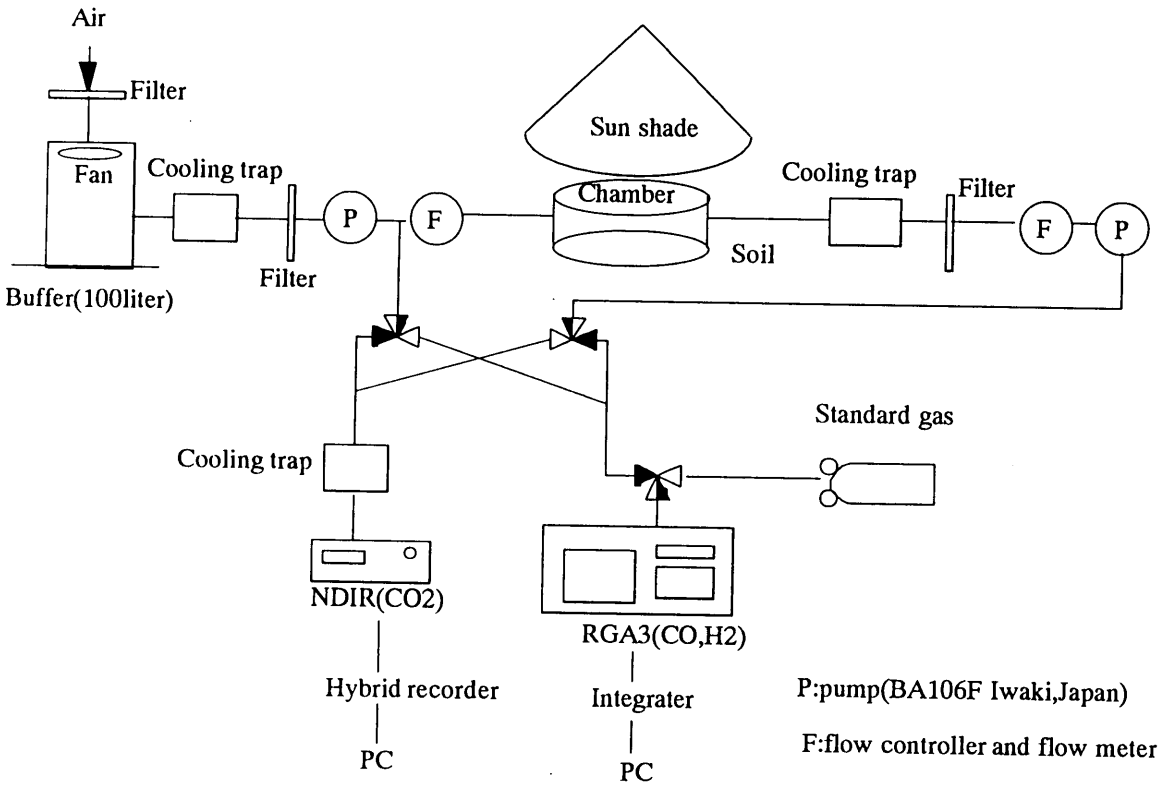

Figure 3.12 Schematic diagram of open-flow chamber technique.

Chapter 4

Field measurements of CO and H_2 uptake by soil

4.1 Introduction

This Chapter presents deposition velocities of CO and H_2 as measured in an arable field and a forest under temperate Japan by both the OFT (Yonemura et al., 1999b) and the CCT (Yonemura et al., 2000a) and seeks to elucidate the factors controlling those velocities. Furthermore, the relationship between deposition velocities and soil temperature and moisture content was investigated, which were continuously measured for a year by sensors using Time Domain Reflectometry (TDR). In Asia, few data are available on the soil influx of CO and H_2.

CH_4 uptake was also measured because CH_4 is similarly absorbed by soil and because the mechanisms involved in the CH_4 uptake may be a good information on CO and H_2 uptake. CH_4 is widely absorbed by aerated soils in various ecosystems (King, 1992; Dörr et al., 1993; Minamí et al., 1993). Soils, even under severe conditions such as in tundra (Whalen and Reeburgh, 1990) and desert (Striegl et al., 1992), can utilize CH_4. The uptake strength of CH_4 in forest soils is generally larger than in arable fields (Priemé and Christensen, 1997), due largely to the enhanced nitrification process in the latter soils because of the use of fertilizer, which reduces the oxidation of CH_4 (e.g., Adamsen and King, 1993; Arif et al., 1996; Hütsch, 1996). Priemé et al. (1997) show that CH_4 consumption rates took more than 100 years to reach pre-cultivation levels in abandoned fields in Denmark and Scotland. Mosier et al. (1997) shows that the conversion from grassland to croplands typically leads to a decrease in the soil's consumption of atmospheric CH_4. Among factors controlling CH_4 uptake by soils, soil diffusivity is considered to be the most prominent (Born et al., 1990; Dörr et al., 1993). However, biological processes are important as well (e.g., Adamsen and King, 1993). Thus, the processes of CO, H_2, and CH_4 deposition onto soils of an arable field and forest are discussed systematically.

Besides, CO_2 efflux was measured in the OFT measurements because it reflects the

total activity of microorganisms in soil.

4.2 Field description and experiments

Both experimental sites (arable field and forest) are situated on the campus of the NIAES (National Institute of Agro-Environmental Sciences; lat 36°01N', long 140°07'E) at Tsukuba Science City, 60 km northeast suburb of Tokyo. Tsukuba has a typical temperate climate. Mean annual air and soil temperatures at Tsukuba are about 13 and 14°C, respectively; mean annual precipitation at Tsukuba is about 1300 mm. In winter, under the influence of the continental anti-cyclone, sunny and dry conditions prevail, because Tsukuba is situated on the downward wind side of the central mountains of Honshu Island; in spring and autumn, cyclones and anti-cyclones come from the west by turns; from the middle of June to the middle of July is the rainy season; after the rainy season, under the influence of the pacific anti-cyclone, sunny conditions again prevail.

Meteorological data such as precipitation were measured at a distance of several hundred meters from the measurement site.

4.2.1 Arable field

The arable field experimental site (Photo 4.1) had been used as an agricultural experimental field for at least 20 years. The soil was an Andisol Hydric Hapludands (United States Department of Agriculture, Soil Conservation Service, 1994) developed to 200 cm depth in volcanic ash from Mt. Fuji and Mt. Asama. Soil pH (in H_2O) was about 6.4. The soil, designated "Kuroboku" in Japan, was very dark in color with a fine granular structure; the soil-particle density of the top soil (0-5 cm depth) was 2.66 g cm^{-3}. Carbon and nitrogen contents in the top soil (0-5 cm depth), analyzed with a MT-700 CN analyzer (Yanagimoto Co. Ltd., Japan), were 4-5% and 0.35-0.42% by weight, respectively. Carbon content can be considered identical to organic-carbon content at this pH. Particle-size distribution in the AP1 layer (0-5 cm depth) is 55% clay, 26% silt, 15% fine sand, and 4.4% coarse sand. Previous measurements of CO_2 fluxes were carried out in this arable field using the OFT (Osozawa and Hasegawa, 1995).

In summer 1995, a crop (*Vicia villosa*) belonging to *Fabaceae* was grown in the field.

In 1995, four plots were set up in an arable field to study the effects of soil moisture, gas-filled porosity as an index of gas diffusivity in the soil, and the vegetation on the fluxes of the above gases. The field was divided into 2 main plots in the middle of May 1995, and plowing and compaction were carried out using a plow and a roller. Soil three phases, solid, liquid, and gas and therefore gas diffusivities in the plots were changed by these management practices. The depth of the plowed soil was about 15 cm. Each main plot was sub-divided into a sub-plot with vegetation cover vegetative (*Vicia villosa*) and a bare sub-plot. Each sub-plot measured 5 m × 3 m. Two chambers of the OFT were installed in each sub-plot.

From November 1995 to the middle of May 1996, wheat (*Triticum*) was grown in the field. From the middle of May 1996 to the end of May in 1997, organic-matter content of the soil was modified by the application of dead crop material following the growing season of the crop. In the winter season from October 1995 to 15 May 1996 wheat was grown in the field. On 15 May 1996, the wheat was plowed into the soil. The depth of plowing was about 20-30 cm. At this time, the arable field was divided into 3 plots (3m×5m). In plot 0, the wheat was removed from the field and not plowed into the soil; in plot 1, the wheat was plowed in; and in plot 2, both the wheat that had grown on that plot and the wheat that had been removed from plot 0 was plowed into the soil. Thus, plot 2 had twice as much dead plant material plowed into the soil as did plot 1. On 25 May, *Cannabina* was planted. *Cannabina* belongs to *Fabaceae*, and its height at maturity is about 2 m. On 15 October 1996, the *Cannabina* was plowed into the soil and the plots were treated as they had been on 15 May 1996. After the plowing of the *Cannabina*, the field lay fallow until May 1997, when the measurements were stopped. The carbon contents of the surface-soil (0-5cm) from 0, 1, 2 plot, measured after passing the soil through a 5 mm stainless steel sieve, were 4.4, 4.5, 4.5 before the plowing on 15 October 1996 and 4.5, 4.7, 4.8 after the plowing, respectively (Fig. 4.1).

4.2.2 Forest

The forest experimental site was 360 m from the arable field (Photo 4.2). The site was covered by a secondary forest in transition from pine trees to deciduous trees. The site

had been forested for at least 20 years. The forest consisted mainly of pine trees (*Pinus densiflora*) and some deciduous trees (e.g., *Quercus myrsinaefolia*). Bamboo grasses (*Pleioblastus chino*) grew on the forest floor, which was covered by fallen trunks and dead leaves from the trees and dead bamboo grasses. The forest was typical of those of the plains of Japan.

The parent material of the forest soil was the same as that of the arable field. Therefore, the particle-size distribution of the forest soil was assumed to be similar to that of the arable field soil. The soil type was Typic Hapludand medial over loamy (United States Department of Agriculture, Soil Conservation Service, 1994) . The detailed characteristics of the soil are described by the Soil Management Support Services, USDA Soil Conservation Service and Japanese Committee of the Ninth International Soil Classification Workshop (1987) . The Ap horizon (basically A horizon but under plowing when the field was used as an arable field) extended to 3 to 5 cm depth at the chamber sites selected for flux measurements. The soil-particle density of the dark surface Ap horizon was 1.93 g cm^{-3} and that of the Ap horizon was 2.41 g cm^{-3}; the soil-particle density averaged over 0-5 cm soil depth was 2.28 g cm^{-3}. The carbon and nitrogen content of the Ap horizon was 29.1% and 1.7%, respectively, for dry soil and 10.99% and 0.66%, respectively, in the A horizon (Mineral horizons that have formed at the surface or below an O horizon). The carbon and nitrogen content averaged over 0-5 cm soil depth was 16.1% and 0.92%, respectively. The pH (in H_2O) of the Ap and A horizons were 5.0 and 5.1, respectively. Carbon content is identical to organic-carbon content at this pH.

4.3 Measurements

4.3.1 Characteristics of the gas profiles in the soil

Soil concentration profiles of CO, CH_4, and CO_2 were measured because these profiles reflect the gas diffusivity in soil. Samples of the soil air were taken at depths of 0, 5, 10, 20, 30, 50, and 70 cm at five locations in the field using stainless steel tubes inserted into the soil. CO and H_2 concentrations were measured by immediately injecting 10 ml samples into the RGA3 system using a gas-tight syringe. Further samples were injected into 5 ml or 10 ml evacuated vials for the analysis of CO_2 and CH_4.

4.3.2 Continuous measurements by the OFT

CO, H_2 uptake, and CO_2 efflux were measured by the OFT (Chapter 3.8) from 26 June 1995 which corresponds to the end of the rainy season until 26 August 1995 which corresponds to the end of summer. The schedule of the measurements in the plots subjected to different treatments is shown in Table 4.1. Measurement instruments, data loggers, and the flow control unit were set up in a temperature controlled cabin at the field site to apply the OFT. An auto-sampler was fitted to the system to allow the continuous automatic measurements necessary for the application of the OFT. The instruments were calibrated in the field. Data acquisition of CO_2 was conducted every 3 minutes to be synchronized with those of CO and H_2. The soil temperature at a 5 cm depth under the chamber and soil temperature profiles in the plots were also measured. The variations in deposition velocities were measured mainly in bare plots. In the OFT measurements, the net deposition velocity v_{nd} were used to express the intensity of CO deposition onto soil; deposition velocity v_d was used for H_2.

4.3.3 Long-term measurements by the CCT

In the arable field, six chamber bases for experiments by CCT (Chapter 3.7) were installed in the arable field in July 1996 and 9 were installed in October 1996, after the *Cannabina* was plowed into the soil. Two (July) or 3 (October) bases were installed in each plot. Each chamber was constructed from transparent Pyrex® glass and was 30 cm by 30 cm by 20 cm high with septum holes, holes for gas sampling, and valves. The chambers were covered with aluminum foil to avoid temperature enhancement. Hence, CO flux (deposition) data obtained in this study do not include photoproduction at the soil surface. The chamber bases were made from stainless steel with a groove where the chamber attached. The joint between the chamber and the chamber base was sealed by water.

Since summer 1995, before the experimental application of dead plant material, CO and H_2, and CH_4 uptake had been measured. CO and H_2 uptake was measured on 19 February, 28 February, 8 March, 26 March, 2 April, 9 April, and 17 April 1996. CH_4 uptake was measured on 11 July, 17 July, and 27 July 1995, and on 19 February, 28 February, 8 March, and 26 March 1996.

The measurements were made about 9:00 AM at least twice a month from July 1996 to May 1997. CO and H_2 uptake was measured on the following dates: 19, 23 July; 3, 12, 17, 24 September; 2, 7, 17, 18, 21 October; 4, 13, 18 November; 2, 12, 25 December 1996; 18, 27 January; 4, 10, 18, 24 February; 3, 10, 17, 25, 31 March; and 16, 26 May 1997. CH_4 uptake was measured on similar dates.

Gas sampling time was counted beginning about 30 s after enclosure. CO and H_2 were sampled using a gas-tight precision syringe at 0, 6, 12, and 18 min. Sometimes additional samples were taken after 18 min. CO and H_2 were analyzed immediately after sampling. CH_4 and CO_2 were collected in vials or 0.5 L Tedler® bags at -0.5 min (enclosed time) and at either 18 or 24 min. CH_4 and CO_2 were analyzed within 6 h of sampling.

In the forest, six chamber bases, the same as were used in the arable field, were installed in August 1996. The chamber sites were several meters apart. Flux measurements were conducted at about 9:00 AM from September 1996 to September 1997 on the following dates: 10, 18, 25 September; 3, 9, 15, 22 October; 1, 12, 19 November; 3, 10, 24 December 1996; and 16, 29 January; 5, 12, 19, 26 February; 5, 12, 19, 26 March; 2 April; 6, 13, 20, 27 May; 17 June; 8, 16, 23, 29 July; 6, 13, 20, 27 August; 3, and 17 September 1997.

Gas sampling in the forest was done by the CCT in the same way as in the arable field. At 0 min, a valve was open to the outside. Samples were collected in 0.5 L Tedler® bags. The gas samples were analyzed within 3 h after sampling. In this study, the concentrations at 0 and 6 min were employed mainly to calculate deposition velocities both in the arable field and in the forest , not to be subject to disturbance due to gas sampling by Tedler® bags. The difference (<5%) in calculated deposition velocities resulting from the difference in sampling methods between gas tight syringe and Tedler® bags was smaller than the precision (<15%) of CCT.

In the CCT experiments, to describe CO deposition onto soil, the phrase "deposition velocity" by itself is employed to mean "gross deposition velocity". To describe net CO deposition in soil, the explicit phrase "net deposition velocity" is employed as in the measurements by OFT. For H_2 and CH_4, only the phrase "deposition velocity" or v_d, is employed because H_2 and CH_4 production in aerated soil is negligible and only eqs. (3.1) and (3.2) are used for the calculation.

To understand what factors are responsible for controlling deposition velocities, linear

correlations of the deposition velocities with soil temperature and soil moisture was calculated. Unless otherwise noted, the correlation was expressed as R^{2*} in the CCT results, which is the coefficient of determination adjusted by degrees of freedom.

4.3.4 Measurements of $[CO]_{eq}$ in the arable field

We measured $[CO]_{eq}$ in the arable field by shading the surface with a chamber in March and July 1996 in order to continuously investigate the balance of CO production and uptake in the soil as expressed by eq. (1.17), using the equilibrium box technique (Conrad and Seiler, 1985a) . The shading chamber was made of vinyl chloride and could cover 2500 cm^2 (50 cm $\times$ 50 cm) of soil. $[CO]_{eq}$ was measured by continuously pumping air between the chamber and the injection line for the measurement of CO concentration. The error in $[CO]_{eq}$ introduced by the production of CO by the chamber material was experimentally estimated to be <3 ppbv at 40°C.

To calculate CO production rates, CO deposition velocities were measured by injecting gases containing a high concentration of CO (500 ppmv) at 3-h intervals during July 1996. CO concentration varied exponentially with time and was fitted using first-order kinetics.

4.3.5 Measurements of factors on deposition velocities- soil temperature and moisture

4.3.5.1 During OFT measurements

Soil core samples (100 ml) were taken from 0-5 cm surface soil in all the sub-plots and the soil moisture content was measured gravimetrically as an index of soil diffusivity. The sampling dates were June 16, 17, 18, 19, 20, 22, 24, 25, 28, 31 and August 2, 22. During the other days, the soil moisture data were interpolated using the thermoconductivity data recorded on a data logger (21X; Campbell Co. LTD., California U. S. A.). Soil thermoconductivities were measured in the field from 16 July to 21 August. The heat probe sensors were set at depths of 5 cm and 10 cm in each plot. The mean value of the two probes in each plot was correlated (R=0.78) with the soil moisture values. Gas-filled porosity was calculated from the soil moisture content and the soil particle density.

4.3.5.2 During measurements by CCT

Soil temperature was measured with Copper-Constantan thermocouple thermometers. The temperature signals were transmitted every 30 (arable field) and 60 min (forest) to a data logger model 21XL (Campbell Scientific Inc., CA, USA) and later transferred to a PC.

Soil moisture was continuously measured with Time Domain Reflectrometry (TDR) probes. Data were collected at 30-min or 1-h intervals by CS615 TDR sensors (Campbell Scientific Inc., CA, USA). The CS615 sensor has 30 cm-long double probes, and the measured value of soil moisture was averaged over a column of soil as high as the length of the probes and extending a few centimeters horizontally around the probes. Soil moisture could not be directly read from the output of the CS615 TDR sensors in volcanic-ash soils. The present study used a relationship proposed by Hatano et al. (1995) who calibrated for Japanese soils by the same method as used by Topp et al. (1982) :

$$q_{real} = 0.9454 q_{CS615} + 0.1168 \qquad (4\text{-}1),$$

where q_{CS615} is the volumetric water content calculated from the CS615 TDR sensor (dimensionless) and q_{real} is the real volumetric water content (dimensionless).

Soil temperature and moisture were measured in the arable field from 5 July 1996 to the end of May 1997. Three TDR sensors were installed horizontally at 3-5 cm depth near the chamber bases in each plot. Soil temperature was also measured at 0, 1, 2, 5, 10, and 20 cm depth at 2 sites in plot 0. Temperature and soil moisture data were saved every 30 min.

Soil temperature and moisture were measured in the forest soil from the beginning of December 1996 to September 1997. Three TDR sensors were installed horizontally in the soil surface at 3-5 cm depth in November 1996. Soil temperature was measured at 0, 2, 5, and 10 cm depth at 2 sites near the chamber bases. Temperature and soil moisture data were saved every hour.

4.4. Results

4.4.1 Characteristics of the gas profiles in the soil

When the soil gas was repeatedly extracted from 5 cm or 10 cm soil-depth, first extraction showed high CO value; later extractions showed constant values, CO concentrations showed small constant values, implying the equilibrium concentrations in soil (Fig. 4.2). The high concentrations observed in the first extraction were probably due to the contamination of tubes made of stainless. Extractions after that should have extracted soil gases around the soil depth probably also from ground. The almost constant concentrations after second extraction exhibit that both production and consumption reactions for CO (and H_2) are rapid in soil.

Samples were collected on June 26, July 9, 12, 19, 26, August 2, 24 1995, February 12, and March 13 1996. H_2 concentrations in soil were always below the detection limit, because of the strong oxidizing activity of enzymes and the lack of any production in soil (Conrad and Seiler, 1985a).

Figure 4.3 shows profile data of the CO, CH_4, and CO_2 concentration. Concentrations of CO in soil decreased rapidly from atmospheric concentrations on the soil surface to <20 ppbv at 5 and 10 cm indicating the presence of a strong CO oxidation (Fig. 4.3a). Therefore, the oxidation of CO occurred mainly on the surface soil (<5 cm). CO concentrations were higher in daytime rather than in nighttime, reflecting higher CO production in daytime due to high temperature. The CH_4 concentration decreased with increasing soil depth , but the rate of decrease was lower than that for CO , indicating that the oxidation rates of CH_4 in soil were lower (Fig. 4.3b). In contrast, the concentration of CO_2 in soil increased with the soil depth (Fig. 4.3c).

During the rainy season (July 9 and 12), CH_4 concentrations near the soil surface were low whereas those of CO_2 were high, suggesting that at that time the precipitated water acted as a barrier near the soil surface and limited the gas exchange between the atmosphere and soil. Spring data (February 12 and March 13) showed smaller gradients only for CO_2, showing the distinct presence of seasonal variation in CO_2 flux; less seasonal variation in CH_4 (, CO, and H_2) uptake.

4.4.2 Deposition velocities continuously obtained by the OFT

Figure 4.4 shows the changes in (a) rainfall, soil moisture level, and temperature, (b) CO_2 efflux, (c) CO deposition, and (d) H_2 deposition velocity throughout the OFT experiments. In 1995, since rainfall was above average and soil deposition of CO and H_2 was negligible due to the water cover until 26 June, the data prior to this date were not shown. The rainy season ended in the middle of July and afterwards the soil moisture level gradually decreased while the temperature increased (Fig. 4.4a). Similarly, CO and H_2 deposition velocities gradually increased during the measurement period (Fig. 4.4b, c). Deposition velocities of 0-6×10^{-2} cm s^{-1} for CO and 0-10×10^{-2} cm s^{-1} for H_2 of the present study were in the same order as those reported previously (Liebl and Seiler, 1976; Moxley and Smith, 1998a).

The CO_2 efflux (Fig. 4.4d) did not affect directly on CO and H_2 deposition velocities. Intermittent peaks of CO_2 effluxes which were observed in the beginning of July, coinciding with high rainfall (Fig. 4.4a), were not observed for CO and H_2 deposition velocities.

CO and H_2 deposition velocities were higher in the plowed plots. The effect of compaction or plowing on CO and H_2 deposition velocities was more conspicuous than that on CO_2 efflux. No striking differences in CO and H_2 deposition velocities between the measured deposition velocities in the vegetated and the bare sub-plots were observed.

Figure 4.5 depicts typical variations in CO and H_2 deposition velocities and CO_2 efflux over a few sunny days. During that time, CO mixing ratios ranged from approximately 180 ppbv to 1 ppmv. However, this wide range of CO mixing ratios did not affect the velocities. Daytime deposition velocities for CO and H_2 were smaller than nighttime values, and the diurnal variation in CO deposition velocities in August (Fig. 4.5b) was larger than that in July. Fig. 4.5c shows the effect of the soil temperature (5 cm) on CO and H_2 deposition velocities and CO_2 efflux. The latter was positively correlated with the soil temperature, while CO deposition velocities showed a slight decrease at higher temperatures. The daily averaged deposition velocities were higher when the surface soil was drier and gas-filled porosity in the surface soil had increased. Daily averaged CO and H_2 deposition velocities increased approximately 2% per day as the soil became drier (Fig. 4.5b).

Generally, the pattern of CO and H_2 deposition velocities obtained by the OFT

experiments was similar. The relationship between CO and H_2 deposition velocities measured in all the plots is shown in Fig. 4.6. The relationship appeared to be linear and the value of the ratio was similar to that reported by Liebl and Seiler (1976).

The relationship between the moisture content of the surface soil (0-5 cm) and CO and H_2 deposition velocities is shown in Fig. 4.7, and the relationship between the surface gas-filled porosity (0-5 cm) and CO and H_2 deposition velocities is shown in Fig. 4.8. Good correlations were found in the data shown in Figs. 4.7 and 4.8. In Fig. 4.7, in the lower range of CO and H_2 deposition velocities, there was a difference between plowed and compacted plots. On the other hand in Fig. 4.8, in the higher range of CO and H_2 deposition velocities, there was a difference between plowed and compacted plots.

4.4.3 Deposition velocities and production rates in the arable field obtained by CCT experiments

4.4.3.1 CO production from the arable soil

$[CO]_{eq}$ data obtained using the equilibrium box technique was higher in the summer than in the spring (Fig. 4.9) (eqs. 3.3-3.5). In the spring, $[CO]_{eq}$ was just a few ppbv, which is close to the detection limit of RGA3 at temperatures < 2°C. $[CO]_{eq}$ increased exponentially with soil temperature (Fig. 4.10). The net balance between production and soil uptake determine $[CO]_{eq}$ (eq. 1.17). Because production responds to soil temperature much more than does uptake (Conrad and Seiler, 1985a), $[CO]_{eq}$ increased with the soil temperature.

$[CO]_{eq}$ was also obtained by curve fitting of CO concentrations from the CCT measurements (eq. 3.3). Because the data that were taken for an enclosure time longer than 18 min were limited, the present study used the data from 28 February, 8 and 26 March, 9 and 17 April , 3 September, 19 July, and 12 and 17 September. CO production rates calculated from $[CO]_{eq}$ correlated positively with soil temperature (Figs. 4.11 and 4.12). The relationship between temperature and CO production rates obtained from the CCT experiments was of the same order as those reported previously (Conrad and Seiler, 1985a; Zepp et al., 1996).

To investigate what part of the soil profile accounted for the CO production rates measured at the soil surface by the CCT experiments, the present study calculated the correlation between CO production rates and soil temperature at various depths. The squared correlation coefficients were larger near the surface (Fig. 4.13) indicating that the several cm of soil near

the surface were responsible for the CO production rates observed at the soil surface.

4.4.3.2 Variation in deposition velocities in the arable field

Data from the period July 1996 to May 1997 is shown in Fig. 4.14. During this period, peaks in soil moisture corresponded to episodes of precipitation (Fig. 4.14b). In summer, when soil temperature was higher and precipitation was less, soil moisture rapidly decreased because of higher evapotranspiration. On the other hand, in winter (December to February), soil moisture varied only within a range of 0.05, even though the days were sunny. Frequent precipitation was recorded in November 1996 and from the end of March to May 1997.

Net CO, H_2, and CH_4 deposition velocities were calculated using eqs. (3.1) and (3.3) (Fig. 4.14c-f). CO gross deposition velocities were calculated iteratively, based on the relationship between soil temperature and CO production rates (Fig. 4.12). A clear seasonal cycle in CO, H_2, and CH_4 deposition velocities was not detected. Variations in CO, H_2, and CH_4 deposition velocities largely corresponded to the moisture pattern.

In July 1996, after the rainy season, soil moisture was high but rapidly decreasing due to high evaporation, and CO and H_2 deposition velocities were 1.5-4 and 3.8-7 cm s^{-1}, respectively. In September 1996, after continuous sunny days, deposition velocities were large. On 3 September 1996, a CO deposition velocity >8 cm s^{-1} was recorded at plot 2, which was the highest value obtained during this study. The H_2 deposition velocity could not be measured because the gas concentration rapidly fell under the detection limit after only 6 min. On that date, soil moisture was 23%, the lowest recorded on dates when deposition velocities were measured. From 12 September until 15 October, soil moisture data are lacking because of a measurement problem. However, from the middle of September, soil moisture probably increased because of high levels of precipitation. Corresponding to this precipitation, deposition velocities decreased. Just after the plowing on 15 October, CO emission was observed at plot 2. CH_4 emission was observed in the beginning of November at plot 2. Also in November 1996, higher soil moisture was observed (Fig. 4.14b). From December 1996 to the middle of May 1997, there were only a few episodes of precipitation and soil moisture gradually decreased. Correspondingly, CO and H_2 deposition velocities gradually increased. During that period, the increase in the CH_4 deposition velocity was

smaller than the increases in CO and H_2 deposition velocities. Not only such long-term trends, but also the detailed variation pattern in deposition velocities during the period correlated negatively with soil moisture. After the end of May, as precipitation continued, soil moisture began to increase. At that time, CO and H_2 deposition velocities decreased strikingly. In contrast, the CH_4 deposition velocity did not decrease.

CO_2 efflux (Fig. 4.14g) data indicate that more CO_2 was emitted from plots higher in organic-matter and when the temperature was higher. With respect to CO, H_2, and CH_4 deposition velocities, the most clear difference among the plots was observed in the case of H_2. The H_2 deposition velocity recorded in plot 2 was almost always higher than those recorded in the other plots. Before the field was plowed in October 1996, the difference in CO deposition velocities among the plots was clear; after the field was plowed, the difference was less clear. No clear difference in CH_4 deposition velocities among the plots was observed.

Overall, the relationship between soil moisture and deposition velocities during all measurement seasons was poor (CO; n=36, R^{2*}=0.246, p=0.0012, H_2; n=37, R^{2*}=0.230, p=0.0016, CH_4; n=28, R^{2*}=0.121, p=0.0389) where p is p value and n is number of samples. However, excluding periods when the variation in soil moisture was large, the correlation was far better during seasons during February 28 1996 to September 12 1996 (COv_d (cm s^{-1})=0.169-0.456*SM*; n=11, R^{2*}=0.861, p<0.0001, H_2v_d (cm s^{-1})=0.218-0.548*SM*; n=10, R^{2*}=0.676, p=0.0021 ,CH_4v_d (cm s^{-1})=0.00225-0.00422*SM*; n=5, R^{2*}=0.113, p=0.3066 where *SM* is soil moisture content (dimensionless)) and during November 13 1996 to March 25 1997 (COv_d=0.186-0.587*SM*; n=15, R^{2*}=0.688, p<0.0001, H_2v_d=0.316-0.988*SM*; n=15, R^{2*}=0.792, p<0.0001, CH_4v_d=0.00506-0.0159*SM*; n=15, R^{2*}=0.588, p=0.0005) (Fig. 4.15). The correlation between soil moisture and deposition velocity was higher in the cases of CO and H_2 than in the case of CH_4.

Even the correlation between deposition velocity and air-filled porosity calculated from soil moisture data and soil-particle density (=2.66 g cm^{-3}) during all measurement seasons remained poor. However, if the values for air-filled porosity are considered, more variation in deposition velocities occurred over a smaller range of variation in air-filled porosity than those by OFT.

It should be noted that the TDR sensors were reinstalled in the field after the plowing on 15 October, and the relation between soil moisture as measured by the TDR sensors and

surface-soil moisture responsible for the first diffusion of gas from the atmosphere to the soil, should have changed. Thus, it is natural that the correlation coefficients obtained before and after the plowing were different (Fig. 4.15). This reasoning is also applicable after precipitation, when the soil moisture gradients have not yet reached a steady state.

Simple correlations between soil temperature and CO and H_2 deposition velocities were poor. However, soil temperature is an important factor that controls the activity of oxidizers. The present study investigated R^{2*}, obtained by multiple correlation analysis of deposition velocities with soil moisture and soil temperature at various depths. Correlations of CO and H_2 deposition velocities could not be improved even when temperature was taken into account. CO and H_2 deposition velocities depended mostly on soil moisture. The present study found a good correlation, R^{2*}=0.569 (n=13), for CH_4 deposition velocity with soil moisture and soil temperature at 10 cm depth during the period from 2 December 1996 to 25 March 1997, when direct plowing and direct precipitation were not factors, although even during that period simple correlations with soil moisture and temperature remained low: R^{2*}= 0.266 (negative correlation) and 0.295 (positive correlation), respectively. At other depths, the correlation was poorer. Hence, during that period, CH_4 deposition onto soil was controlled by both soil moisture and soil temperature at about 10 cm depth.

The correlation between H_2 and CO deposition velocities was high, R^{2*}=0.881 (n=36), but the correlation between H_2 and CH_4 deposition velocities was poor, R^{2*}=0.168 (n=28). However, the correlation between H_2 and CH_4 deposition velocities calculated for the period from 13 November 1996 to 25 March 1997 was higher, R^{2*}=0.406 (n=15).

4.4.4 Deposition velocities and production rates in the forest obtained by CCT experiments

4.4.3.1 CO production from the forest soil

We calculated CO production rates in the forest soil, using data from the CCT experiments (Fig. 4.16). For the correlation with soil temperature (Fig. 4.17) (eqs. 3.3-3.5), the present study used the data from 6 March; 3, 27 May; 6, 23, 29 July; 6, 13, 27 August; and 3 and 17 September 1997, when temperature was being monitored continuously. Under the same soil temperature conditions, the CO production rates in the forest soil were about 2.5 times larger than those in the arable field. The temperature dependence of CO production rates in the forest was larger than in the arable field. The temperature dependence was

greater when correlated with deeper reference soil temperatures, as was the case with the data from the arable field.

The squared correlation coefficient was larger in the correlation with soil depth < 5 cm but deeper than those in the arable field (Fig. 4.18), implying that the CO production rates reflect in-situ CO production near the surface. Hence, the present study chose soil temperature at 2 cm depth for the correlation with CO production rates.

4.4.3.2 Variation in deposition velocities in the forest

We show variations in soil temperature, soil moisture, and deposition velocities in the forest in Fig. 4.19. In the forest, soil moisture content was less in July and August (Fig. 4.19b), as it was in the arable field. The variation in soil moisture content was a little smaller in the forest than in the arable field. Because the volumetric solid ratio was about 10% smaller in the forest soil, air-filled porosity in the forest soil was about 10% larger there than in the arable soil.

Gross CO deposition velocities were calculated iteratively, using the relationship between soil temperature and CO production rates (Fig. 4.17). The values of the CO and H_2 deposition velocities were of similar magnitude as those in the arable field. The values of CH_4 deposition velocity were about 3 times larger than in the arable field.

In comparison to data from the arable field, CO, H_2, and CH_4 deposition velocities were less variable, and these gases were always deposited onto the soil and never emitted. CO, H_2 and CH_4 deposition velocities varied from 1.5-3.5, 5-8, and 0.25-0.55 $\times 10^{-2}$ cm s^{-1}, respectively. A seasonal pattern in the deposition velocity was clear for CH_4; the CH_4 deposition velocity was larger in the summer. Seasonal trends in CO and H_2 deposition velocities were not observed. CO production in the soil effectively lowered net CO uptake by the forest soil; the CO net deposition velocity was smaller in June and July 1997, although the gross CO deposition velocity was not.

Short-term maximums and minimums in deposition velocities corresponded fairly well, but negatively, to the variation in soil moisture (Fig. 4.19b). However, although soil moisture dropped to < 0.25 in July and August 1997, an increase in CO and H_2 deposition velocities was not observed. It appears that only short-term variation in CO and H_2 deposition

velocities corresponded to the variation in soil moisture.

Correlations between soil temperature at 2 cm soil depth, soil moisture, and deposition velocities are shown in Table 4.2. A simple correlation between soil temperature and deposition velocities was positive for CO, H_2, and CH_4 deposition velocities from 2 December 1996 to the end of the experiment. The R^{2*} value calculated for the correlation of CH_4 deposition velocity with soil temperature was the highest obtained. For CO and H_2 deposition velocities, the correlation with soil temperature was not clear. The correlation for the period from 2 December 1996 to 27 May 1997, excluding the summer months, was even worse.

Simple correlations between soil moisture and deposition velocities were negative (Table 4.2, Fig. 4.20). The R^{2*} value for the CH_4 deposition velocity was largest. For the period from 2 December 1996 to 27 March 1997, excluding the summer months, R^{2*} values between soil moisture and CO and H_2 deposition velocities increased to 0.430 and 0.491, respectively.

Multiple correlation analysis between deposition velocities and soil moisture and temperature showed that deposition velocities positively correlated with soil temperature but negatively correlated with soil moisture.

The correlation between H_2 and CO deposition velocities in the forest was less striking than the results obtained in the arable field (Table 4.2). This difference is partly because the control range in deposition velocities was less than in the arable field. The correlation between H_2 and CH_4 deposition velocities was positive. For the period from 2 December 1996 to 27 May 1997, the correlations were much larger.

It should be noted that soil temperature and moisture are not completely independent variables--the correlation coefficient between soil temperature and moisture was not zero--and care should be taken to determine which factor is most important in controlling deposition velocities.

4.5 Discussion

4.5.1 Differences in exchange between emitted and absorbed gases by soil.

CO_2 efflux was less affected by the soil moisture content (Figs. 4.4a, d and 4.14b, g). CO_2 once produced in soil was eventually emitted from soil unless it was dissolved in water

and transported downward into deeper layers. Hence, higher CO_2 concentrations (Fig. 4.3c) and intermittent high CO_2 effluxes (Fig. 4.4d) were observed in the beginning of July, regardless of the lower production rate under lower temperature conditions (Fig. 4.4a). The CH_4 profiles (Fig. 4.3b) indicate that the CH_4 concentrations were lower in the beginning of July. CH_4 deposition was lower when the soil moisture level was higher because the diffusivity in soil was hindered and CH_4 oxidation occurred only in the top soil layer.

In contrast to the CO_2 efflux and in the same way as CH_4 deposition, CO and H_2 deposition velocities were strongly controlled by the soil moisture content which predominantly controlled the gas-filled porosity (Figs. 4.4b, c, 4.7, and 4.8). Hence, the gas transport from the atmosphere to soil was considered to be more important for the gases deposited onto soil.

4.5.2 CO, H_2, and CH_4 deposition velocities

4.5.2.1 General

The gross CO deposition velocities obtained by the CCT experiments ranged from $0\text{-}7 \times 10^{-2}$ cm s^{-1} in the arable field and from $1.5\text{-}4.5 \times 10^{-2}$ cm s^{-1} in the forest. The mean values were $2.42 \pm 1.60 \times 10^{-2}$ cm s^{-1} (n=38) in the arable field and $2.70 \pm 0.60 \times 10^{-2}$ cm s^{-1} (n=37) in the forest. The data in the arable field by the CCT lack measurements in August and may underestimate the deposition velocities. Although the averaged CO deposition velocity was slightly higher in the forest, the highest CO deposition velocity was observed in summer in the arable field. Variation in CO deposition velocities was larger in the arable field. These averaged values are within a reasonable range of those reported for mid- or high latitudes prior to this study (Liebl and Seiler, 1976; Conrad and Seiler, 1980b; Zepp et al., 1997; Sanhueza et al., 1998) . CO and H_2 deposition velocities from various studies are summarized in Table 4.3. Values of CO deposition velocities are high at sites in mid-latitudes; vice versa at sites in dry and high-latitudes. The globally averaged CO deposition velocity on biologically active lands excluding desert and snow areas is likely to be $2\text{-}3.5 \times 10^{-2}$ cm s^{-1}.

The difference between net and gross CO deposition velocities was roughly similar in both arable field and forest. Initial concentrations of CO in the chamber ranged from 180 to 800 ppbv. On the other hand, the CO equilibrium concentration in the soil changed from a

few ppbv to >100 ppbv. The ratios of gross CO deposition velocities to net deposition velocities were usually within several percentage points in winter and within 20% in other seasons. However, a larger correction, as much as 20-50%, was needed under high moisture conditions because high equilibrium concentrations were observed/estimated (eq. 1.17) when air-filled porosity was lower (Figs. 4.14c, d and 4.19c, d).

The H_2 deposition velocities obtained by the CCT experiments ranged from 0-9 $\times 10^{-2}$ cm s^{-1} in the arable field and from 5-8 $\times 10^{-2}$ cm s^{-1} in the forest. The mean values were 4.29±2.19 $\times 10^{-2}$ cm s^{-1} (n=38) in the forest and 6.26±0.94 $\times 10^{-2}$ cm s^{-1} (n=38) in the forest. As with CO, high H_2 deposition velocities in the summer were not incorporated in the averaged value. Variation in H_2 deposition velocities was larger in the arable field, as was the case with CO. These averaged values are smaller than those reported by Liebl and Seiler (1976) (Table 4.3). The globally averaged H_2 deposition velocity on biologically active lands is likely to be 5-7 $\times 10^{-2}$cm s^{-1} (Table 4.3).

The CH_4 deposition velocities obtained by the CCT experiments ranged from 0.05-0.1 $\times 10^{-2}$ cm s^{-1} in the arable field and from 0.3-0.6 $\times 10^{-2}$ cm s^{-1} in the forest. The mean values were 0.0857±0.0371 $\times 10^{-2}$ cm s^{-1} (n=32) in the arable field and 0.410±0.083 $\times 10^{-2}$ cm s^{-1} (n=37) in the forest. There was a distinct difference in CH_4 deposition velocities between the arable field and the forest. These averaged values are large compared to previous results (e.g., Dörr et al., 1993; Dobbie and Smith, 1996; Priemé and Christensen, 1997; Savage et al., 1997) in both arable field and forest. It may also have been caused in part by the higher in-situ uptake because of higher temperatures in Japan compared to Europe. High temperatures may create good conditions for the CH_4 oxidizers. The difference between CH_4 and CO and H_2 deposition velocities must be caused by the difference in the order of in-situ uptake as was shown by core/incubation studies (e.g., Adamsen and King, 1993; Bender and Conrad, 1994b; Moxley and Smith, 1998a) because it cannot be explained by soil physical properties. The reason why CH_4 deposition velocities were different between the arable field and the forest has been discussed (e.g., Keller et al., 1990; Lessard et al., 1994) and can be partly explained by the difference in in-situ uptake rates (e.g., Keller et al., 1990; Priemé et al, 1997) largely

resulting from nitrogen fertilization effect and, by the disturbance by tillage in arable fields (Mosier et al., 1991; Bender and Conrad, 1994), and by the high gas diffusivity in the forest soil as expected from the lower soil densities (Keller et al., 1993).

Previous core/incubation studies (Hendrickson and Kubiseski, 1991; Moxley and Smith, 1998a) show that CO utilization rates are positively correlated with soil organic-matter content, and forest soils have larger uptake potential than do arable soils. However, according to data of the present study, CO deposition in the arable field and forest were of the same magnitude, although the forest soil had a high organic-matter content. This is attributed to compensation caused by the diffusional resistance of the leaf layer (Sanhueza et al., 1998). Moreover, it should be noted that the positive relationship between soil organic-matter content and in-situ uptake obtained by the core/incubation experiments may not be applicable simply to the top soil responsible for the oxidation of CO and H_2.

4.5.2.2 Soil moisture and deposition velocities

From Figs. 4.7, 4.15, and 4.20, it can be seen that deposition velocities correlated strongly with soil moisture (3-5 cm) both in the arable field and in the forest. Soil moisture changes various factors, including the molecular diffusion of gases in the soil and the activity of oxidizers of CO, H_2, and CH_4. Soil gas diffusivity increases as soil moisture decreases because the gases diffuses 10^4 times more rapidly in air than it does in water. Furthermore, it should be noted that the fertilization effect of the gas itself (Ingersoll et al., 1974; Spratt and Hubbard, 1981) induced by the change in soil diffusivity resulting from a change in soil moisture leads to more diffusional control on deposition velocities.

Deposition velocities in the forest were controlled to a far smaller extent by soil moisture than results in the arable field. Hence, the control exerted by soil moisture on deposition velocities because of soil diffusivity was less effective in the forest than in the arable field. This observation is also supported by high WFPS (Water-filled pore space, namely intra-aggregate pore space; Saxton et al., 1986) values reported by Sanhueza et al. (1998).

Soil within the uppermost 5 cm is responsible for the oxidation of CO and H_2, (Liebl and Seiler, 1976; Sanhueza et al., 1998; Kuhlbusch et al., 1998) , and the uppermost 1 cm of

surface-soil is especially important as an interface between the atmosphere and soil. For CH_4, the oxidation layer is several centimeters deep, and the top <1cm of soil does not show uptake (Adamsen and King, 1993; Koschorreck and Conrad, 1993; Bender and Conrad, 1994b) . However, top soil is also important for CH_4, because the top soil is a diffusion path from the atmosphere to the oxidizers. Soil moisture measured by TDR sensors installed at a soil depth of several centimeters may not reflect the soil moisture content of the oxidation layers or of the diffusion path from the atmosphere to the oxidizers. Accordingly, the relationship between soil moisture content as measured by TDR sensors and top soil moisture (TSM) relevant to the deposition of CO, H_2, and CH_4, should be made clear.

We show short-term variation in TDR soil moisture values for the arable and forest soils in Figs. 4.21 and 4.22. Diurnal variation in soil moisture was far larger in the arable soil than in the forest soil. The diurnal variation was caused by high evaporation in the arable field at high temperatures and was larger than the seasonal increase in summer (Fig. 4.21a, b, c). Because a certain soil moisture gradient could be established by evaporation from the soil surface without direct precipitation, TSM is considered to be lower than the TDR soil moisture value. Thus, even if the TDR soil moisture content is the same, TSM should be much lower compared to values obtained by TDR in the summer when the soil temperature is high. During sunny days in summer, soil moisture decreased considerably, and the diurnal variation was quite small (Fig. 4.21c). Under these conditions, water is supplied from the deeper soil layer and a constant upward water flux is realized and the relationship between TSM and TDR soil moisture contents should be fairly stable.

As seen by the small diurnal variation (Fig. 4.22), evaporation in the forest was partly suppressed by the leaf layer present above the soil and lower daily-maximum soil temperature. However, even in the forest, the decrease in soil moisture in the summer (Fig. 4.22b) was larger than in other seasons (Fig. 4.22a). Therefore, the relationship between TSM and TDR soil moisture can be changed even in the forest.

Precipitation greatly disturbed the soil moisture profile, particularly the relation between TDR sensor values and TSM (Figs. 4.22d and 4.23c). With respect to diurnal variations, it took a few days for the soil moisture profile to reach a steady state. It is also possible that the oxidizing activity was lower immediately after rain because the fertilization effect was inactive during rain. The scattering observed in the relationship between TDR soil moisture and

deposition velocities during all measurement seasons in the arable field can be attributed to the poor relationship between TSM and TDR soil moisture contents throughout the period of measurements as well as to the tillage and to the application of dead plant material to the field. When the correlation period was suitably chosen to ensure a steady relation between TSM and TDR soil moisture content, good correlations were obtained (Fig. 4.15). In Fig. 4.15, the data from 24 September 1997 and from 31 March and 16 and 26 May 1997 were excluded because these dates fell just after episodes of precipitation. On these days, diurnal variation in soil moisture amounted to 0.02 (Fig. 4.22d), supporting the unstable state of water distribution in soil. Data from 17 and 18 October and from 4 November 1997 were also excluded because the soil might have been unstable soon after plowing. A similar discussion is applicable to the correlations found in the forest soil (Fig. 4.20).

Noteworthy is that the CH_4 deposition velocity decreased on 24 September 1996 but not on 31 March, or on 16 or 26 May 1997, although CO and H_2 deposition velocities were low on all these dates. This discrepancy can be explained by the differences in the depth of the oxidation layer of CO, H_2, and CH_4. On 24 September 1996, the TDR soil moisture was high, indicating that the soil was wet in all layers, including in the CH_4 oxidation layer. On the other hand, on 31 March, and on 16 and 26 May 1997, the TDR soil moisture was low, so the layer responsible for CH_4 uptake was relatively dry. Only the top soil responsible for CO and H_2 oxidation could have been wet.

4.5.2.3 Soil temperature and deposition velocities

The daily temperature dependency of CO and H_2 deposition velocities obtained by the OFT experiments (Fig. 4.5c), supports the data presented in fig.6 by Liebl and Seiler (1976). In Fig. 4.5b, only a slight decrease in net deposition velocities was detected even during the days when the soil temperature was higher (Fig. 4.5a) and the abiological CO production from organic matter was highest. High net deposition velocities were not only recorded in the night but also during the day and may be explained as follows: nitrogen application to the arable soil may have stimulated the bacterial/enzymatic uptake ability of CO and H_2, as reported in previous studies (Conrad, 1988; Bender and Conrad, 1994a) who addressed nitrifiers as the most effective CO oxidizers in soils. Soil temperature as well as moisture conditions were optimal for nitrification in the study area.

Seasonal trends largely attributable to the trends in soil temperature affected CH_4 deposition velocities slightly in the arable field (Fig. 4.14f) and clearly in the forest (Fig. 4.19f, Table 4.2) although CO and H_2 deposition velocities did not. The seasonal trend in CH_4 deposition velocity (~50%) is partly explained (~12%) by the increase in molecular diffusivity induced by higher summer temperatures (Chapter 5). Furthermore, the temperature dependence of CH_4 in-situ uptake of soil samples from laboratory experiments in the physiological temperature range of 5-30°C, is almost insignificant at atmospheric concentration of CH_4 (King and Adamsen, 1992; Whalen and Reeburgh, 1996). Therefore, the seasonal trends in CH_4 deposition velocity should be attributable to variation in the diffusivity because of the trends in soil moisture influenced by the trends in soil temperature (e.g., Crill, 1991; Castro et al., 1995).

Seasonal trends in CO and H_2 deposition velocities driven by soil temperature should be masked by strong control by soil moisture because a short-term relationship can be established by laboratory experiments between CO and H_2 in-situ uptake and temperature; the temperature dependence of CO and H_2 in-situ uptake of soil samples from laboratory experiments in the physiological temperature range of 5-30°C, is not large but significant, at about E_a=5-30 kJ mol^{-1} (Liebl and Seiler, 1976; Conrad and Seiler, 1985a; Schuler and Conrad, 1991; Kuhlbusch et al., 1998) where E_a is the activation energy by Arrhenius equation (Conrad and Seiler, 1985a, b).

4.5.3 Differences in deposition velocities resulting from management practices in the arable field

Although Liebl and Seiler (1976) suggested that vegetation enhances deposition velocities, this was not reflected in the results by OFT experiments, since no difference between the measured CO and H_2 deposition velocities in the vegetated and the bare sub-plots were observed. The lack of striking differences in the CO and H_2 deposition velocities between vegetated and plowed plots may be due to the low vegetation density, and also due to the fact that the duration of the experiment was too short to detect differences. Further studies should be carried out on the role of vegetation.

Through plowing and compaction, soil showed the similar moisture content but higher and lower gas-filled porosity, respectively (Figs. 4.7 and 4.8). The differences in the CO

and H_2 deposition velocities between plowed and compacted soils are consistent with the measurements of Rust et al. (1957) who suggested that the decrease in the gas-filled porosity by water affects diffusion more than the decrease in gas-filled porosity by solids, i.e. due to compaction. Gas diffusivities in soil were controlled not only by the gas-filled porosity but also by the soil moisture content. Therefore, to explain the details of CO and H_2 sorption, not only gas-filled porosity but also liquid to solid ratio should be considered in the diffusion calculation.

The emission of CO and CH_4 from plot 2 after the plowing of plant dead materials on 15 October 1996 (Fig. 4.14) was apparently a result of the plowing of the dead plant material. Two reasons might account for the CO emission; first, $[CO]_{eq}$ may have risen because soil moisture content was higher after the plowing (Fig. 4.14b); second, emission from the dead plant material that had been plowed into the soil may have occurred. Both reasons could account for the CO emission. The CH_4 emission might have been caused by the degradation of the dead plant material applied under conditions of high soil moisture.

Averaged H_2, CO, CH_4 deposition velocities and CO_2 efflux for each plot for the period from 13 November to 25 March 1997 are shown in Fig. 4.23. H_2 and CO deposition velocities were about 8 and 12% higher, respectively, in plot 2, which had had more dead plant material plowed into the soil, compared to plot 0. A difference in CH_4 deposition velocities among the plots was not observed, probably because of the lower precision of CH_4 data.

The application of dead plant material changed the physical properties of the soil. The clear difference in CO and H_2 deposition velocities among the plots may be partly because of the difference in soil moisture among the plots. One percent of the difference in soil moisture (0-5cm) between 0 and 2 plots was observed by gravimetric method (data not shown). This difference could account for a variation in deposition velocity of about 10% (Fig. 4.15), which is about the amount of variation observed among the plots. Nevertheless, that increased bacterial/enzymatic activity and consequent absorption of CO and H_2 results from the application of dead plant material is undeniable.

In arable fields, various management practices modify soil properties: CH_4 uptake is hindered by nitrogen fertilizer applications (e.g. Hütsch, 1996; Arif et al., 1996) ; CH_4 uptake profile is modified by plowing (Bender and Conrad, 1994b) ; CO and H_2 uptake is accelerated

by plowing (Figs. 4.7 and 4.8; Sanhueza et al., 1994a). To understand the variation in deposition velocities in arable fields, the impact of management practices on the deposition velocities must be investigated on the emphasis of both physical and biological aspects.

4.5.4 Relationship between deposition velocities

In both the arable field and the forest, R^{2*} between H_2 and CH_4 deposition velocities was larger if calculated using the data collected from December 1996 to March 1997 than if data collected over the entire period of measurement were included. This difference can be partly explained by the difference in temperature dependence of the CH_4 and H_2 deposition velocities as discussed earlier: H_2 deposition is not much controlled by soil temperature; CH_4 deposition is dependent on soil temperature. Hence, during the period when the temperature variation is large, the correlation is poor.

The relationship between H_2 and CO deposition velocities found by this study and by previous studies (Liebl and Seiler, 1976; Conrad and Seiler, 1985a) , is shown in Fig. 4.24. The slope of the correlation line for the forest in this study is shallow in comparison to the other slopes. This difference can be explained by the diffusional resistance of the leaf layer in the forest (Sanhueza et al., 1998). In the forest, CO deposition velocities were more effectively lowered than those of H_2 because of diffusional resistance by the leaf layer. There is also a slight difference in slope between the arable field data of this study and the data of Liebl and Seiler (1976) . Just as the leaf layer caused diffusional resistance in the forest soil, the biologically non-active surface layer, which also causes diffusional resistance, may be thicker in this study because measurements in this study were conducted over several seasons, including periods when the field was fallow and the surface-soil may have been stressed by drought and high temperature. This drought or high temperature effect is clearer in aid soils as Andalusia and Transvaal.

Although the oxidizers of H_2 and CO are considered to be different (see 1.3.2), the one-to-one relationship is striking. If the enzyme/bacterial utilization efficiency of H_2/CO in the liquid matrix of oxidizers is very large, the diffusion in the path from the atmosphere to the matrix of the oxidizers determines the H_2 and CO uptake rates. CO and H_2 are not very different with respect to water solubility, which is responsible for their diffusion from the ambient soil air to the oxidizer, but their molecular diffusivity is different. Considering the

pathway to matrices of the relevant oxidizers for H_2 and CO uptake, the difference between CO and H_2 deposition velocities reflects the difference in their molecular diffusivities.

4.5.5 CO production in soil

For the characterization of CO production in soil, both absolute values and its dependence on temperature are important factors. The present study express the temperature dependence of CO production rates by the activation energy, E_a (kJ mol^{-1}) using the Ahhrenius equation (Conrad and Seiler, 1985a, b):

$$\ln P_{CO} = \text{const} - E_a/(R_g T), \quad (6.2)$$

where R_g is gas constant (8.31 J mol^{-1} K^{-1}) and T is soil temperature (K).

CO production obtained from CCT experiments in an arable field and a forest (Figs. 4.12 and 4.17), increased exponentially with soil temperature at E_a= 67 and 106 kJ mol^{-1}, respectively. A short-term experiment using equilibrium box techniques in the arable field (Fig. 4.9) also showed an exponential relationship between CO production rates and soil temperature at E_a=75 kJ mol^{-1}.

The similarity of the temperature dependence obtained from the chamber experiments in the arable field and from the equilibrium box techniques indicates that the temperature dependence is stable over a long time frame. Previous studies (Conrad and Seiler, 1985b; Moxley and Smith, 1998b) show that CO production rates are not greatly altered by changes in soil moisture (10-35%) when the soil temperature is constant.

Conrad and Seiler (1985a) obtained E_a=57-102 kJ mol^{-1} in arid soils at Andalusia, Spain; and the Transvaal and Karoo, South Africa by the CCT. This value is comparable to the value obtained in the arable field of this study. However, the E_a value obtained in the forest soil in this study is larger. Firstly, the larger forest value was caused by the difference in temperature variation at the two sites and the difference in the depth at which temperature was referred. Temperature gradients under field conditions were steep in the top soil. If the sensors are installed close to the soil surface, then temperature is sensitive and temperature dependence (E_a) is small. This observation is consistent with the reference depth of 2 cm in the forest and deeper than 1 cm in the arable field. Secondly, the E_a value from the forest

may have been larger because the forest soil was humic acid rich near the surface, which could significantly change not only the absolute value of CO production but also its kinetics (Conrad and Seiler, 1985b; Moxley and Smith, 1998b) . However, the E_a was larger in the forest and the pH of the forest soil was low, contrary to the results reported by Conrad and Seiler (1985b) that E_a becomes larger as pH becomes larger. Then, the first explanation more probably accounts for the difference between E_a in the arable field and the forest.

The absolute values of CO production at 25°C in the arable field and the forest are 12.3 and 38.6 $\times 10^9$molecules cm^{-2} s^{-1}, respectively, (a ratio of 3.1) and the carbon contents are about 4.6 and 29.1%, respectively, (a ratio of 6.3) (Figs. 4.12 and 4.17). Previous laboratory experiments (Conrad and Seiler, 1985b; Moxley and Smith, 1998b) , show that CO production is proportional to the organic-matter ratio of the sample soils. At first glance, data of this study, which show different ratios, contradict their studies. However, as is shown in eq. (1.17), the $[CO]_{eq}$ and therefore the CO production rate observed at the soil surface are related to the in-situ production rate on the spatial base, $P_{in\text{-}situ}$ (s^{-1}). The solid-phase ratio of the forest soil (12.7±1.2%, n=28) was about half that of the arable soil (24.0±1.1%, n=23); the particle densities of the arable and forest soil near the surface were 2.66 and 1.92, respectively. Adjusting for these differences and assuming deposition velocity to be 2.7 $\times$ 10^{-2} cm s^{-1}, the CO production from a unit mass of carbon in the arable-field and forest soils is estimated to be 1.55 and 2.01 $\times 10^{12}$ molecules Cg^{-1}, respectively. Hence, it is concluded that a unit mass of carbon, equal to organic-carbon in this study, considering pH, emits a similar amount of CO both in the arable field and in the forest. From this point of view, CO production rates observed at the soil surface should be interpreted taking into account the solid-phase ratio of the soil as well as the organic-carbon content. Thus, even though in-situ CO production is proportional to organic-carbon content in the laboratory studies, this observation is simply not applicable to the CO production rates observed in the soil surface when the soil physical properties are different to a large extent.

It should be noted that the CO production rates obtained reflect CO production only in the top soil (Figs. 4.14 and 4.19). The deeper soil does not contribute to CO production at the soil surface because the CO produced in the deeper layer is rapidly utilized by in-situ oxidizers. Deeper soil may contribute to CO production rates when CO gradients are gentle,

as expected when diffusivities are low. When air-filled porosity is low during precipitation, CO may be emitted from the soil because CO oxidation is weak, so CO production in the deeper layer may contribute to CO at the surface.

Hence, CO production rates at the soil surface obtained with the CCT depend not only on in-situ production rates but also on in-situ uptake rates. The above estimated values might have been lower in the forest soil if the in-situ CO uptake rates of the forest soil had been larger than in the arable soil.

4.6 Summary

In this Chapter, firstly, CO and H_2 deposition velocities and CO_2 efflux were measured by the open-flow technique (OFT) during the summer of 1995. This is the first trial of measurements of CO and H_2 soil uptake by OFT. The deposition velocities were very low during the rainy season, then increased gradually as the soil surface became drier. The gas profiles in the soil also reflected the moisture conditions. Deposition velocities in the plowed plots were higher than those in the compacted plots. The ratio of the deposition velocity of H_2 to that of CO were approximately 1.6. The deposition velocities were not directly correlated to the CO_2 efflux. The changes in the gas diffusivity resulting from the soil moisture content affected more on the CO and H_2 deposition velocities than on CO_2 effluxes. In temperate and moist climates such as Japan, soil moisture level regulates the exchanges of CO and H_2 between the atmosphere and soil through two mechanisms. One is related to gas transport; higher soil moisture leads to lower gas diffusivity. The other is associated with the bacterial/enzymatic uptake activity of CO and H_2 which decreases under the optimum moisture level for the oxidizers.

Secondly, in the closed chamber experiments, CO, H_2, and CH_4 deposition onto soil was measured in an arable field and in a forest 360 m apart in temperate Japan for about a year. It is first time to monitor CO and H_2 deposition velocity along with high-precision soil moisture measurements by TDR sensors. The results of these experiments reconfirmed in longer measurements that soil moisture controls CO and H_2 uptake by the soil.

The CO production rate observed at the soil surface by the closed-chamber experiments was dependent exponentially on surface-soil temperature. CO production was larger in the

forest than in the arable field when the soil temperature was the same.

The deposition velocities obtained by the closed chamber technique are of the same magnitude as those obtained by previous studies (Table 6.3). The difference between the deposition velocity of each gas in the arable field and forest was largest for CH_4, smaller for H_2, and smallest for CO. However, net uptake of CO was larger in the arable field because of larger production rates in the soil. The net uptake of CO correlated negatively with soil temperature. This was attributed to the greater production rate when the soil temperature was higher.

In the arable field, the deposition velocities were controlled mainly by soil moisture content of the top soil. The clear correlation between CO and H_2 deposition velocities and soil temperature was not observed. Application of dead plant material to soil led to slight (~20%) acceleration of CO and H_2 deposition onto the soil, partly because of the increase in diffusivity caused by the physical transformation of the soil.

Variations in the deposition velocities were smaller in the forest than in the arable field and corresponded to the soil moisture. Long-term (seasonal) trends caused by variation in temperature were observed only for CH_4 deposition in the forest. A slight positive temperature dependence of CO and H_2 deposition velocities was observed, but it could have been masked by their strong dependence on soil moisture and therefore soil diffusivity. CH_4 deposition velocities were clearly dependent on soil temperature.

The deposition velocities of CO and H_2 were positively correlated both in the arable field and in the forest, indicating similar factors controlling the deposition velocities. The correlation between H_2 and CH_4 deposition velocities was poor both in the arable field and in the forest, but better over a shorter period when the temperature variation was small.

In the next Chapter, based on the results of this Chapter, model analysis is done to soil uptake of CO and H_2.

Table 4.1 Dates of measurements by the open-flow technique (OFT) in the different treatment plots during the period from June 26 to August 26, 1995 in Tsukuba, Japan (indicated by shaded areas).

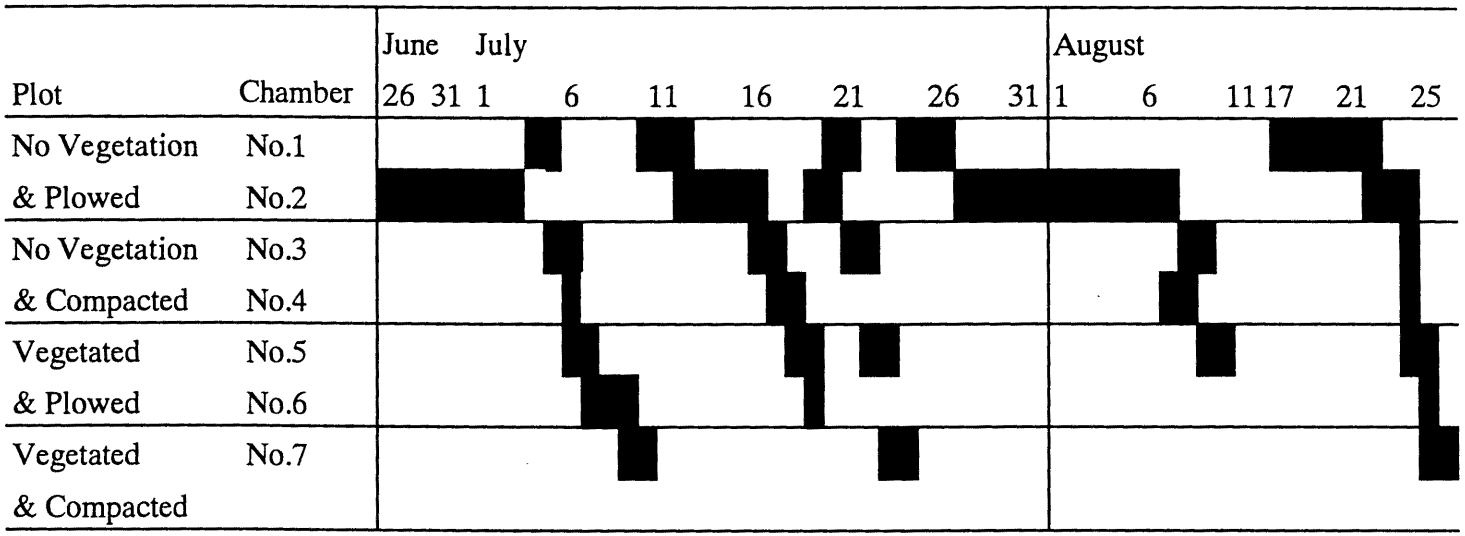

Table 4.2 Relationship between soil temperature, soil moisture, and deposition velocities in the forest. The correlation between soil temperature at 2 cm depth and deposition velocities was calculated from data collected from 3 Dec 1996 to 18 September 1997, when temperature and soil moisture were monitored continuously. To describe the relationship between deposition velocities, H2 is chosen as a independent variable, because the soil layer responsible for deposition is expected to be deeper in the order CH4, H2, and CO (Lieble and Seiler, 1976; Adamsen and King, 1993; Bender and Conrad, 1994b).

Period	y=ax+b y dependent	x independent	n	a slope	b interception	R^{2*}	p
2.Dec 1996 - 17.Sep 1997	H_2 v_d	Soil temperature	28	0.0590	0.000450	0.137	0.0300
	CO v_d	Soil temperature	27	0.0240	0.000220	0.054	0.1259
	CH_4 v_d	Soil temperature	27	0.0029	0.000077	0.569	<0.0001
2.Dec 1996 - 27.May 1997	H_2 v_d	Soil temperature	18	0.0584	0.000635	0.070	0.1507
	CO v_d	Soil temperature	18	0.0256	0.000050	0.000	0.8509
	CH_4 v_d	Soil temperature	16	0.0030	0.000070	0.334	0.0112
2.Dec 1996 - 17.Sep 1997	H_2 v_d	Soil moisture	28	0.112	-0.159	0.340	0.0070
	CO v_d	Soil moisture	27	0.056	-0.095	0.266	0.0035
	CH_4 v_d	Soil moisture	27	0.010	-0.020	0.673	<0.0001
2.Dec 1996 - 27.May 1997	H_2 v_d	Soil moisture	18	0.197	-0.419	0.491	<0.0001
	CO v_d	Soil moisture	18	0.100	-0.232	0.430	0.0019
	CH_4 v_d	Soil moisture	16	0.011	-0.023	0.341	0.0103
10.Sep 1996 - 17.Sep 1997	CO v_d	H_2 v_d	37	0.00083	0.416	0.408	<0.0001
	CH_4 v_d	H_2 v_d	36	0.00174	0.367	0.167	0.0077
2.Dec 1996 - 27.May 1997	CO v_d	H_2 v_d	18	-0.00154	0.437	0.523	0.0004
	CH_4 v_d	H_2 v_d	16	0.00029	0.051	0.523	0.0009

Table 4.3 Comparison of CO and H_2 deposition velocities (v_d) from various studies.

Sites	Vegetation	Season	CO v_d (10^{-2}cm s^{-1})	H_2 v_d (10^{-2}cm s^{-1})	Reference
Agricultural, savannah, unplanated field					
Guri Venezuela	grassland savannnah	Oct.1988	2.5 (0-4.5)		Scharffe et al. (1990)
Transvaal S. Africa	savannah	Wet season Feb.1983	5.1 (4.7-6.4)	13.1 (12-14)	Conrad and Seiler (1985a)
Namib S.W. Africa	desert	Feb.1982	0		Conrad and Seiler (1982)
Karoo S. Africa	semidesert	Dry season Feb.1982	0	1	Conrad and Seiler (1982) Conrad and Seiler (1985a)
Andalusia Spain	unplanted field	Dry season Sep.1982	1.1 (0.98-1.26)	3.3 (3.1-3.6)	Conrad and Seiler (1984) Conrad and Seiler (1985a)
Tsukuba Japan	agricultural	Year-based	2.3 (0-5)	4.29 (0-9)	This work
Mainz Germany	Various sites	Nov./Dec.1974 Apr./May 1975	3-4 (0.5-7)	6-7 (3-12)	Liebl and Seiler (1976)
Mainz Germany	grass/small plants	Year-based 1978/1979	4 (0.5-7)		Conrad and Seiler (1980b)
Bush Scotland	agricultural	Year-based	0.14		Moxley and Smith (1998a)
Woodland					
Guri Venezuela	semideciduous forest	October,1988	3.8		Scharffe et al. (1990)
Tsukuba Japan	deciduous forest (secondary forest)	Year-based	2.7 (1.5-3.5)	6.26 (5-8)	This work
Darmstadt Germany	deciduous forest	Year-based	2.7 (1-6)		Sanhueza et al. (1998)
Bush Scotland	coniferous deciduous	Year-based	0.23		Moxley and Smith (1998a)
Manitoba Canada	boreal forest Jack pine forest	Summer	0.85		Zepp et al. (1997)
	Black spruce forest		1.5-1.8		Zepp et al. (1997) Kuhlbusch et al. (1998)

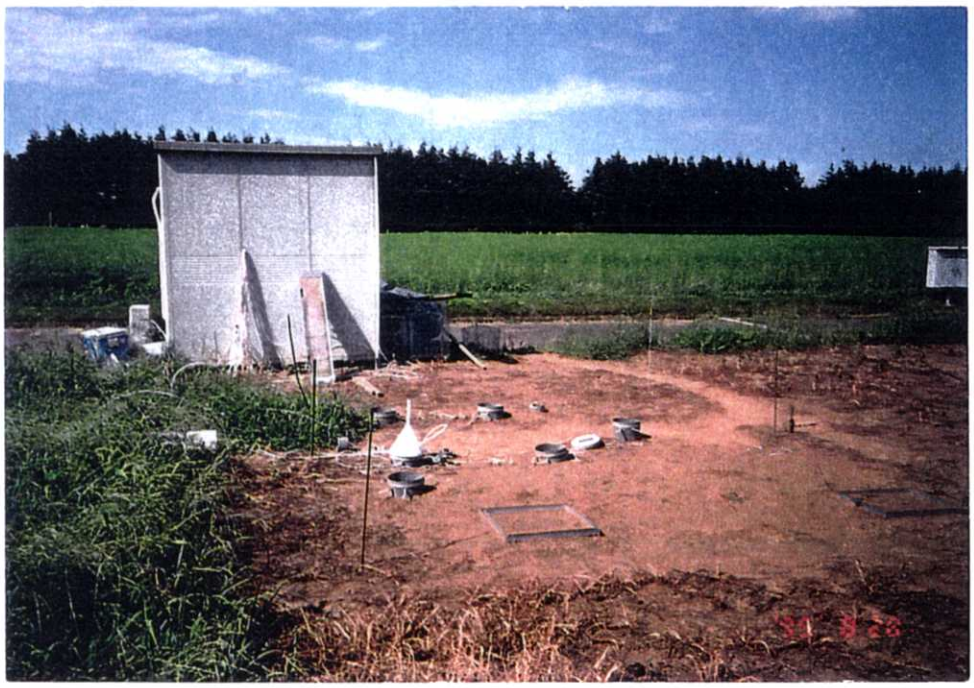

Photo 4.1 Measurements in the arable field.

Photo 4.2 Measurements in the forest.

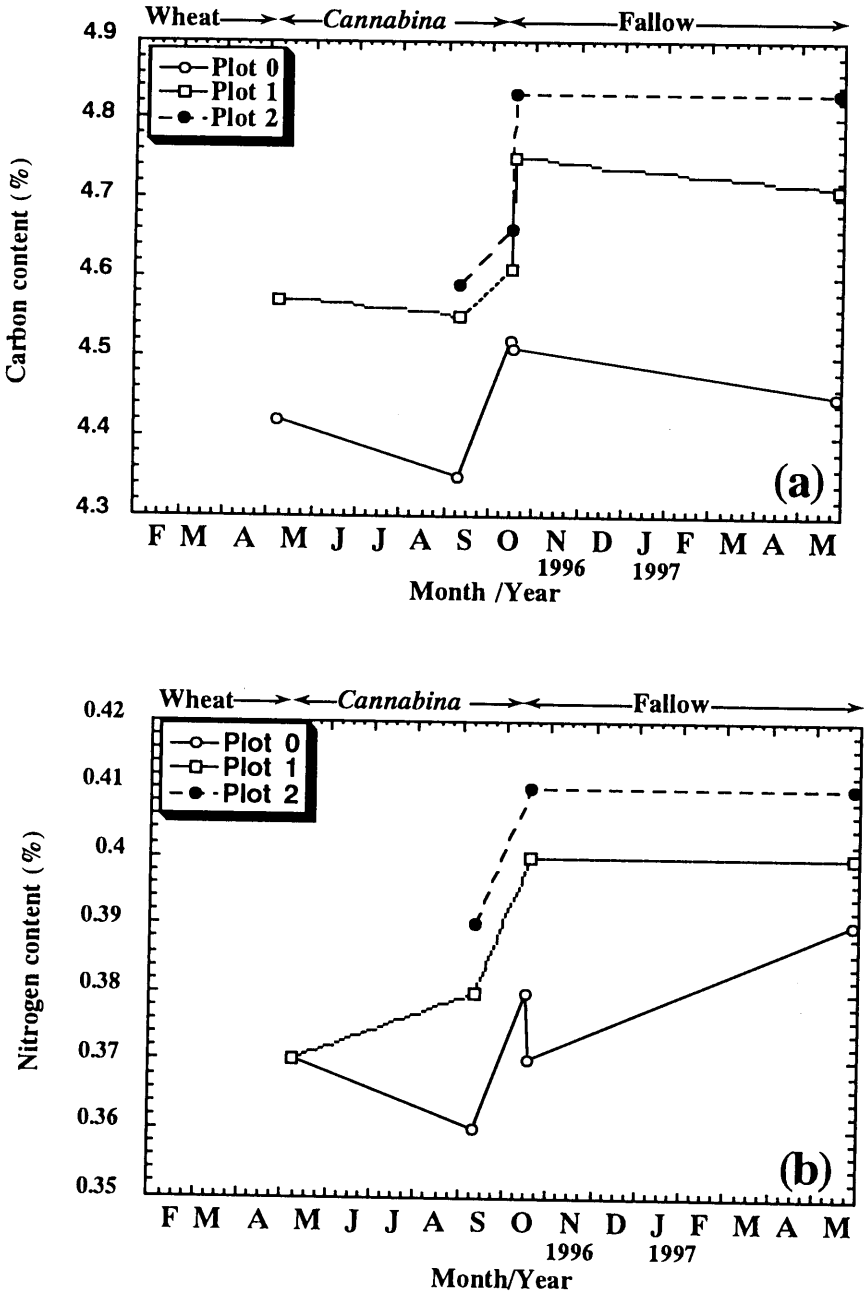

Figure 4.1 Variation in (a) carbon and (b) nitrogen contents in the arable field from 1996 to 1997

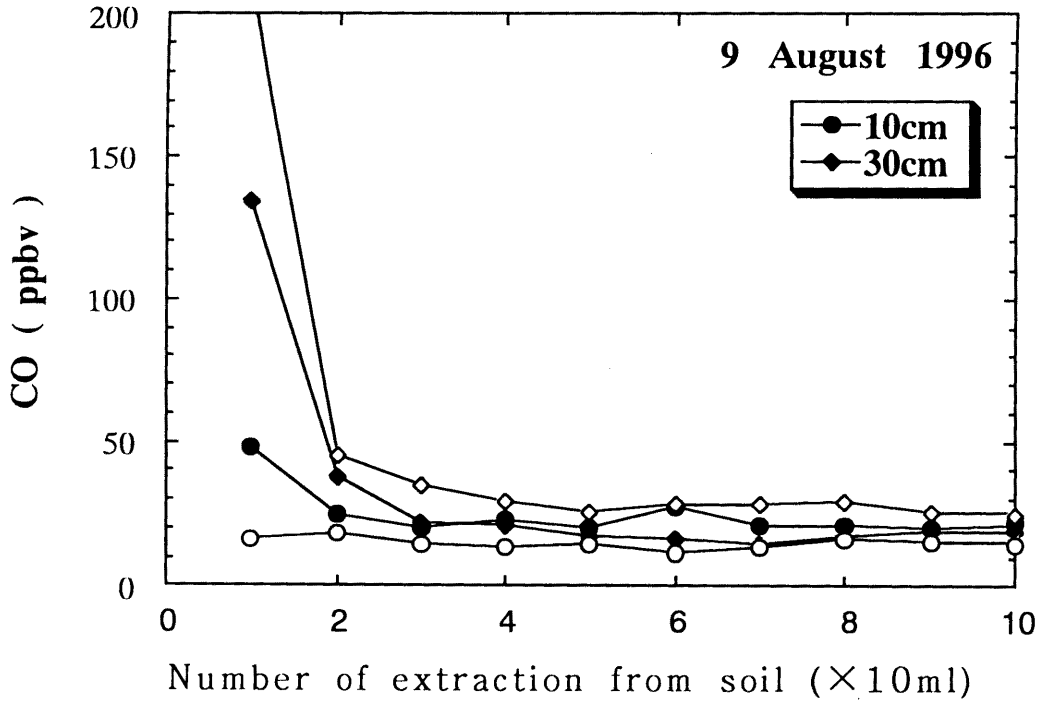

Figure 4.2 Variation in CO concentration from soil air samples by repeating extraction.

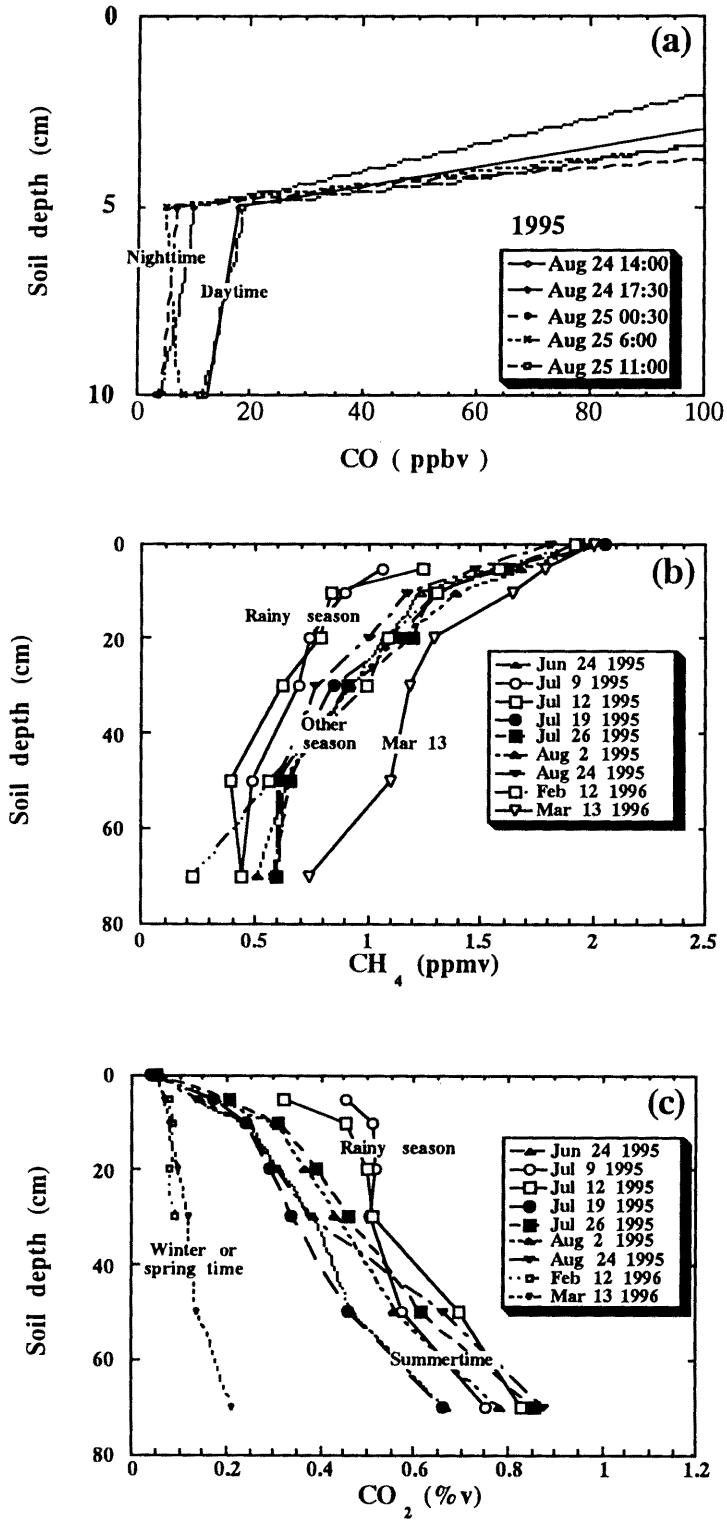

Figure 4.3 Changes in soil air concentrations of (a) CO, (b) CH_4, and (c) CO_2 with soil depth on different dates during the period from June 25 to August 24, 1995, and February 12 and March 13, 1996 in Tsukuba . Only the August 24 measurements are shown for CO due to sample contamination.

H_2 in soil always could not be detected.

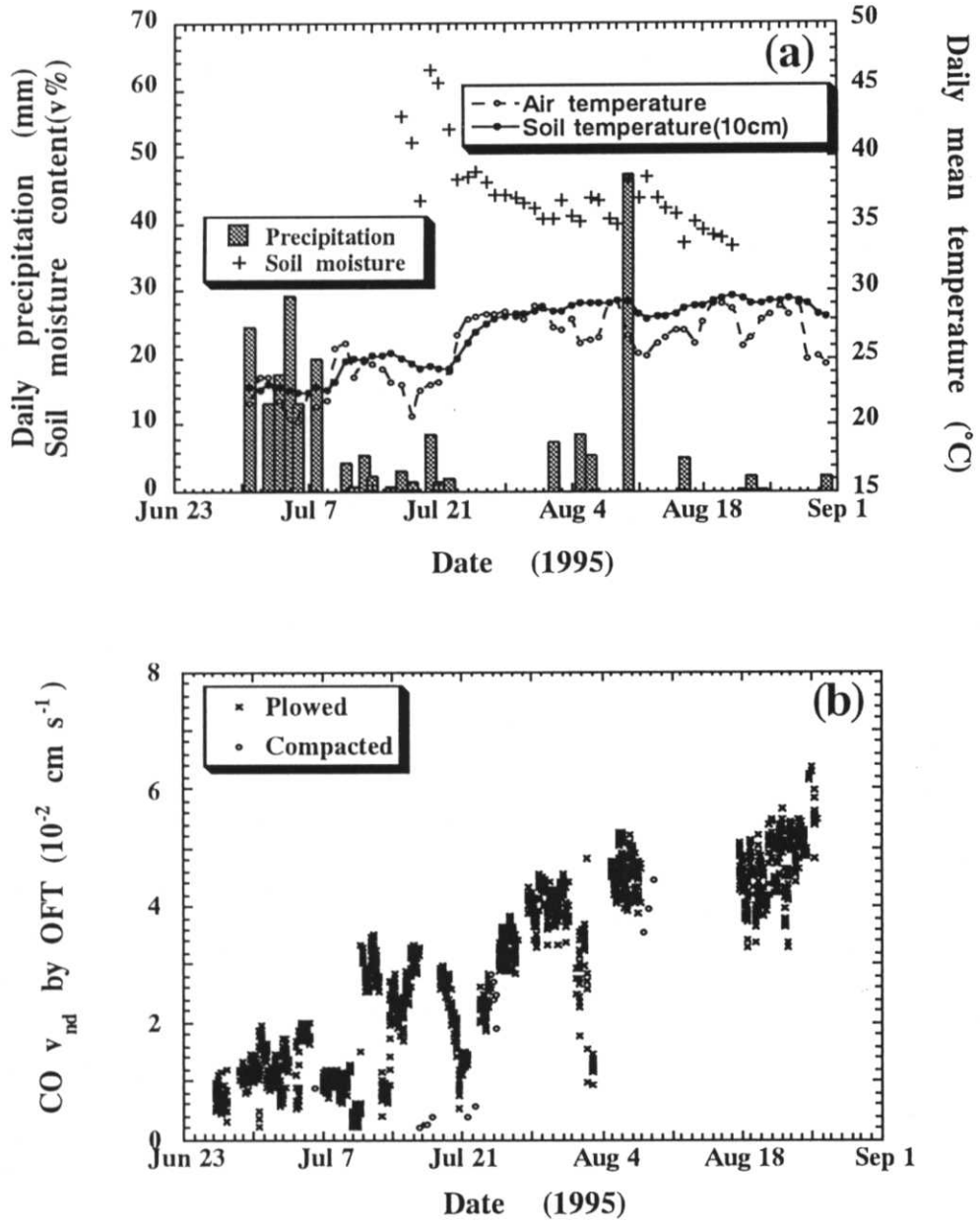

Figure 4.4 continues to next page.

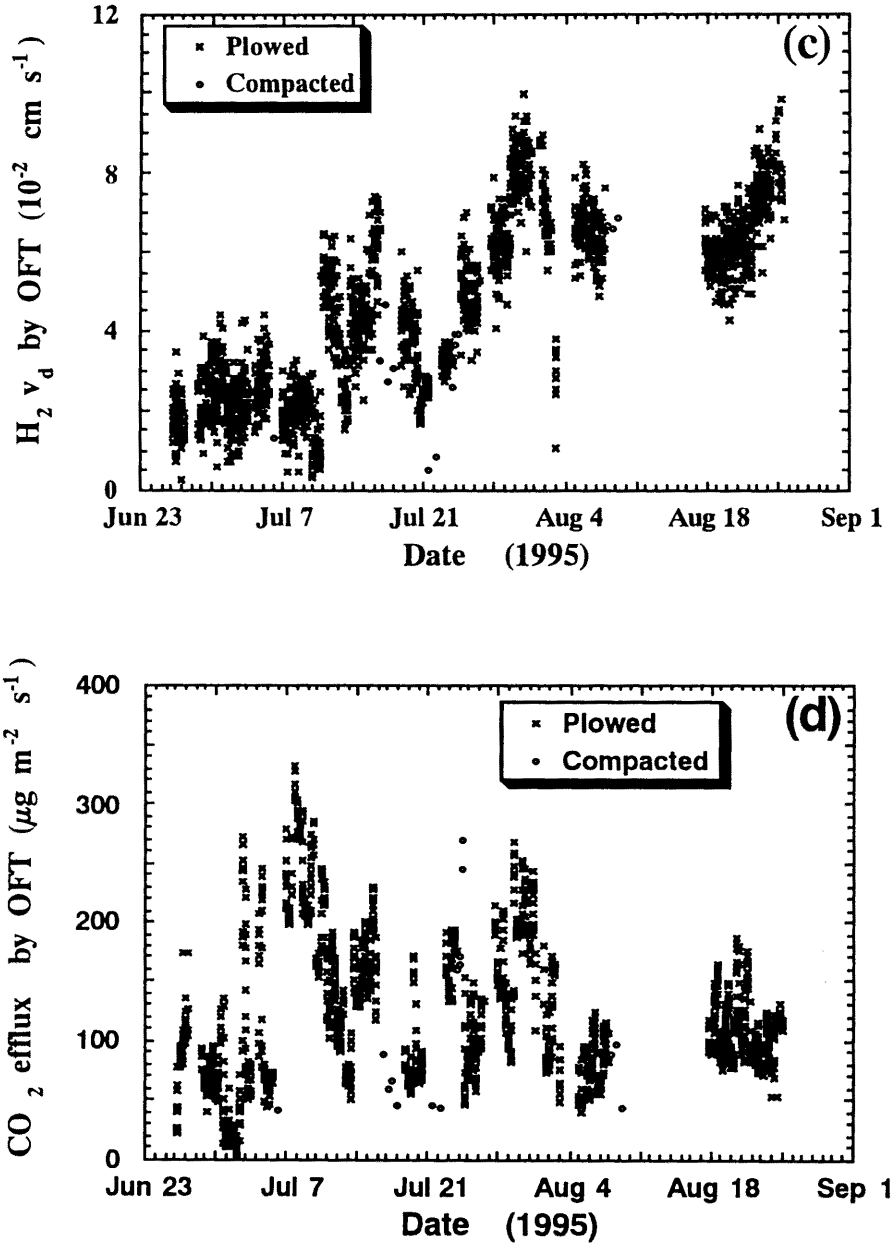

Figure 4.4 Changes in (a) daily rainfall, daily temperatures taken at a meteorological station located at a distance of several hundred meters from the measurement site, and soil moisture level (0-5 cm) measured in the field; (b) soil CO net deposition velocity; (c) soil H_2 deposition velocity; and (d) CO_2 efflux by the OFT during the summer season in 1995 in Tsukuba. Each data point on the graphs (b, c and d) represents a 30 minute average. The vertical scatter for each date denotes diurnal variations.

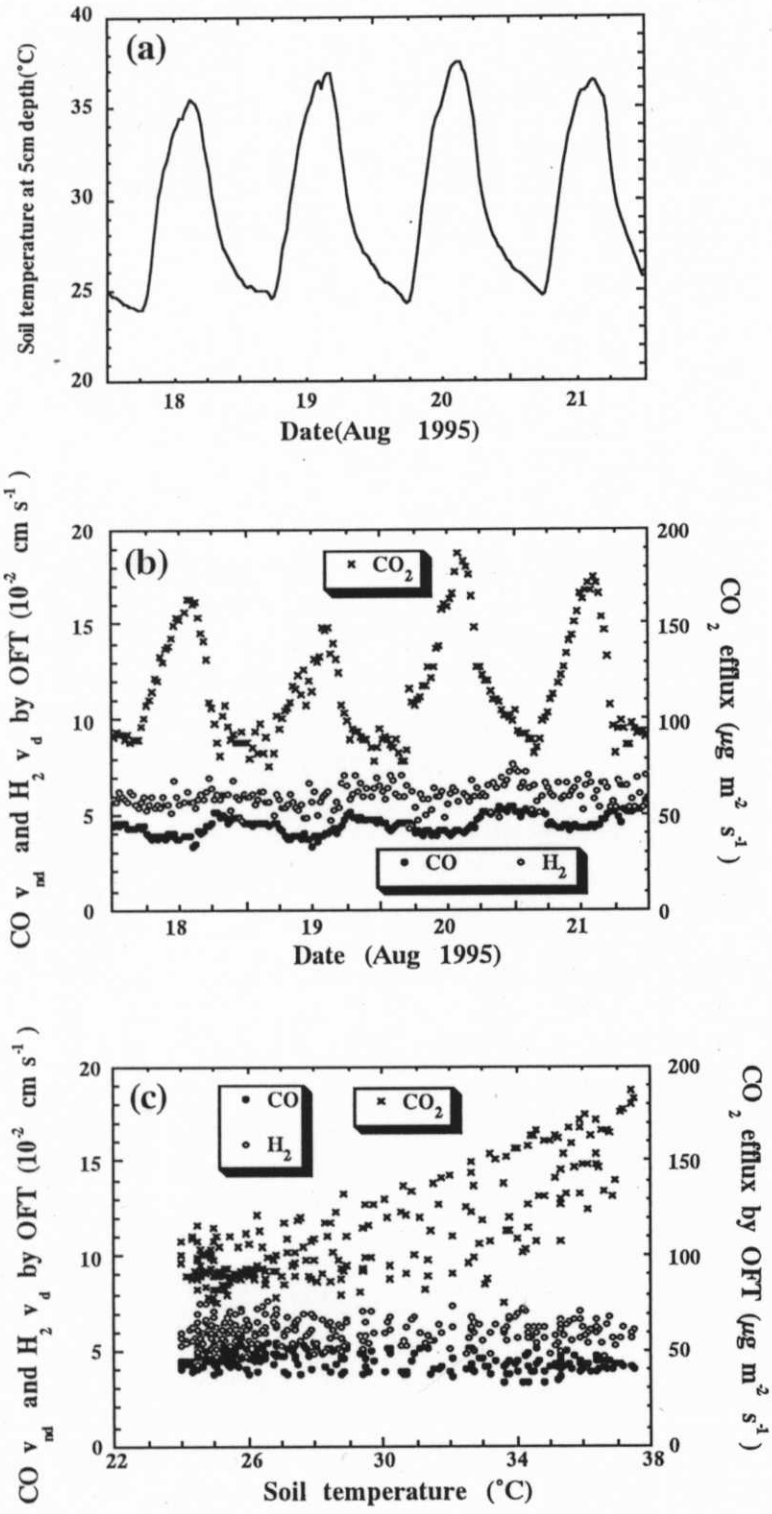

Figure4.5 Changes in (a) soil temperature, (b) CO and H_2 deposition velocities, and CO_2 efflux obtained by the OFT during 4 sunny days between August 18 and 21 in 1995 and (c) relationship between the soil temperature and deposition velocities and flux rates of CO, H_2 and CO_2 during the same period. Date and time are JST.

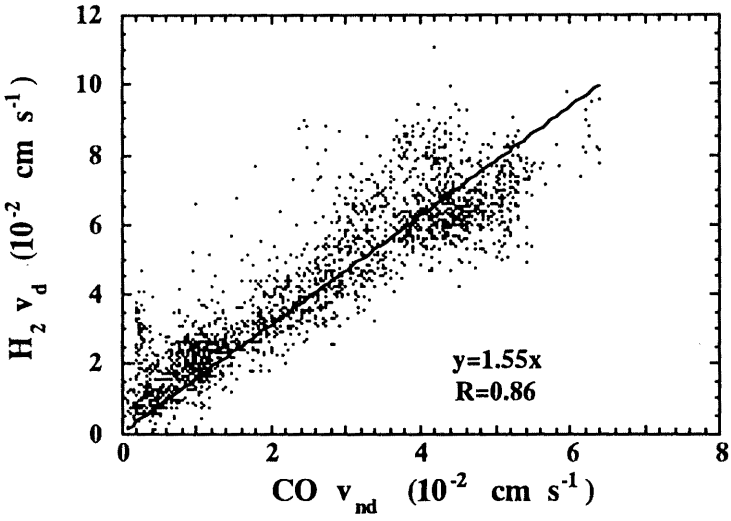

Figure 4.6 Relationship between CO and H_2 deposition velocities obtained by the OFT. Each point represents a 30-minute average from 3-minute data.

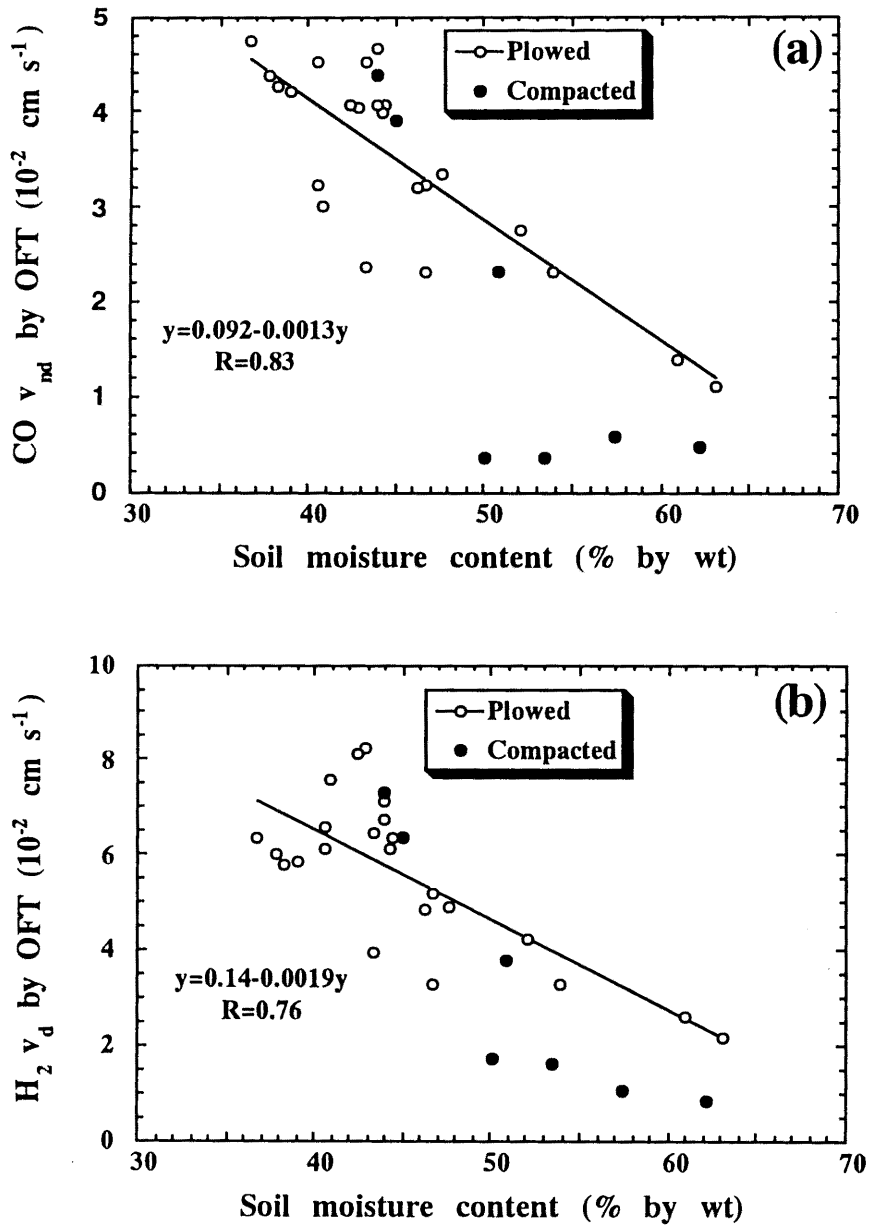

Figure 4.7 Relationship between soil moisture content (0-5 cm) and the deposition velocities of (a) CO and (b) H_2 obtained by the OFT experiments: the data points represent 12 or 24-hour averages to eliminate diurnal variation. Regressions were calculated for plowed plots.

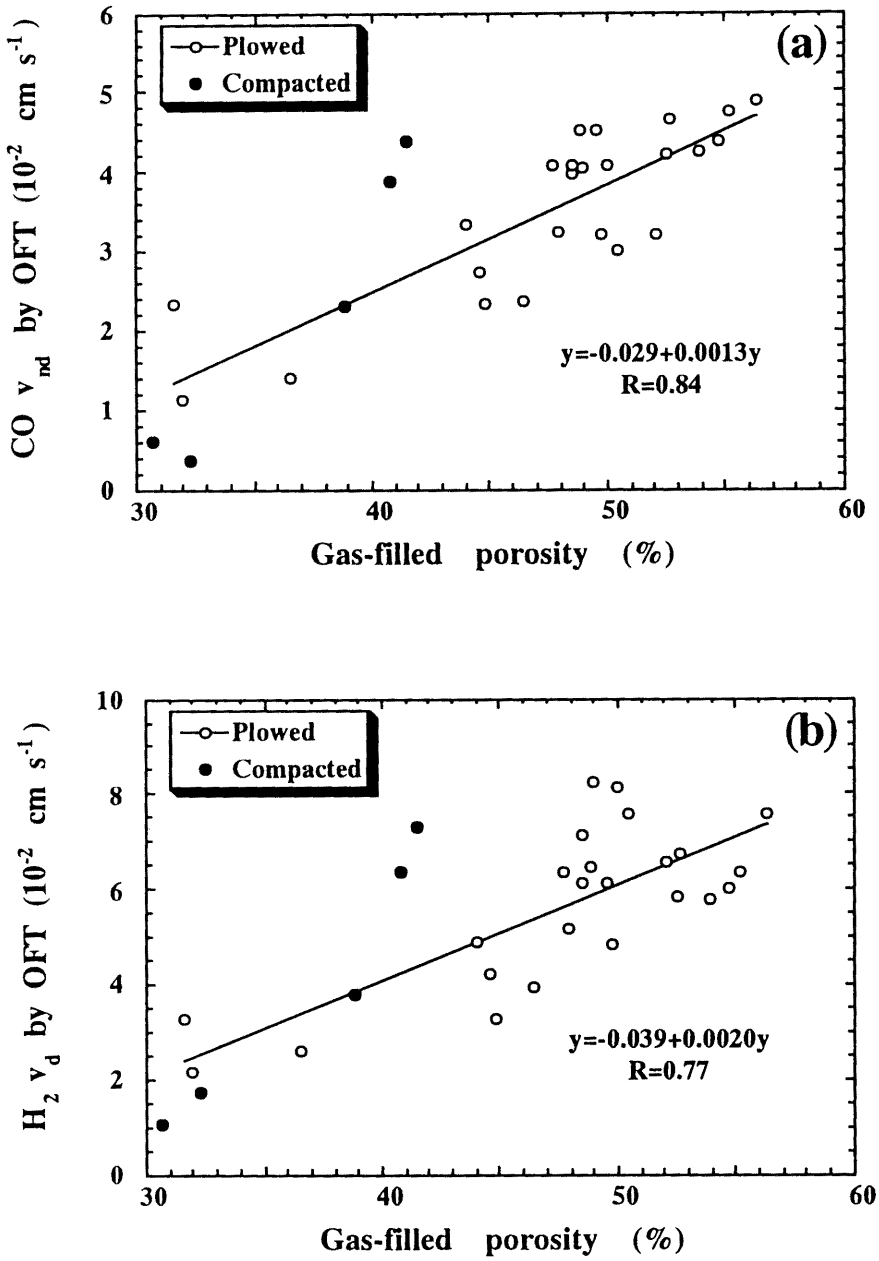

Figure 4.8 Relationship between gas-filled porosity (0-5 cm) and the deposition velocities of (a) CO and (b) H_2 obtained by the OFT experiments: the data points represent 12 or 24-hour averages to eliminate diurnal variation. Regressions were calculated for plowed plots.

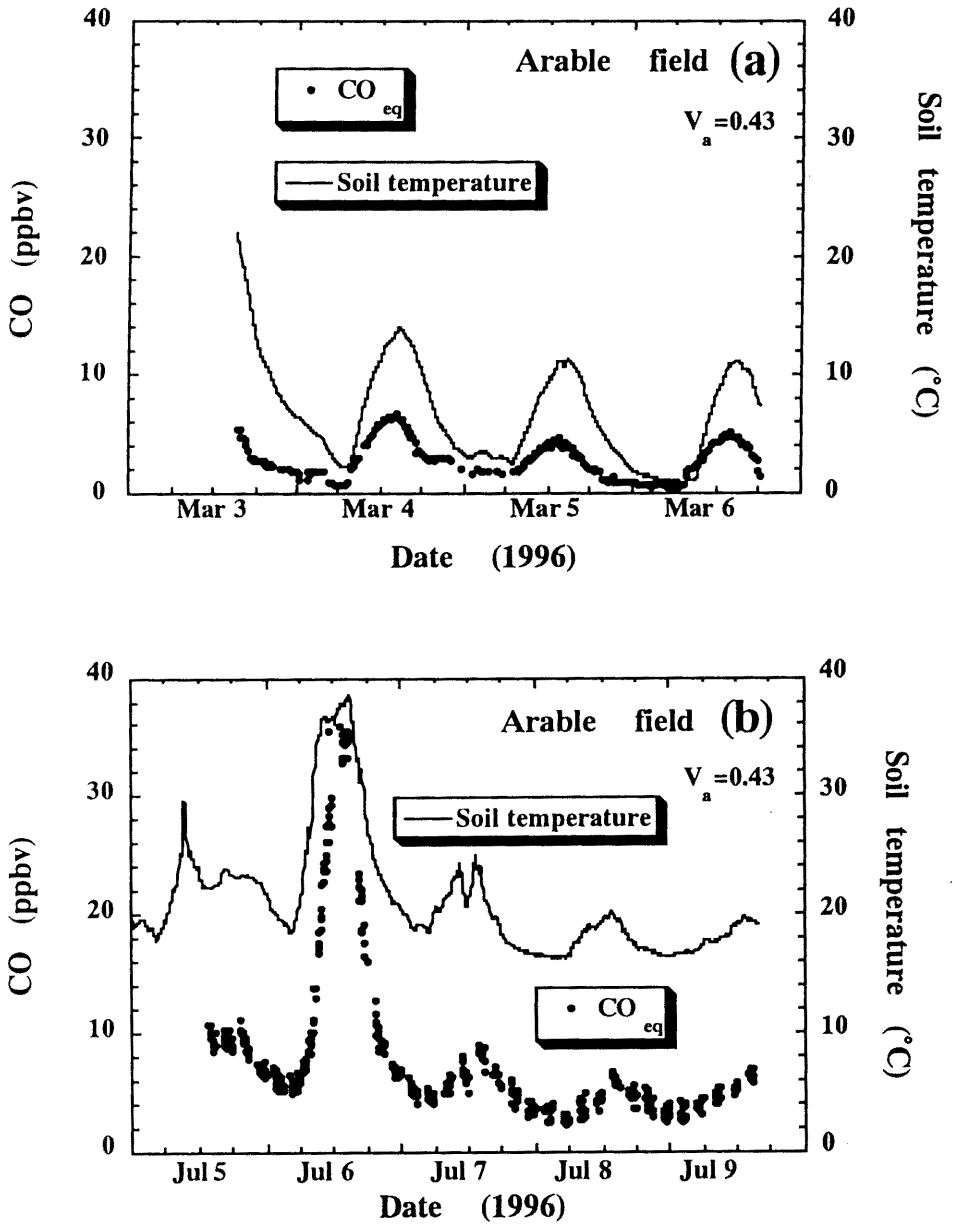

Figure 4.9 CO equilibrium concentration in soil for several days in (a) March 1996 and (b) July 1996 by the equilibrium box technique. The $[CO]_{eq}$ data at lower concentrations (a) were close to detection limit. Vertical scattering in $[CO]_{eq}$ data (b) H_2 was caused by injecting gases containing a high concentration of CO (500 ppmv) at 3-h intervals. H_2 always could not be detected within the detection limit.

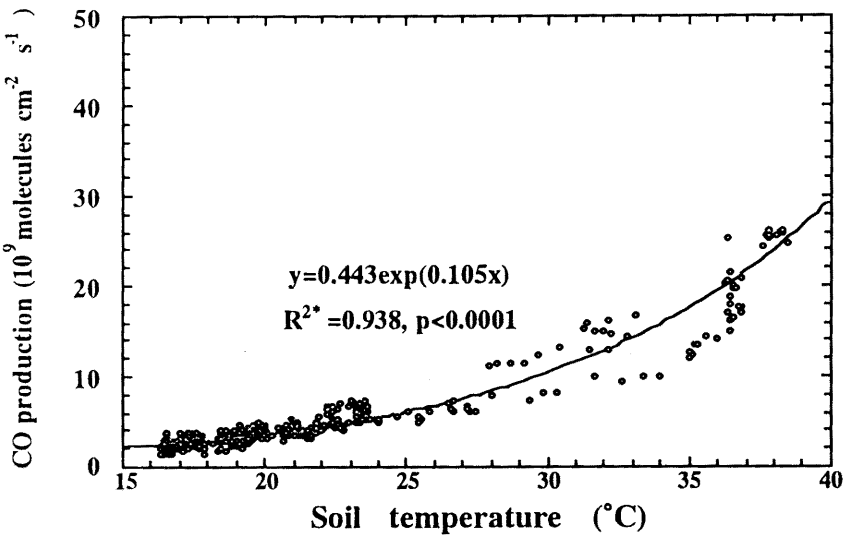

Figure 4.10 The relationship between CO production estimated using the equilibrium box technique in July 1996 (Fig. 4.9b) and soil temperature in the arable field.

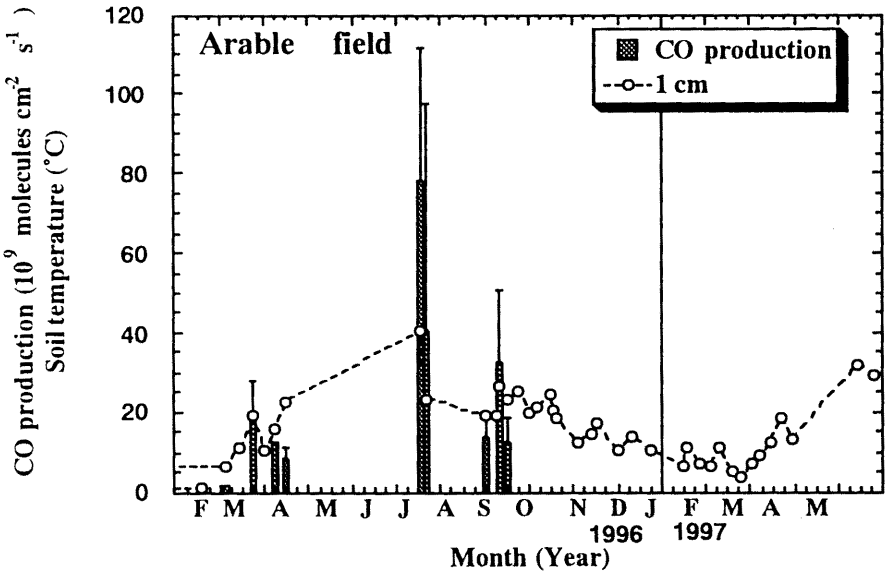

Figure 4.11 Variation in CO production rates and soil temperature at 1 cm depth estimated from data collected by the closed-chamber technique in the arable field. CO production rates were not always obtained without large errors because, when the temperature was low.

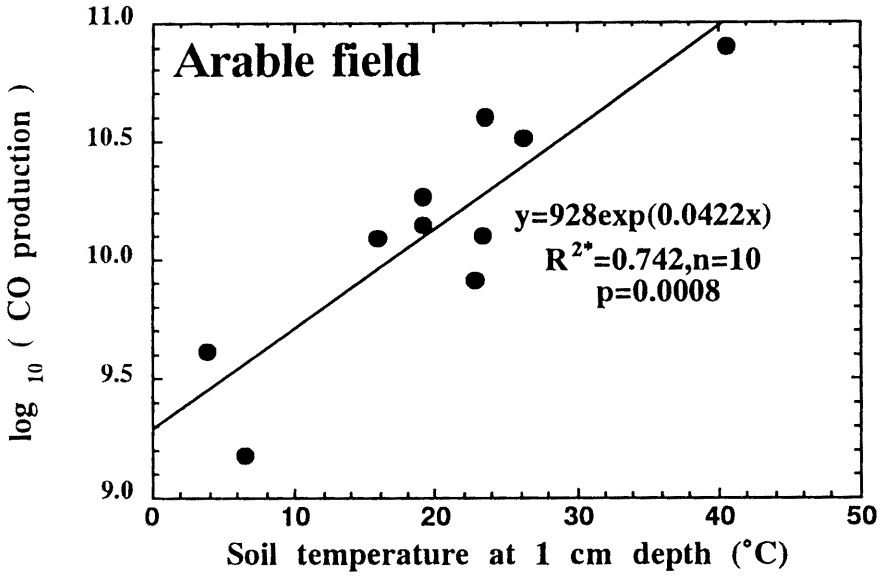

Figure 4.12 The relationship between soil temperature at 1 cm depth and CO production rates estimated from data collected by the closed-chamber technique in the arable field.

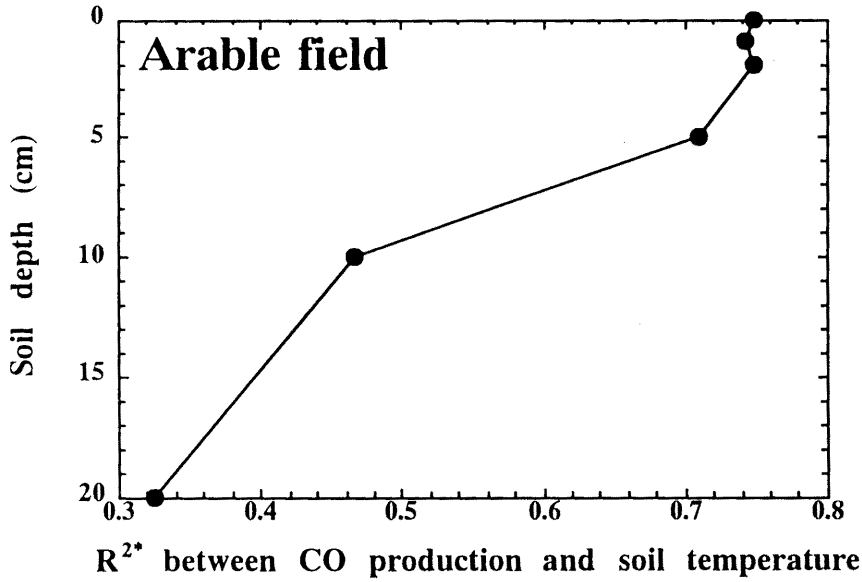

Figure 4.13 Squared correlation coefficients between CO production and soil temperatures in the arable field.

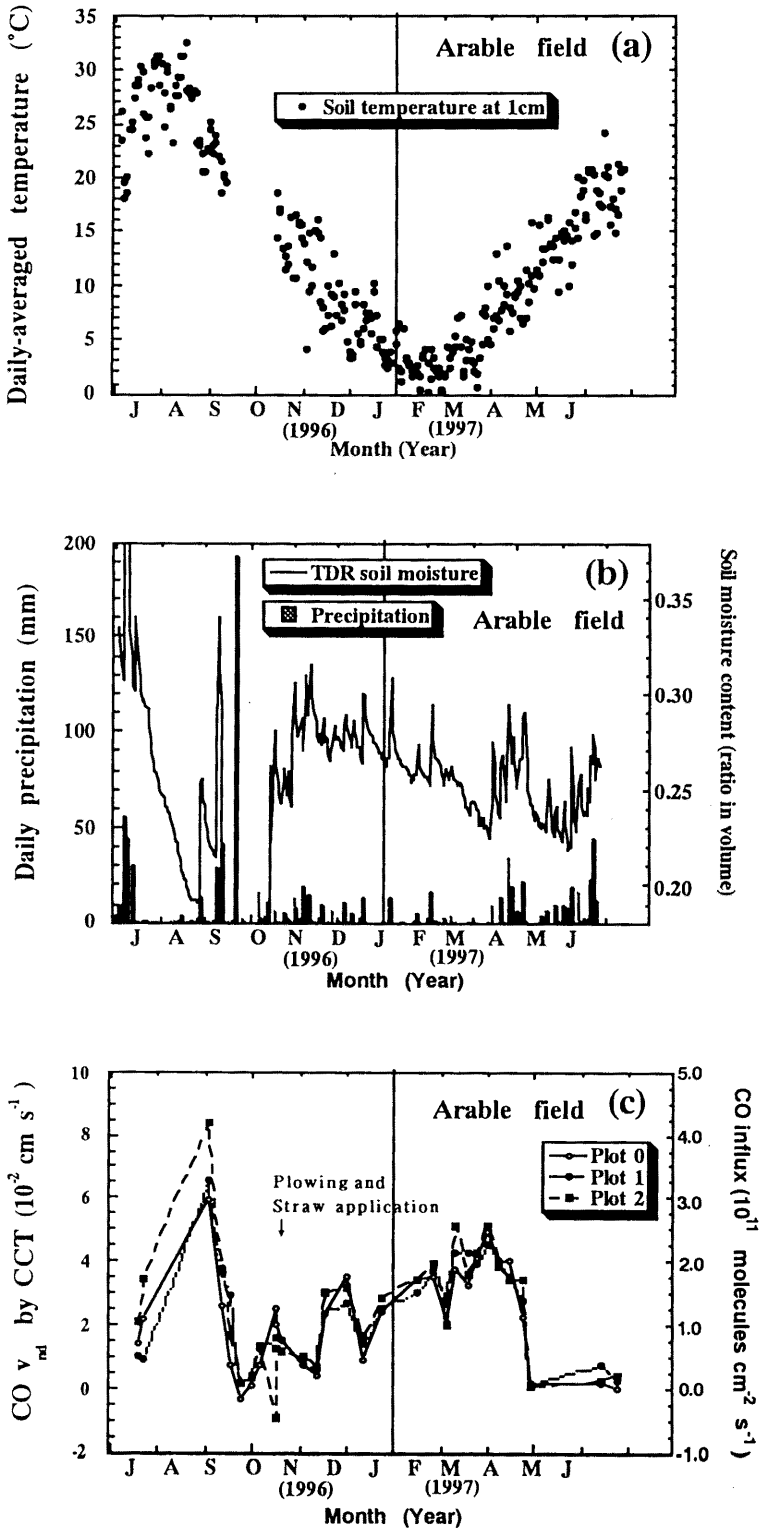

Figure 4.14 continues to next page.

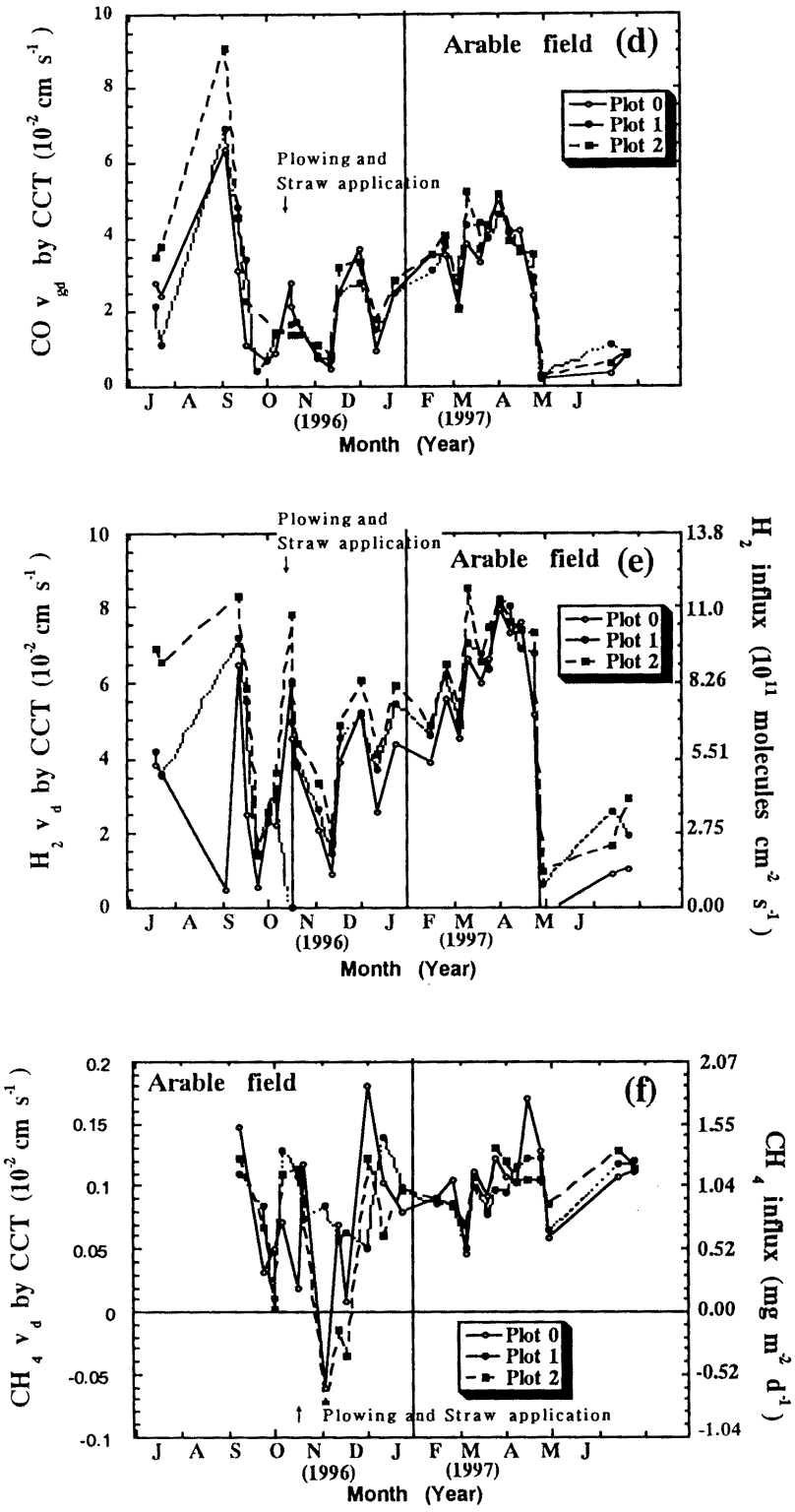

Figure 4.14 continues to next page.

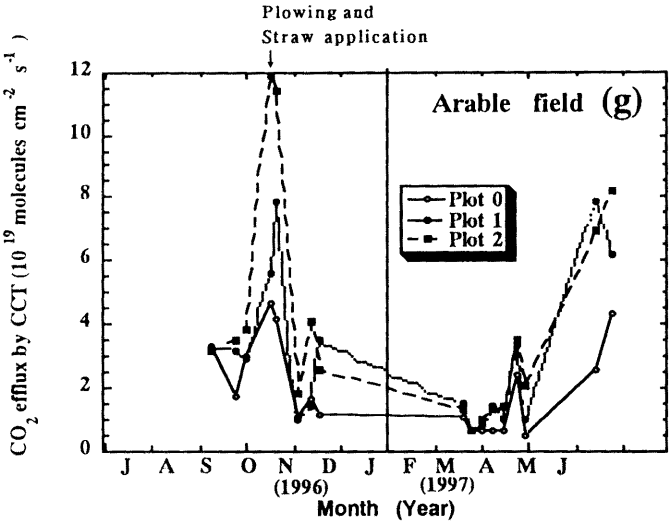

Figure 4.14 Variation in the arable field from July 1996 to June 1997 in (a) soil temperature at 1 cm depth, and (b) precipitation and soil moisture content, (c) CO net deposition velocity, (d) CO gross deposition velocity, (e) H_2 deposition velocity, (f) CH_4 deposition velocity, and (f) CO_2 efflux obtained by the CCT. From 13 September to 14 October 1996 (Fig. 4.14a), soil moisture data were not obtained. On the right vertical axis, CO and H_2 deposition velocities are converted to the unit molecules cm^{-2} s^{-1} assuming that atmospheric concentrations of CO (c) and H_2 (e) are 200 and 550 ppbv, respectively, temperature is 20°C, and pressure is 1 atm. On the right vertical axis, CH_4 (f) deposition velocity was converted to the unit mg m^{-2} d^{-1} assuming that atmospheric CH_4 concentration is 1.8 ppmv, temperature is 20°C, and pressure is 1 atm. Error bars in deposition velocities are omitted for clarity.

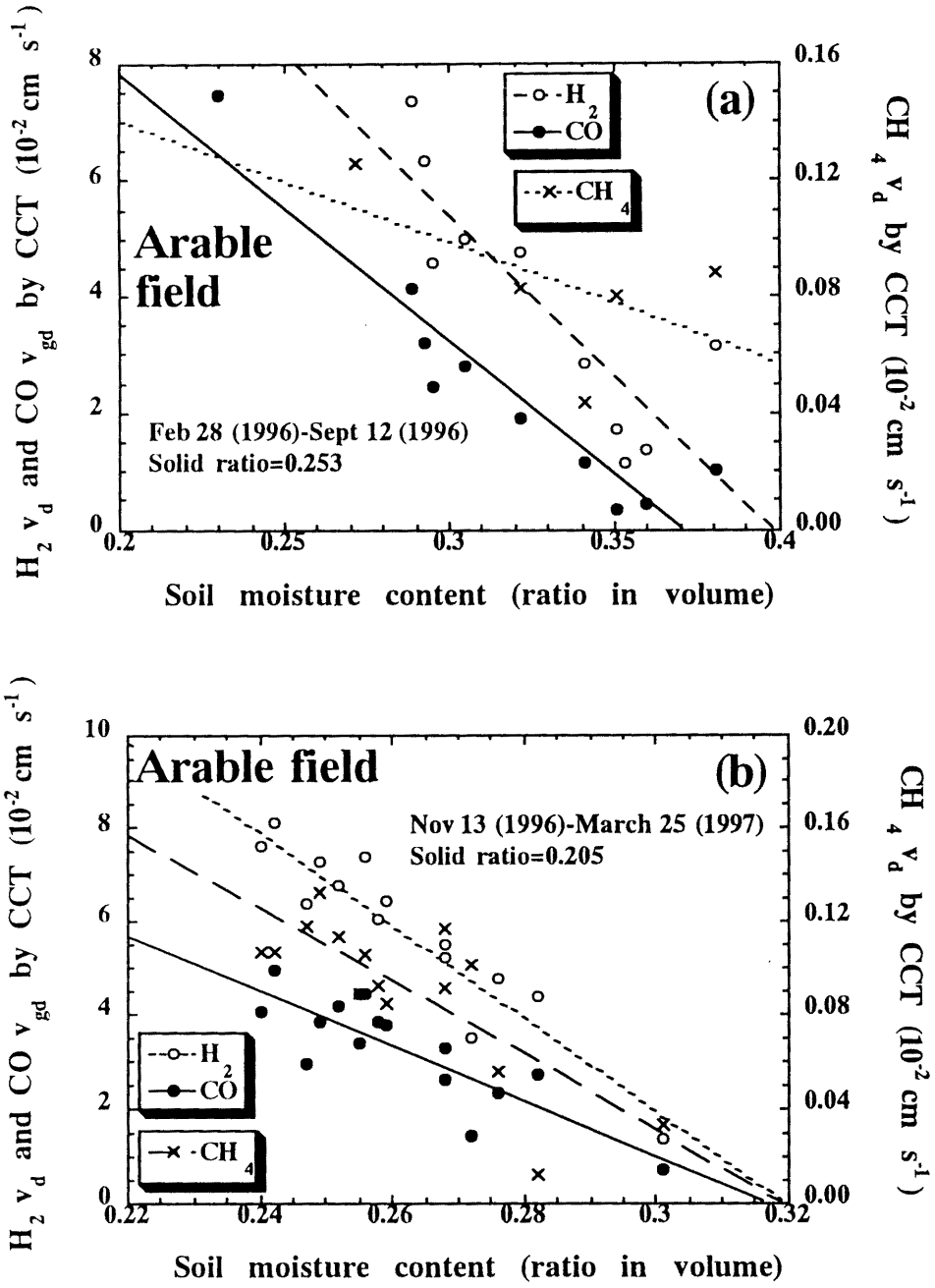

Figure 4.15 The relationship between soil moisture content and deposition velocities of CO ,H_2 , and CH_4 for (a) data from 28 February to 12 September 1996 and (b) data from 2 December 1996 to 25 March 1997. Data shown are values averaged for each date. Values from each plot are not shown.

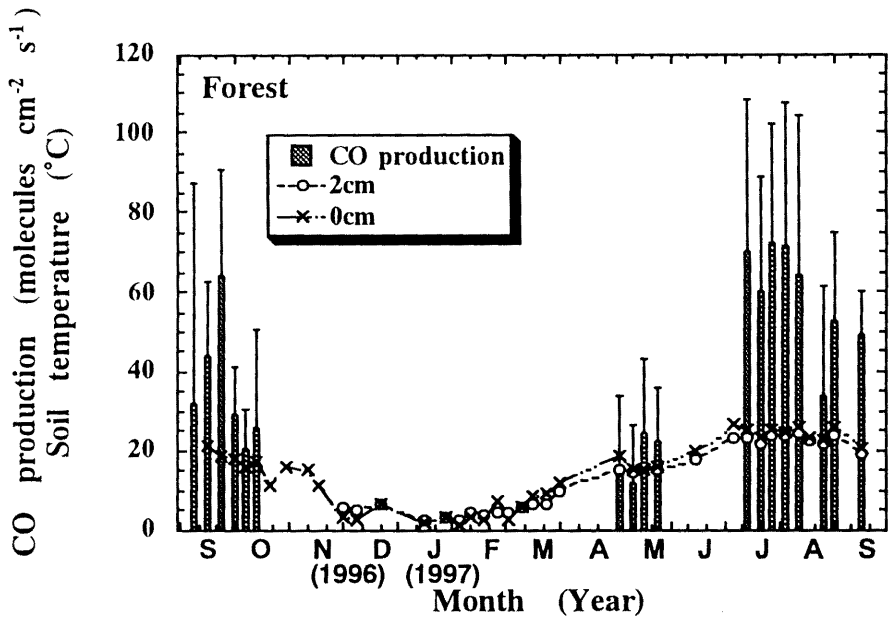

Figure 4.16 Variation in CO production rates and soil temperature at 2 cm depth in the forest. CO production rates from November 1996 to May 1997 are not shown because, when the temperature was low, CO production rates could not be obtained without large errors.

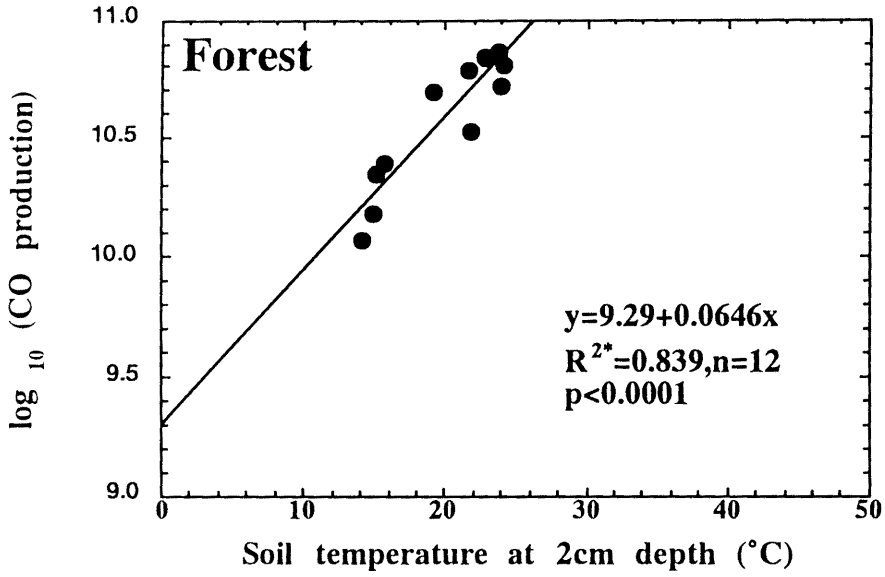

Figure 6.17 CO production rates versus soil temperature at 2 cm depth in the forest.

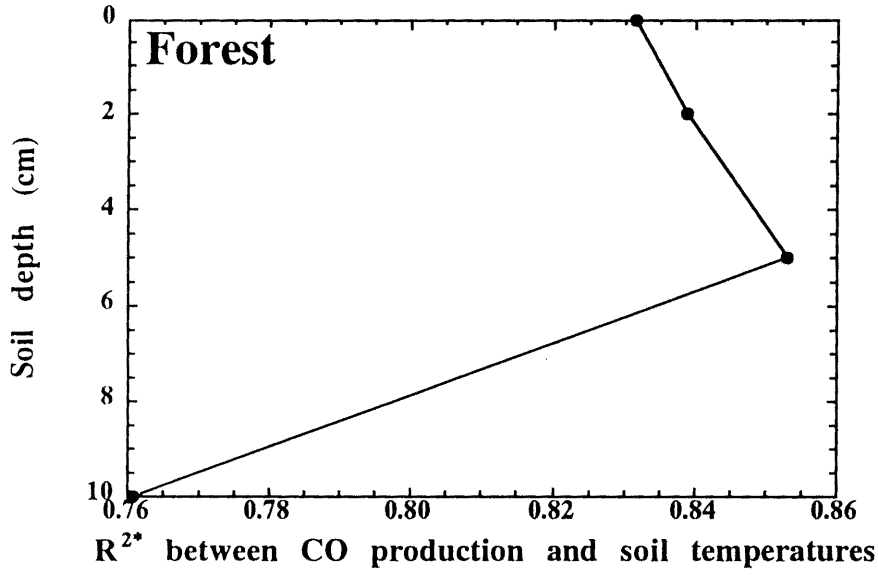

Figure 6.18 Squared correlation coefficients between CO production and soil temperature in the forest.

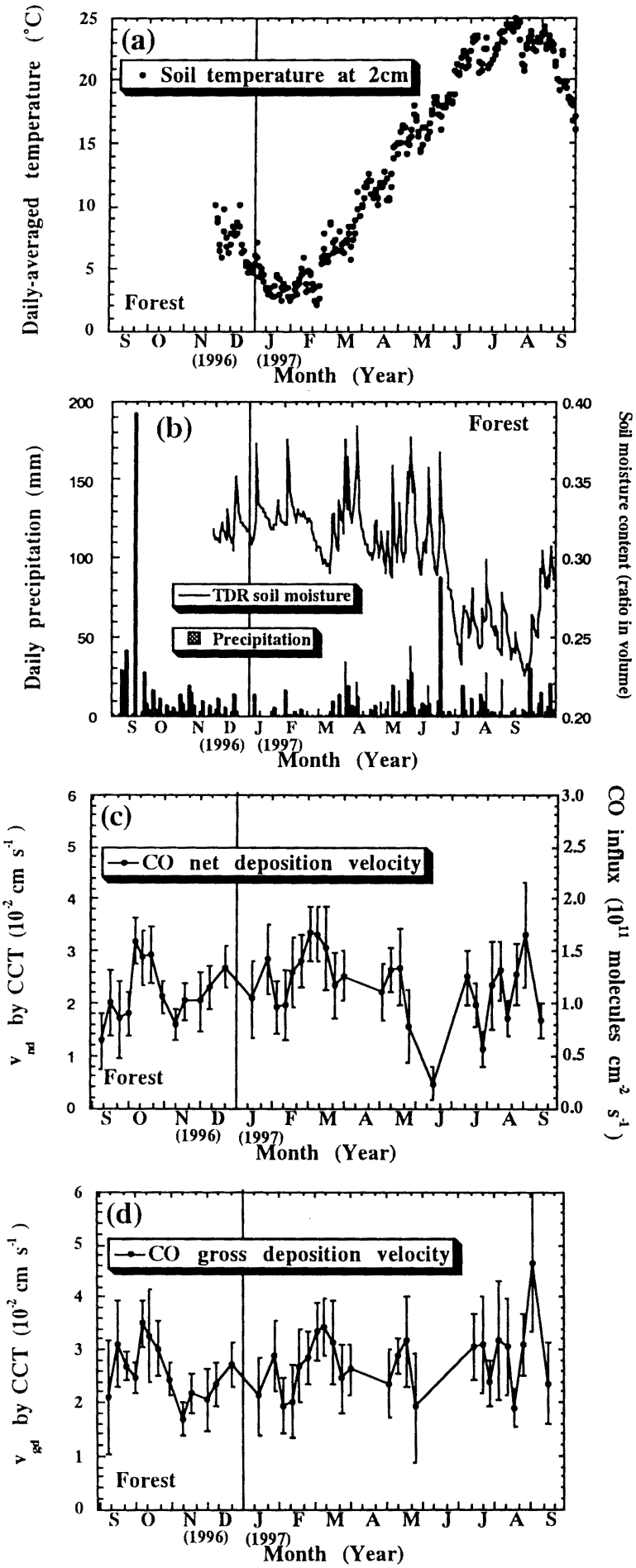

Figure 4.19 continues to next page.

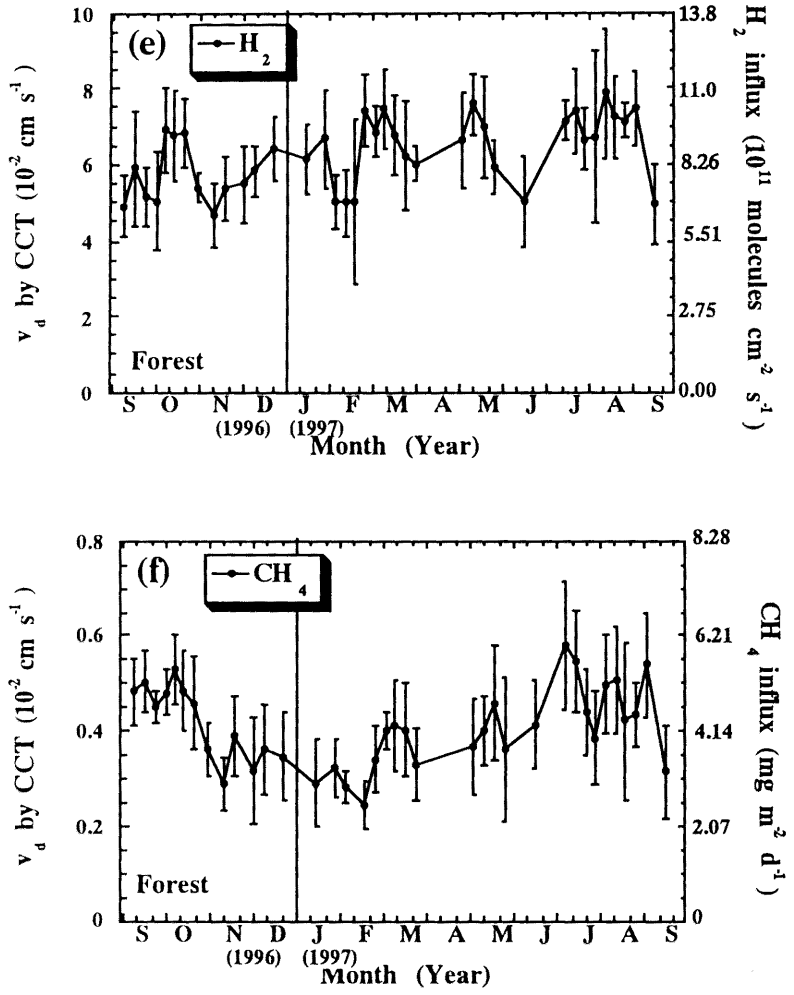

Figure 4.19 Variation in (a) soil temperature at 2 cm depth, (b) precipitation and soil moisture content, (c) CO net deposition velocity, (d) CO gross deposition velocity, (e) H_2 deposition velocity, and (f) CH_4 deposition velocity in the forest. Error bars in deposition velocities are standard errors for 6 chambers. On the right vertical axis, CO and H_2 deposition velocities are converted to the unit molecules cm^{-2} s^{-1} assuming that the atmospheric concentrations of CO (c) and H_2 (e) are 200 and 550 ppbv, respectively, temperature is 20°C, and pressure is 1 atm. On the right vertical axis, CH_4 deposition velocity is converted to the unit mg m^{-2} d^{-1} assuming that CH_4 (f) concentration is 1.8 ppmv, temperature is 20°C, and pressure is 1 atm.

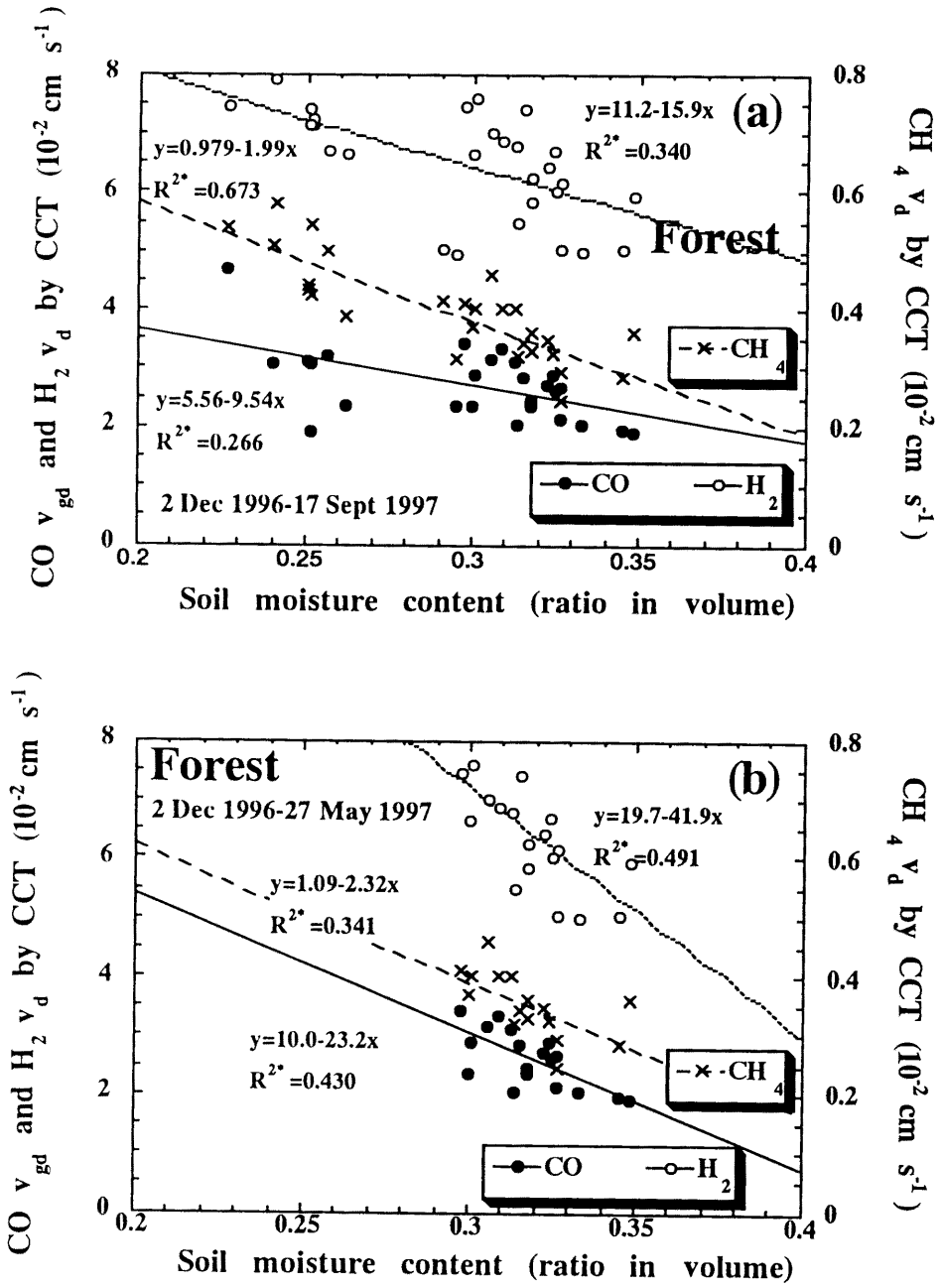

Figure 4.20

The relationship between soil moisture content and deposition velocities of CO, H_2, and CH_4 in the forest. The correlation was calculated from data collected from 3 Dec 1996 to 18 September 1997, when temperature and soil moisture were monitored continuously. Please see Table 6.2 on detailed description of correlation coefficients.

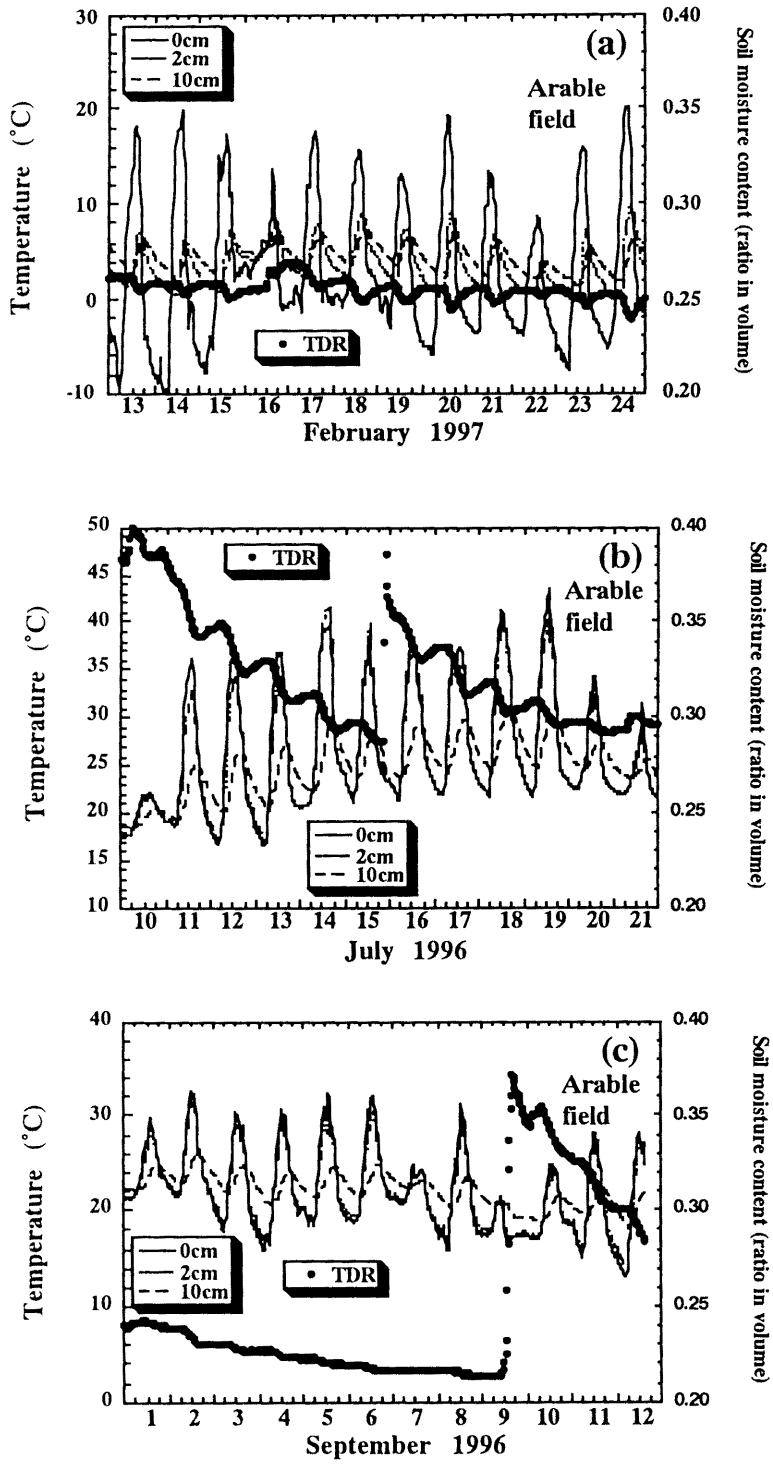

Figure 4.21 continues to next page.

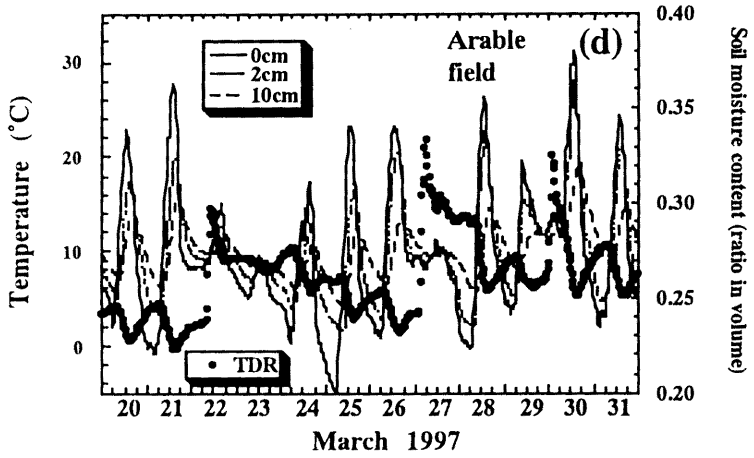

Figure 4.21 Examples of variation in soil temperature and soil moisture content measured by TDR sensors in the arable field for (a) winter, (b) summer after precipitation, (c) summer with long drought, and (d) spring. Soil moisture contents are averages of data from 9 probes of all plots.

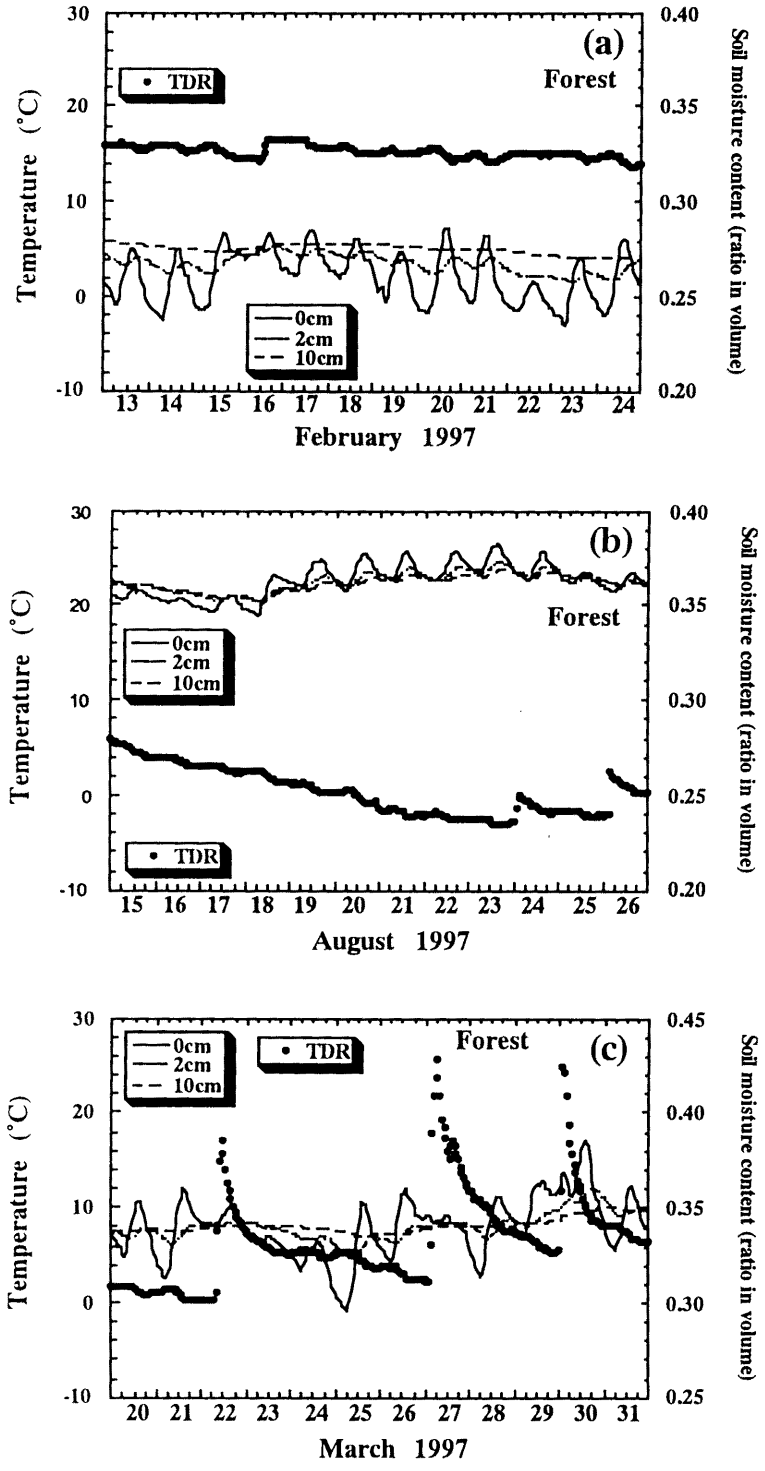

Figure 4.22 Examples of variation in soil temperature and soil moisture content measured by TDR sensors in the forest for (a) winter, (b) summer , and (c) spring. Soil moisture contents are averages of data from 3 probes.

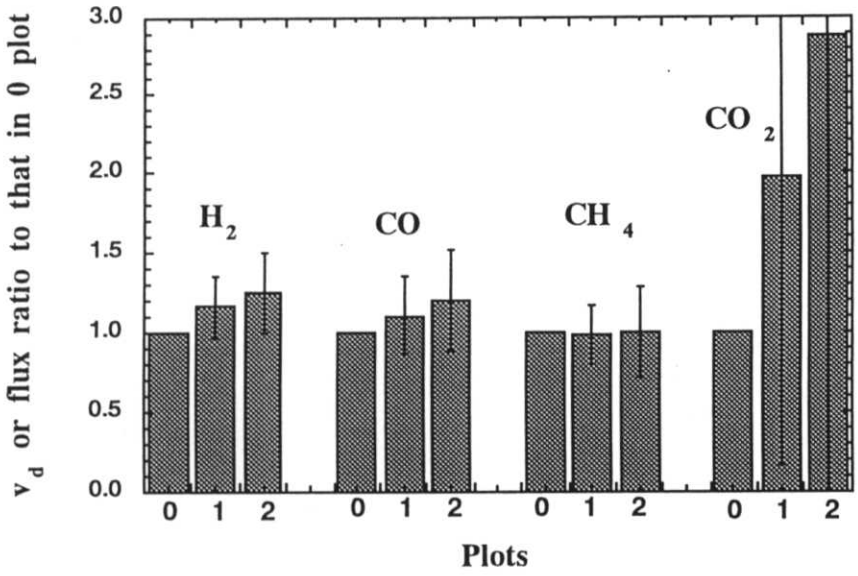

Figure 4.23 Averaged ratios of deposition velocities in the plots in the arable field. Data for H_2, CO, and CO_2 were averaged from 13 November 1996 to 25 March 1997. Data for CH_4 were averaged from 2 December 1996 to 25 March 1997. Error bars are standard deviations of the three ratios at each plot.

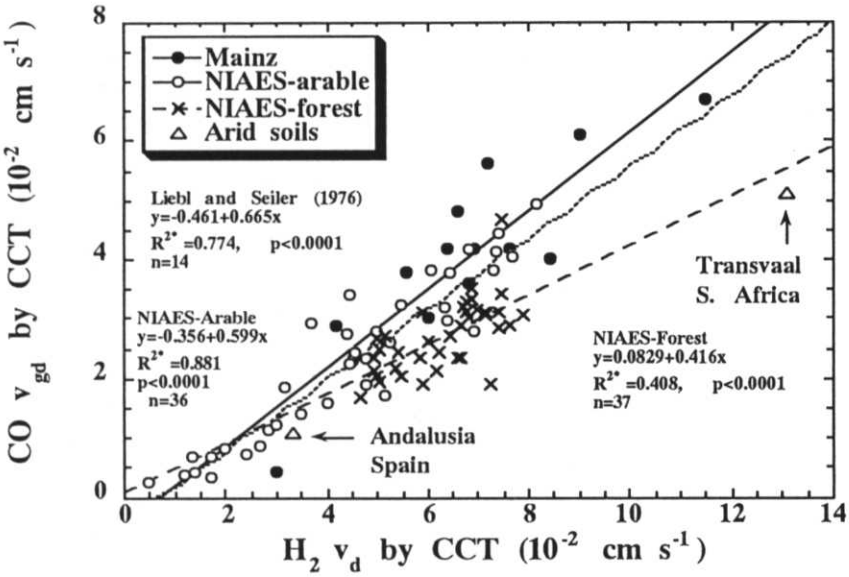

Figure 4.24 The relationship between H_2 and CO deposition velocities from this study and from Liebl and Seiler (1976). Data for the graph from the study of Liebl and Seiler (1976) are taken from their tables. Liebl and Seiler (1976) collected data from several sites near Mainz, Germany. Conrad and Seiler (1985a) collected data from arid or semi-arid sites. H_2 deposition velocities were always higher than those of CO.